NASA Contractor Report 177626

Aerodynamic Control of NASP-Type Vehicles Through Vortex Manipulation

Volume I

Static Water Tunnel Tests

Carlos J. Suárez, T. Terry Ng, Lih-Yenn Ong, and Gerald N. Malcolm

CONTRACT NAS2-13196
September 1993

National Aeronautics and Space Administration

NASA Contractor Report 177626

Aerodynamic Control of NASP-Type Vehicles Through Vortex Manipulation

Volume I

Static Water Tunnel Tests

Carlos J. Suárez, T. Terry Ng, Lih-Yenn Ong, and Gerald N. Malcolm

Eidetics International, Inc.
3415 Lomita Blvd.
Torrance, CA 90505

Prepared for
Ames Research Center
CONTRACT NAS2-13196
September 1993

National Aeronautics and
Space Administration

Ames Research Center
Moffett Field, California 94035-1000

PAGE _____ INTENTIONALLY BLANK

TABLE OF CONTENTS

NOMENCLATURE

A_{ref}	reference wing area
A_{base}	forebody base area
b	wing span
c	wing chord
$C\mu$	momentum coefficient of blowing = $\dot{m}j\ Vj / q_\infty\ A_{ref}$ (A negative $C\mu$ denotes left-hand-side blowing)
C_{nref}	reference yawing moment coefficient = $YM / q_\infty\ A_{ref}\ b$
L	reference length = total length of the model
LF	left forebody vortex (from a pilot's view point)
LW	left wing vortex (from a pilot's view point)
$\dot{m}j$	mass flow rate of the blowing jet
q_∞	free-stream dynamic pressure
RF	right forebody vortex
RW	right wing vortex
V_∞	free-stream velocity
Vj	average exit velocity of the blowing jet
α, AOA	angle of attack
ϕ	angle from the windward meridian
YM	yawing moment

LIST OF FIGURES

SUMMARY

Water tunnel tests were conducted on a NASP-type configuration to evaluate different pneumatic Forebody Vortex Control (FVC) methods. Flow visualization and yawing moment measurements were performed on a 1/50th-scale full configuration model and on a 1/25th-scale forebody model at angles of attack from 0° to 30°. The pneumatic techniques tested included jet blowing (aft and forward) and slot blowing. In general, blowing can be used efficiently to manipulate the forebody vortices, which are naturally symmetric up to $\alpha = 25°$ and asymmetric between 25° and 30° angle of attack. None of the techniques seem to produce noticeable effects at angles of attack below 20°. Results indicate that tangential aft jet blowing is the most promising method for this configuration and angle of attack range. Aft jet blowing produces a yawing moment towards the blowing side and the trends with blowing rate are well-behaved. The size of the nozzle is not the dominant factor in the blowing process; the change in the blowing "momentum", i.e., the product of the mass flow rate and the velocity of the jet, appears to be the important parameter in the water tunnel (incompressible and unchoked flow at the nozzle exit). For this condition, circular nozzles give better results than elliptic nozzles. Forward jet blowing is very unpredictable and sensitive to mass flow rate changes. Slot blowing (with the exception of very low blowing rates) acts as a flow "separator"; it promotes early separation on the blowing side, producing a yawing moment towards the non-blowing side for the $C\mu$ range investigated.

AERODYNAMIC CONTROL OF NASP-TYPE VEHICLES THROUGH VORTEX MANIPULATION

VOLUME I: STATIC WATER TUNNEL TESTS

1.0 INTRODUCTION

One of the most significant and ambitious programs in the aerospace industry in the near future will be the development and eventual flight test of the National Aero-Space Plane (NASP). A high proportion of the technological research now being conducted to support the development of a NASP is concentrated in the hypersonic regime. In addition to excellent hypersonic performance, however, high-quality low-speed flight must also be achieved. Conceivably, configurations optimized for hypersonic flight may experience adverse aerodynamic phenomena which could complicate the effort for achieving good handling qualities during the takeoff and the approach and landing phases, which are dominated by separated and vortex flows. Using larger conventional control effectors to overcome the effects of these adverse phenomena and satisfy low-speed flight quality criteria, such as a larger vertical tail and rudder to counteract forebody vortex generated yawing moments, may result in a weight increment over and above that for hypersonic flight. Using non-conventional vortex control effectors, on the other hand, may potentially satisfy low-speed flight quality criteria with a substantially lower weight penalty. The principal mechanism to accomplish a saving in weight is with fluid amplification, where a small fluidic input, such as surface blowing in the forebody region, results in large output control forces and moments to the airframe by influencing the vortex flow field.

The powerful forebody vortices are one of the main causes of aircraft instabilities at high angles of attack. An effective means of suppressing the instabilities in this flight regime is, therefore, to directly control these vortices. Recent research efforts on fighter-type aircraft indicated that some of the most promising methods for Forebody Vortex Control (FVC) are movable forebody strakes, rotatable nose-tip devices, and blowing on the forebody surface. The use of symmetrically deployed forebody strakes has been shown to be effective in forcing naturally-occurring asymmetric vortices at high angles of attack to be symmetric. The large forebody sideforces and resulting yawing moments at zero sideslip are therefore reduced or eliminated. The use of asymmetrically deployed forebody strakes has been investigated for possible application to controlling the yawing moment[1,2]. Rotatable nose-tip devices are also found to be effective in controlling the forebody flow. These devices are in the forms of a small cylinder attached to the tip[3], machined flats[3], elliptic tips[4], and small vortex generators[5]. Due in part to the concern about strakes and mechanical surfaces interfering with forebody radar operation, various forebody blowing techniques to control the forebody vortex orientations have also been investigated as alternatives to mechanical devices. Two main forms of blowing have been studied: (1) blowing from a localized jet and (2) blowing from a tangential slot[2,6-8]. In either form, blowing was found to be highly effective in controlling the vortex orientation.

The Phase I technical results (water tunnel tests on a similar configuration which are discussed in detail in Ref. 9) show that it is potentially feasible to utilize vortex manipulation with blowing to provide the necessary control forces for a NASP-type configuration at low speeds. The blowing requirement scaled to a full-size NASP based on sub-scale experiments appears to be low, well within practical limits of acquiring the required mass flow through engine bleed or similar sources. The resulting control moments, based on wind tunnel studies of fighter configurations, can be greater than those generated by a typical rudder. The vertical tail area and structural weight may be reduced, and thus, can potentially lead to an improvement in the hypersonic drag performance. It is important to note that at the time the research contract with NASA was awarded, there was no specific design for the NASP yet selected. The models used in the Phase I study and in this investigation are based on drawings of a generic, preliminary NASP configuration provided by the duPont Aerospace Co., Inc. The configuration that now appears from the consolidated NASP design team, however, is significantly different. Even though it still has highly-swept wings, the fuselage has a chined forebody and a blunt nose, so the lateral stability problems will be different. This by no means diminishes the value of this research program; the general results obtained in this study can be applied to similar configurations, such as the High Speed Civil Transport (HSCT) or any other supersonic/hypersonic advanced configuration. Also, the basic fluid mechanics associated with blowing will be better understood. Despite the dissimilarity between the current NASP and the configurations used in this investigation, the models will still be referred to as NASP-type configurations.

The Phase II research effort includes static and dynamic ("free-to-roll") water tunnel tests, static and dynamic wind tunnel tests, and a simulation exercise. It is the intention of this report (Volume I of a Final Report) to only summarize the results of the static water tunnel tests performed on this configuration. The free-to-roll tests in the water tunnel will be reported in Volume III.

2.0 TECHNICAL OBJECTIVES

The principal objectives of the Phase I study were to identify, early-on in the technology development phase of NASP, the potential adverse low-speed aerodynamic phenomena associated with typical NASP configurations (which are optimized for high-speed flight), and to investigate potential solutions to these problems. The idea was to utilize vortex control methods similar to those investigated for fighter aircraft at high angles of attack as an alternative method or an augmentation to conventional methods of aerodynamic control of the National Aero-Space Plane. The Phase I study showed that blowing could be utilized to manipulate the forebody vortices and to create forces that could be used for control. That study, however, was all qualitative and was based on flow visualization. The Phase II study is structured to quantify and optimize those changes, first in a water tunnel test, and finally in a wind tunnel test. The overall goal is to develop the technology of forebody blowing for vortex control to a level where it can be seriously considered as a viable candidate for incorporation into the flight control system of this type of aircraft. Results from the Phase II research are expected to provide high-confidence in the aerodynamic performance benefits to the generic NASP configuration with forebody blowing. Based on this data, a very limited conceptual design exercise will identify potential control

system approaches to incorporate blowing. Finally, a six degree-of-freedom simulation will be performed to evaluate the advantages of the blowing system for take-off and approach and landing tasks, where the angle of attack is sufficiently high to require enhanced controllability.

Water tunnel tests were conducted to evaluate different blowing techniques and to perform a preliminary "screening", so only the best blowing configurations are studied in the wind tunnel test. The specific objectives of the static water tunnel tests are listed below:

1. Evaluate different blowing techniques, such as blowing jets and slots, for controlling the forebody vortices on a highly-slender, highly-swept-wing configuration.

2. Investigate the effects of different parameters on each of the blowing methods. Flow visualization and force measurements will be performed for different blowing nozzle locations and blowing directions, and for different size and shape nozzles and slots. Changes in the flow field and changes in the yawing moment will be recorded.

3. Reduce the test matrix necessary for evaluating FVC by blowing, so only selected configurations are tested in the wind tunnel test.

3.0 EXPERIMENTAL SETUP

The experiments were conducted in the Eidetics 2436 Flow Visualization Water Tunnel. The facility is a continuous flow tunnel with a horizontal test section 0.91 m high x 0.61 m wide x 1.83 m long (36" x 24" x 72"). The test section is a channel constructed of tempered glass which allows both side and planform views. In addition, a downstream transverse window provides an upstream end view without any obstruction. The tunnel speed can be varied from 0 to 30.5 cm/sec (0 to 1 ft/sec). A pressurized dye-injection system was used for flow visualization which was recorded using both a 35-mm camera and a video tape recorder. Two different experiments were performed in the water tunnel, which are described as follows.

3.1 Flow Visualization and Force Measurements on a 1/50th-scale NASP Configuration

A generic 1/50th-scale model of a NASP configuration was tested in the water tunnel in an effort to determine the effects of jet blowing on this configuration (Fig. 1). The forebody of the model has a length-to-base diameter ratio of 6, and is circular in cross-section. The wing is a sharp-edge delta with a 78° sweep. The blowing fluid was supplied by a pressurized canister and metered by a rotameter. Blowing on the left and right sides was turned on or off by fast-acting solenoid valves. Blowing was tangential to the forebody surface in the aft direction, and the two circular nozzles (0.076 cm (0.03" i.d.)) were located at 1.9 cm (0.75") from the tip and at 150° radially from the windward side. A single-component strain gage balance was used to measure the changes in the reference yawing moment (Cn_{ref}) that were produced by blowing. The test setup is seen in Fig. 2. Blowing was applied to the left and right-

hand-sides independently at different rates, and the changes in the vortex flow field and in the reference yawing moment were recorded. The tests were run at a velocity of 12.7 cm/sec (5.0 in/sec), which corresponds to a Reynolds number of 1.1×10^5 per m (3.3×10^4 per ft). The angle of attack was varied from 0° to 30°.

3.2 Flow Visualization and Force Measurements on a 1/25th-scale NASP Forebody

One of the main goals of this research program was to clearly understand the effects of various parameters (size, shape, location of blowing devices) on pneumatic forebody vortex control. In order to get better resolution of the changes produced by blowing, a larger model was desirable. Due to size limitations of the water tunnel test section, it was decided to use only the forebody of a 1/25th-scale NASP configuration. Various blowing techniques were investigated: tangential aft jet blowing, forward jet blowing and slot blowing (leeward and windward directions). Two models, which have exactly the same dimensions, were used for this experiment: forebody model # 1 was provided with nozzles for jet blowing in the aft direction (Fig. 3), and forebody model # 2 was provided with slots and nozzles for jet blowing in the forward direction (Fig. 4).

The first model was used to perform an investigation of nozzle size and shape effects on jet blowing (aft). Three different circular nozzles were tested: 0.152 cm i.d., 0.102 cm i.d., and 0.076 cm i.d. (0.06" i.d., 0.04" i.d., and 0.03" i.d.). Nozzles with horizontal and vertical elliptic cross-sections were also investigated. The size of these nozzles was comparable to the large and medium circular nozzles (0.152 cm and 0.102 cm i.d., respectively). The two blowing ports were located at 3.2 cm (1.25") from the tip and at 150° radially, based on the results of the Phase I experiments.

Forebody model # 2 was used for evaluating forward jet blowing and slot blowing. For the forward jet blowing investigation, the two nozzles (0.076 cm i.d.) were located at 1.0 cm (0.4") from the tip and 150° radially. For the slot blowing study, the slots were cut at 90° radially and had a thickness of 0.013 cm (0.005"). Three different slot lengths were investigated: 1.3 cm, 2.5 cm, and 5.1 cm (0.5", 1", and 2"), starting from a common point 4.4 cm (1.75") from the tip of the model. Two slot blowing techniques were studied: leeward blowing, or upward, and windward (reverse) blowing, or downward.

Flow visualization was performed for an angle of attack range between 0° and 30°. Most of the direct comparisons were conducted at 30° angle of attack and at a speed of 12.7 cm/sec (5.0 in/sec).

4.0 RESULTS AND DISCUSSION

4.1 Static Tests on a 1/50th-scale NASP Configuration

Flow visualization shows that this configuration presents symmetric vortices up to 25° angle of attack, as seen in Fig. 5. At $\alpha = 25°$, the flow becomes slightly asymmetric, and the forebody vortex interacts with the wing vortex causing a portion of the wing vortex near the trailing edge to curve away from the surface. The forebody

vortex asymmetry increases progressively with angle of attack. At $\alpha = 30°$, the forebody flow is strongly asymmetric, and the natural vortex asymmetry favors a right-vortex-high pattern, i.e., the right forebody vortex is farther away from the surface than the left vortex. The left forebody vortex migrates towards the right side underneath the right wing vortex, causing a significant portion of this wing vortex to lift away from the surface.

The effects of blowing at $\alpha = 25°$ can be seen in Fig. 6. Blowing on the left-hand-side with a $C\mu = -0.00069$ (a negative $C\mu$ denotes left-hand-side blowing) makes the right-hand-side vortex move up, farther from the surface. The left vortex is pulled closer to the forebody and the core crosses over the afterbody to the opposite side of the vertical tail. Blowing on the right-hand-side with the same $C\mu$ produces a similar effect, this time making the left vortex move away from the surface. Figures 7 and 8 demonstrate the effect of blowing on the forebody vortex asymmetry at $\alpha = 30°$. Two effects can be observed when blowing underneath the low (left) vortex (Fig. 7). First, the natural right-vortex-high asymmetry is enhanced. Second, the aft portion of the left forebody vortex is lifted from the wing surface and the right vortex is displaced far above the vertical tail, as seen when blowing with a $C\mu = -0.00069$. The interaction between the forebody and the wing vortices is suppressed.

Figure 8 shows the case of blowing underneath the high (right) vortex. Depending on the blowing rate, this blowing technique reduces and eventually reverses the natural forebody vortex asymmetry. Once the right forebody vortex moves sufficiently close to the wing surface, the interaction between the forebody and wing vortices is enhanced and the left vortex crosses over the vertical tail. Increasing the mass flow rate makes the left vortex move far away from the surface, creating a left(blue)-vortex-high asymmetry. Therefore, the forebody-wing vortex interaction on either side of the model can be suppressed or enhanced by inducing, with blowing, a large forebody vortex asymmetry. The wing vortex breakdown asymmetry switches correspondingly when the orientation of the forebody vortex asymmetry is switched by blowing. This indicates that the asymmetry in wing vortex breakdown is dictated to a significant extent by the forebody vortex asymmetry because of the direct interactions of the forebody and wing vortices.

Figure 9 shows a typical output from the one-component water tunnel balance. The procedure for running these force measurements was as follows. The output of the strain gages was zeroed at each angle of attack (tare) with the blowing off. A blowing condition was introduced or modified, and the change in voltage output was recorded. The data were later reduced to moment coefficient form. Results of blowing at different angles of attack can be seen in Fig. 10. Cn_{ref} is the yawing moment at the strain gage location (aft of the trailing edge of the model rather than at a typical model reference C.G. location), explaining the large magnitude of the moment coefficient. Below 20° angle of attack, blowing was not very effective. Strong forebody vortices have to be present in order to get an effect from jet blowing. Trends in yawing moment are predictable and well-behaved with blowing at $\alpha = 20°$ and 25°. Blowing on the left-hand-side pulls the vortex on that side closer to the surface (as seen in the flow visualization), creating a negative (nose-left) yawing moment. The magnitudes of the

changes in moment produced when blowing on the right or on the left sides are similar because the baseline vortex flow field is symmetric. At $\alpha = 30°$, the vortices are asymmetric, as discussed previously. Note that, even though the flow field is asymmetric, the reference yawing moment coefficient for the non-blowing case is zero because Cn_{ref} is zeroed at each angle of attack with blowing off. The magnitude of the Cn_{ref} shown as a function of blowing rate is actually the change in Cn_{ref} produced by blowing. The right vortex is high (resulting in a yawing moment to the left), so blowing on the left side is not as effective as blowing on the right side because a point is reached where the asymmetry cannot be increased anymore. On the other hand, when blowing on the right side, the vortices can be switched completely and a new reversed asymmetry is formed, explaining the larger change in the reference yawing moment when blowing on the right side with the same blowing coefficient. A small magnitude control reversal or instability can be seen at $\alpha = 30°$ when the blowing coefficient is low. This trend was also observed in another study[10], and was attributed to the low exit velocity of the jet (Vj) compared to the free-stream velocity (V_∞).

4.2 Static Tests on a 1/25th-scale NASP Forebody

4.2.1 Jet Blowing (Aft)

Flow visualization performed on the 1/25th-scale forebody model # 1 (equipped with jet nozzles for aft blowing) shows that the baseline flow field is very similar to the 1/50th-scale model (Fig. 11). The vortices are symmetric up to 25° angle of attack, where a slight asymmetry appears. At 30°, the model presents a noticeable asymmetry, with the right-hand-side (red) vortex high.

Once the baseline flow field was clearly understood, aft jet blowing was carefully investigated.

4.2.1.1 Effects of Nozzle Size

This experiment consisted of testing the effect of three different circular nozzles. Flow visualization was performed for each of the nozzles at $\alpha = 30°$, and the results can be seen in Figs. 12 - 17. Figure 12 shows results of blowing under the high (right) vortex with the large nozzle (0.152 cm i.d.). The blowing jet is made visible by means of yellow dye. Blowing is capable of making the forebody vortices symmetric at high $C\mu$, but it is not powerful enough to switch the vortex pattern. The medium and small nozzles (0.102 and 0.076 cm i.d., respectively) are capable of switching the vortex asymmetry when blowing with the same mass flow rate (corresponding to a larger $C\mu$ because of the larger Vj), as seen in Figs. 14 and 16. Blowing under the low vortex (left) enhances the natural asymmetry, again with better results for the medium and small nozzles (Figs. 13, 15 and 17).

Force measurements were performed simultaneously with flow visualization. Figure 18a shows the reference yawing moment (Cn_{ref}) with blowing coefficient for the three different nozzle sizes. Due to the asymmetry in the baseline flow, a stronger effect is seen when blowing on the right-hand-side. Apparently, nozzle size does not

have a strong effect on jet blowing, even though the medium nozzle appears to give the best performance when blowing on the left-hand-side at low $C\mu$. The data in that $C\mu$ range, however, is not sufficient to strongly demonstrate any size effect. When blowing on the right side (positive $C\mu$), the curves for the three nozzle sizes all fall upon each other indicating that the magnitude of the blowing effect is dependent on the jet momentum coefficient, i.e., the product between the mass flow rate ($\dot{m}j$) and the exit velocity of the jet (Vj). This argument is clearly supported by the next two figures. Since the flow at the nozzle exit is not choked, the reduction in area produces an increase in the jet velocity Vj for the same mass flow rate. Figure 18b shows that at the same Vj, the medium nozzle produces larger changes in yawing moment than the small nozzle when the non-dimensionalized Vj (Vj/V_∞) is greater than 5. However, the mass flow rate for the medium nozzle is larger than for the small nozzle for the same Vj. Figure 18c shows that the smallest nozzle is the most effective when blowing on the right-hand-side with the same mass flow rate, but the jet velocity for this nozzle is the highest. Therefore, the important parameter for jet blowing in the water tunnel test (incompressible and unchoked flow) is the momentum of the blowing jet. Yawing moment changes can be produced by increasing or decreasing either the mass flow rate or the velocity of the jet.

Figure 18b reveals another important fact. It seems that there is a "threshold" velocity (Vj/V_∞ between 3 and 4) that needs to be exceeded if yawing moment changes are expected. If the mass flow rate supply is limited, the only way to get higher velocities is by decreasing the nozzle size. That explains why the medium and small nozzles appear to work better than the large nozzle in the flow visualization study and in the force measurements. The jet velocity at the exit of the large nozzle was too low and limitations in the water tunnel blowing supply system did not allow for further increases in mass flow rate.

The results from this study reveal some of the interesting characteristics of jet blowing in the water tunnel, i.e., incompressible and unchoked flow. The wind tunnel test on the same configuration will be extremely important for assessing differences, if any, in the blowing mechanism. Conditions are different in the wind tunnel because the nozzle flow is choked and Vj remains constant, i. e. changes in mass flow rate results in proportional changes in blowing coefficient.

Tangential aft jet blowing is well behaved for both the medium and the small nozzles. Figure 19 shows the change in yawing moment produced by the small nozzle (0.076 cm i.d.) at different angles of attack. The trends are similar to the 1/50th-scale model, i. e. blowing is not effective at angles of attack below 20°. At α = 25° and 30°, blowing under the high vortex (right) is more efficient than blowing on the left side because of the natural asymmetry. Throughout the whole investigation, force measurements correlated very well with flow visualization.

4.2.1.2 Effects of Nozzle Shape

Elliptic nozzles, obtained from the large and medium size tubes (0.152 and 0.102 cm i.d.), were tested at α = 30°, in an effort to improve the effectiveness of the blowing/mixing process, so lower flow rates can be used. For the large size, both

horizontal and vertical elliptic nozzles were studied. Size was a constraint factor in investigating small elliptic nozzles, as they are extremely complicated to machine. It has been demonstrated that the shape of a nozzle can have a significant effect on the mixing process. Results from Ref. 11 show that for an elliptic jet with a 2-to-1 aspect ratio, the mixing rate is 3 to 8 times that of an equivalent circular shape. In this investigation, however, the results show a decrease in effect for the large elliptic nozzles (Figs. 20 and 21). The horizontal elliptic nozzle (Fig. 21) seems to perform slightly better than the vertical nozzle, i.e., it is capable of making the vortex pattern symmetric. The medium elliptic nozzle was also less effective than the circular nozzle (Figs. 22 and 23), and presented almost no change when blowing under the low vortex at low $C\mu$, as seen in Fig. 23. Figure 24 shows a side by side comparison between circular and elliptic nozzles. Starting with the natural right-vortex-high asymmetry, blowing with the large circular nozzle produces a symmetric vortex pattern, while blowing with the medium circular nozzle reverses the asymmetry. The right-hand-side of the figure reveals that the asymmetry cannot be switched when blowing with elliptic nozzles at the same $C\mu$.

Force measurements confirm the flow visualization results. As seen in Fig. 25a, the large circular nozzle is better than both elliptic nozzles, except when blowing under the low vortex, where the horizontal elliptic nozzle produces a larger nose-left yawing moment. The medium circular nozzle (0.102 cm i.d.) is clearly better than the elliptic nozzle with the same size (Fig. 25b).

4.2.2 Jet Blowing (Forward)

The forebody model # 2 was used for this test. Even though the geometry and dimensions are exactly the same as those of the model used for the previous study, it presented a different natural asymmetry. The baseline flow is again symmetric up to 25° angle of attack, but the natural asymmetry observed at $\alpha = 30°$ presented a left-(blue)-vortex-high pattern (Fig. 26).

Flow visualization results reveal again that blowing is not effective at angles of attack below 20°. Figure 27 presents the effect of blowing on the right-hand-side at 20° angle of attack, and some changes in the flow field can be observed. Starting from a symmetric vortex pattern, forward jet blowing at low $C\mu$ seems to promote an early separation on the blowing side. When $C\mu = 0.0003$, the vortex pattern becomes symmetric again and blowing at higher $C\mu$ produces the reverse effect, i.e., the separation on the blowing side is delayed and a left (blue)-vortex-high asymmetry is created. This agrees with the results of a generic fighter reported in Ref. 2, in which a yawing moment pointing towards the non-blowing side was generated at low blowing rates. At $\alpha = 25°$, and especially at $\alpha = 30°$, the trends are the same but forward jet blowing is really unpredictable (Figs. 28, 29 and 30). Any small change in blowing coefficient produces a drastic change in the vortex pattern, with the larger effects occurring when blowing on the left-hand-side (Fig. 30) because of the original baseline asymmetry.

Figure 31 shows the yawing moment coefficient as a function of Cμ for different angles of attack. For $\alpha = 25°$ and 30°, the changes are very non-linear and very unpredictable, with control reversals and enormous moment changes with minimum changes in blowing coefficient. The proximity of the nozzles to the tip of the model probably causes any perturbance added to the flow field to be easily amplified along the forebody, producing large yawing moment fluctuations. Figure 32 presents a direct comparison between aft and forward jet blowing at $\alpha = 30°$. Aft blowing produces larger moment changes than forward jet blowing when blowing on the right-hand side and those changes are well-behaved with increased blowing rate. The magnitudes of the changes produced by forward blowing are larger when blowing on the left-hand-side, denoting again the importance of the initial asymmetry on the blowing process; however, changes are erratic and not well-behaved with blowing rate increases.

4.2.3 Tangential Slot Blowing

4.2.3.1 Leeward Slot Blowing

The effects of slot blowing (short slot, 1.3 cm long) can be seen in Figs. 33 - 39. At low angles of attack ($\alpha = 10°$, Fig. 33), slot blowing does not have a strong effect on the flow field. Starting at $\alpha = 20°$ (Figs. 34 and 35), slot blowing produces large changes in the vortex pattern. These changes are, however, significantly different than the changes produced by jet blowing. Also, the results from this experiment do not seem to agree with results obtained in other studies[6, 10]. In those studies, it was reported that slot blowing operates on the principle of circulation control. Blowing energizes the flow near the surface so that it is more capable of overcoming the adverse pressure gradient. The separation on the blowing side is therefore delayed, and the resultant changes in vortex strength and trajectory determine the eventual flow asymmetry. In the experiments performed on this NASP-type configuration, blowing on the right-hand-side pushes the vortex on that same side away from the surface, inducing a negative (nose-left) yawing moment, while blowing on the left-hand-side has the opposite effect. Besides the difference in configurations, other factors could be affecting the results of this investigation, such as angle of attack range and mass flow rate differences. While the angle of attack during these experiments did not exceed 30°, most of the FVC studies are focused on fighter configurations at higher angles of attack.

The possibility that the mass flow rate used during the slot blowing investigation was too high could also be a valid explanation for the results obtained. It can be seen in most of the figures that the blowing fluid existing the slot is injected into the free-stream flow without interacting directly with the forebody vortices. The blowing "sheet" may actually be acting as a flow "separator", promoting an early separation on the blowing side, rather than delaying it. This is supported by some of the results from Ref. 10, where water tunnel tests were performed on an F/A-18 configuration. Blowing from a slot located close to the forebody tip produced a yawing moment towards the blowing side at low and moderate blowing rates, but at high Cμ values, the sign of the yawing moment was reversed. For this NASP-type configuration, not much effect is seen when blowing at low Cμ. The trends observed at 20° angle of attack are similar to those at $\alpha = 25°$ (Figs. 36 and 37) and at $\alpha = 30°$ (Figs. 38 and 39).

Figure 40 shows the changes in reference yawing moment with Cμ. Force measurements were performed in the same manner as for the jet blowing study: the

balance was zeroed at each angle of attack with the blowing off, and then blowing was initiated. Again, despite the fact that the flow is naturally asymmetric at $\alpha = 30°$, the reference yawing moment for the non-blowing case will be zero. Throughout the experiments, the yawing moment change produced by the natural asymmetries was never more than 20% of the maximum change in yawing moment produced by the different blowing techniques. Blowing on the right side produces a negative (nose-left) yawing moment and the pattern is well-behaved at all angles of attack. Sign reversals can be observed when blowing at low $C\mu$, especially on the left-hand-side. This reinforces the conclusions from the flow visualization study: slot blowing on this configuration and at these conditions is not very effective at low $C\mu$; large yawing moment changes towards the non-blowing side can be produced at higher $C\mu$. Results are similar for the 2.5 cm long slot (Figs. 41 - 47), and for the 5.1 cm long slot (Figs. 48 - 54). These two slots, however, produce more irregular changes than the short slot. Figures 47 and 54 (force measurements for the 2.5 cm and the 5.1 cm long slots, respectively) reveal that first of all, the magnitude of the yawing moment change decreases with slot length. Also, not much effect is seen when blowing on the left side. It was shown in the aft jet blowing study that jet velocity is a very important parameter in the water tunnel test, so it can be concluded that the higher Vj obtained with the 1.3 cm long slot probably is responsible for the better performance. Figure 55 presents a direct comparison of the yawing moment changes produced by the three different slots at various angles of attack.

4.2.3.2 Windward (Reverse) Slot Blowing

Flow visualization for this slot blowing technique ("downward" blowing, i.e., towards the windward side) revealed promising results at low angles of attack. At $\alpha = 5°$, 10° and 15°, shown in Figs. 56, 57 and 58, respectively, windward slot blowing produced noticeable changes in the flow field characteristics and the flow separation. However, force measurements were performed later and no change in reference yawing moment was found. This indicates that the change in separation and in the pressure distribution at low angles of attack is not enough to produce a noticeable change in yawing moment. Also, since vortices are not present at low angles of attack, the local effect produced by blowing does not propagate. Reverse slot blowing is not as effective at changing the vortex flow field as regular slot blowing even at higher angles of attack, as seen in Figs. 59 and 60. Force measurements (Fig. 61) show that the effects produced are smaller in magnitude, and at $\alpha = 30°$ (Fig. 61c), the effects are reversed in sign compared to regular slot blowing, i.e., blowing on the left side produces a negative (nose-left) yawing moment.

5.0 CONCLUSIONS

Different blowing techniques for controlling the forebody vortices of a NASP-type configuration were investigated. Extensive flow visualization and yawing moment measurements were performed in the Eidetics 2 x 3 foot water tunnel. The baseline flow on this configuration presents symmetric vortices up to $\alpha = 25°$; between 25° and 30° angle of attack, the forebody vortices are asymmetric. The orientation of the natural asymmetry depends on the model; the two forebody models, despite having the same geometry and dimensions, show different natural asymmetries at 30° angle of attack. In general, blowing can be used efficiently to produce changes in yawing moment between 20° and 30° angle of attack. However, each of the blowing methods tested has unique effects on the flow field. Figure 62 presents a summary of the reference yawing moment changes that can be obtained with jet blowing (aft and forward) and with slot blowing.

For each of the blowing techniques, the following conclusions can be made:

1. Jet blowing (aft) produces similar results on both models, the 1/50th-scale full configuration and the 1/25th-scale forebody model. Blowing on the right-hand-side produces a positive (nose-right) yawing moment for angles of attack greater that 20°. The size of the blowing nozzles in not the dominant factor, i.e., the effects produced by blowing can be modified by introducing changes in the jet velocity or in the mass flow rate of the jet. For this study, circular nozzles proved better than elliptic nozzles.

2. Jet blowing (forward) produces large changes in the flow field; however, these changes and the trends are non-linear and unpredictable. A yawing moment towards the non-blowing side is produced at low $C\mu$, and the effect is reversed at higher $C\mu$, in agreement with previous studies.

3. Slot blowing towards the leeward side gave good results; however, the trends and effects are opposite to jet blowing. Blowing on the right-hand-side promotes early separation on that side, producing a negative or nose-left yawing moment. The short slot (1.3 cm long) seems to be the most efficient, probably because of the higher Vj obtained. Reverse (downward) slot blowing did not produce a change in the reference yawing moment at low angles of attack despite a noticeable change in the flow field.

It seems that aft jet blowing is the best technique for this configuration. The results are consistent with other data on generic fighter configurations, trends are well-behaved and the mass flow rate requirements seem to be within realistic limits. Jet blowing will be tested in detail in the wind tunnel test performed on a similar configuration as part of this contract. Additional data will be obtained that will help to better understand this method of control and to assess Reynolds number effects, if any.

6.0 ACKNOWLEDGMENTS

Support for this work is provided by NASA-Ames Research Center under contract NAS2-13196. The technical monitor is Mr. Larry Meyn of the Fixed-Wing Aerodynamics Branch. We would also like to acknowledge the efforts of Mr. Bert Ayers for his consistent high quality work in constructing the water tunnel models.

7.0 REFERENCES

1. Murri, D.G. and Rao, D.M., "Exploratory Studies of Actuated Forebody Strakes for Yaw Control at High Angles of Attack," AIAA-87-2557-CP, August 1987.

2. Malcolm, G.N., Ng, T.T., Lewis, L.C., and Murri, D.G., "Development of Non-Conventional Control Methods for High Angle of Attack Flight Using Vortex Manipulation," AIAA-89-2192, July 31-August 1-2, 1989.

3. Zilliac, G., Degani, D., and M. Tobak, "Asymmetric Vortices on a Slender Body of Revolution," AIAA-90-0388, January 1990.

4. Moskovitz, C., Hall, R., and DeJarnette, F., "Experimental Investigation of a New Device to Control the Asymmetric Flowfield on Forebodies at Large Angles of Attack," AIAA-90-0068, January 1990.

5. Ng, T. T. and Malcolm, G. N., "Aerodynamic Control Using Forebody Strakes," AIAA-91-0618, January 1991.

6. Tavella, D.A., Schiff, L.B., and Cummings, R.M., "Pneumatic Vortical Flow Control at High Angles of Attack," AIM-90-0098, January 1990.

7. Rosen, B. and Davis, W., "Numerical Study of Asymmetric Air Injection to Control High Angle-of-Attack Forebody Vortices on the X-29 Aircraft," AIAA-90-3004, August 1990.

8. Ng, T. T. and Malcolm, G. N., "Aerodynamic Control Using Forebody Blowing and Suction," AIAA-91-0619, January 1991.

9. Ng, T. T., "Aerodynamic Control of NASP-type Vehicles Through Vortex Manipulation", Eidetics International TR89-009, 1989.

10. Ng, T. T., Suárez, C. J., Malcolm, G.N., "Forebody Vortex Control Using Slot Blowing," AIAA-91-3254, September 1991.

11. Ho, C. M., Gutmark, E., "Vortex Induction and Mass Entrainment in a Small-Aspect Ratio Elliptic Jet", Journal of Fluid Dynamics, Vol. 179, 1987.

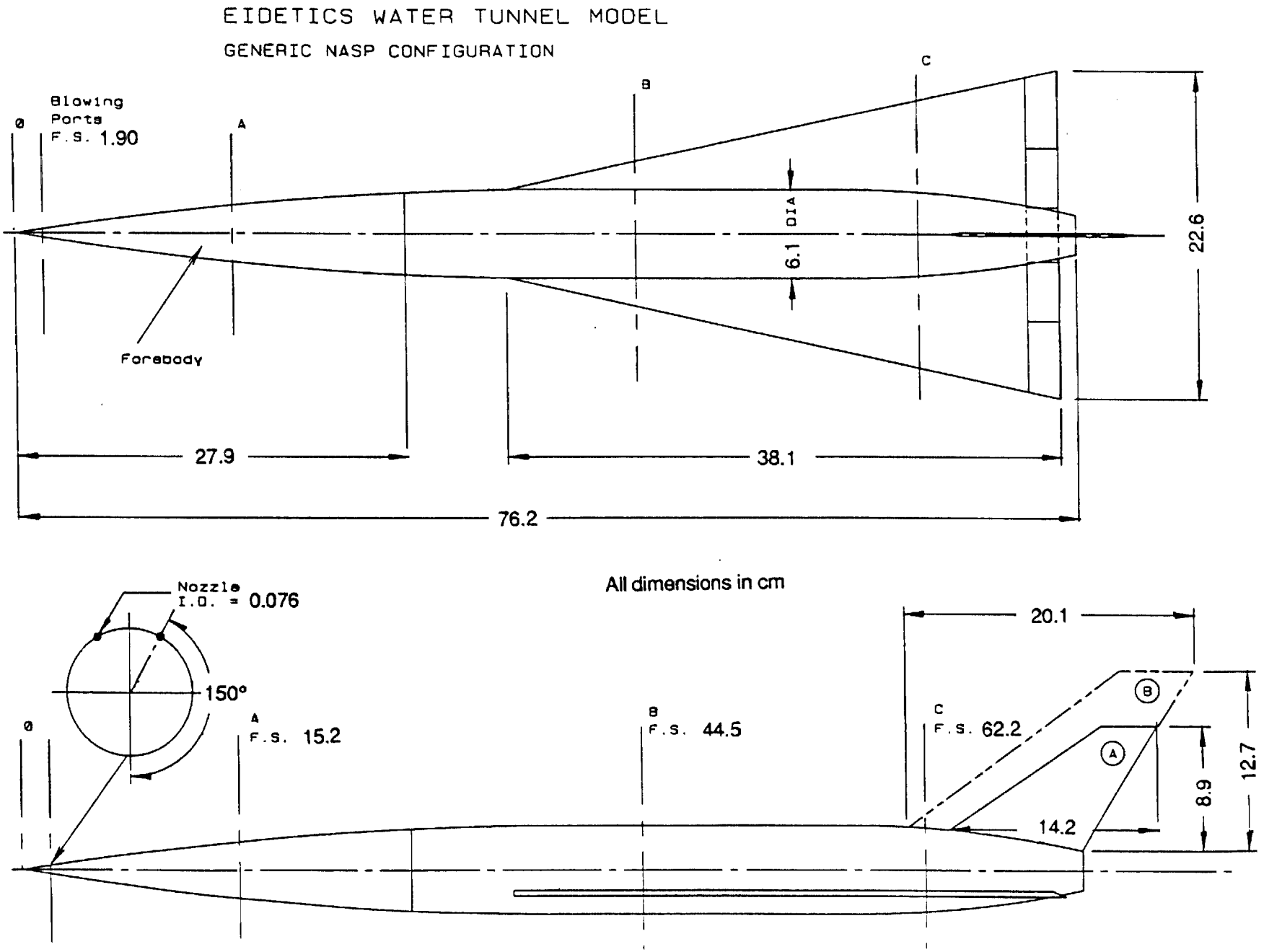

Figure 1 - 1/50th-scale Water Tunnel Model - General Dimensions

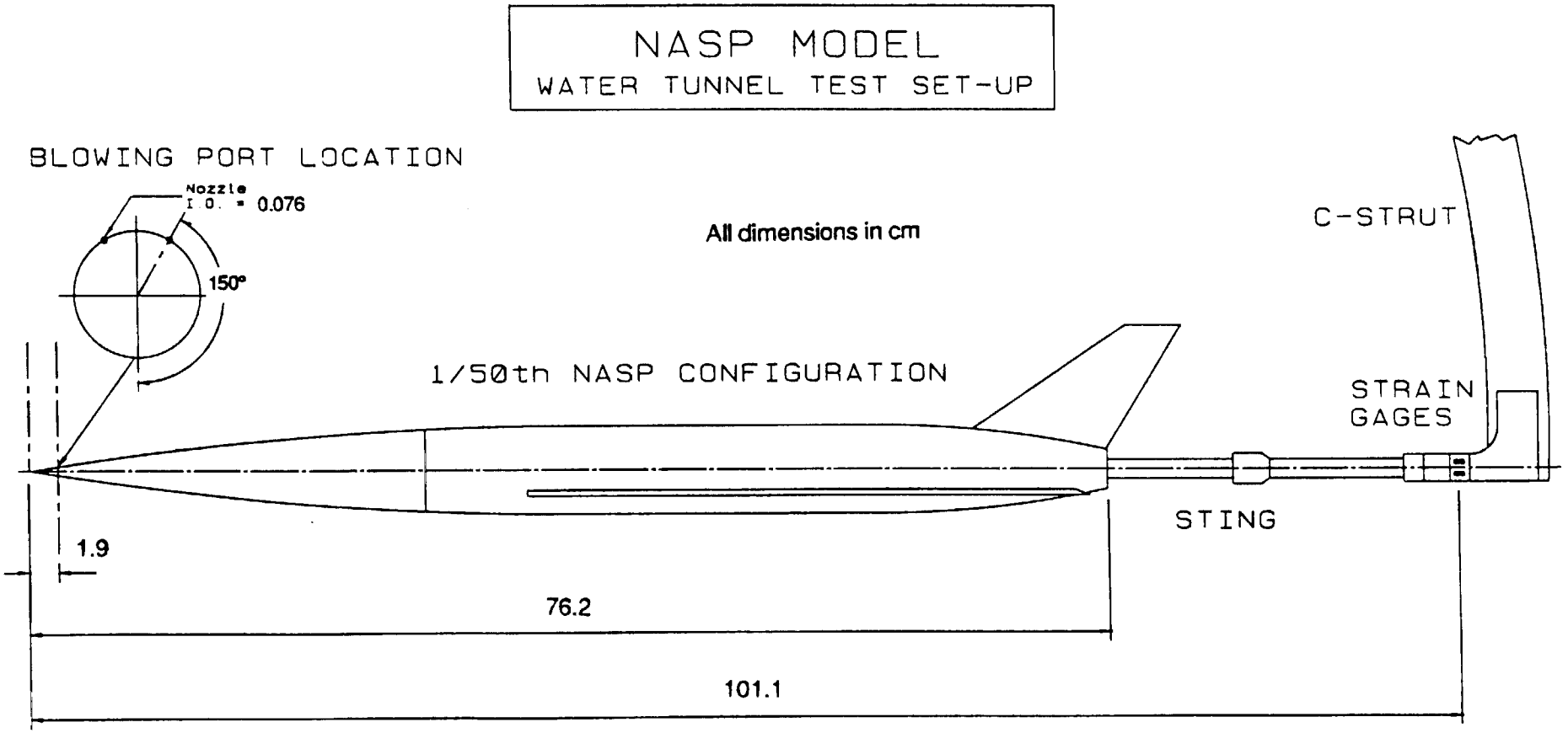

Figure 2 - 1/50th-scale Water Tunnel Model - Experimental Setup

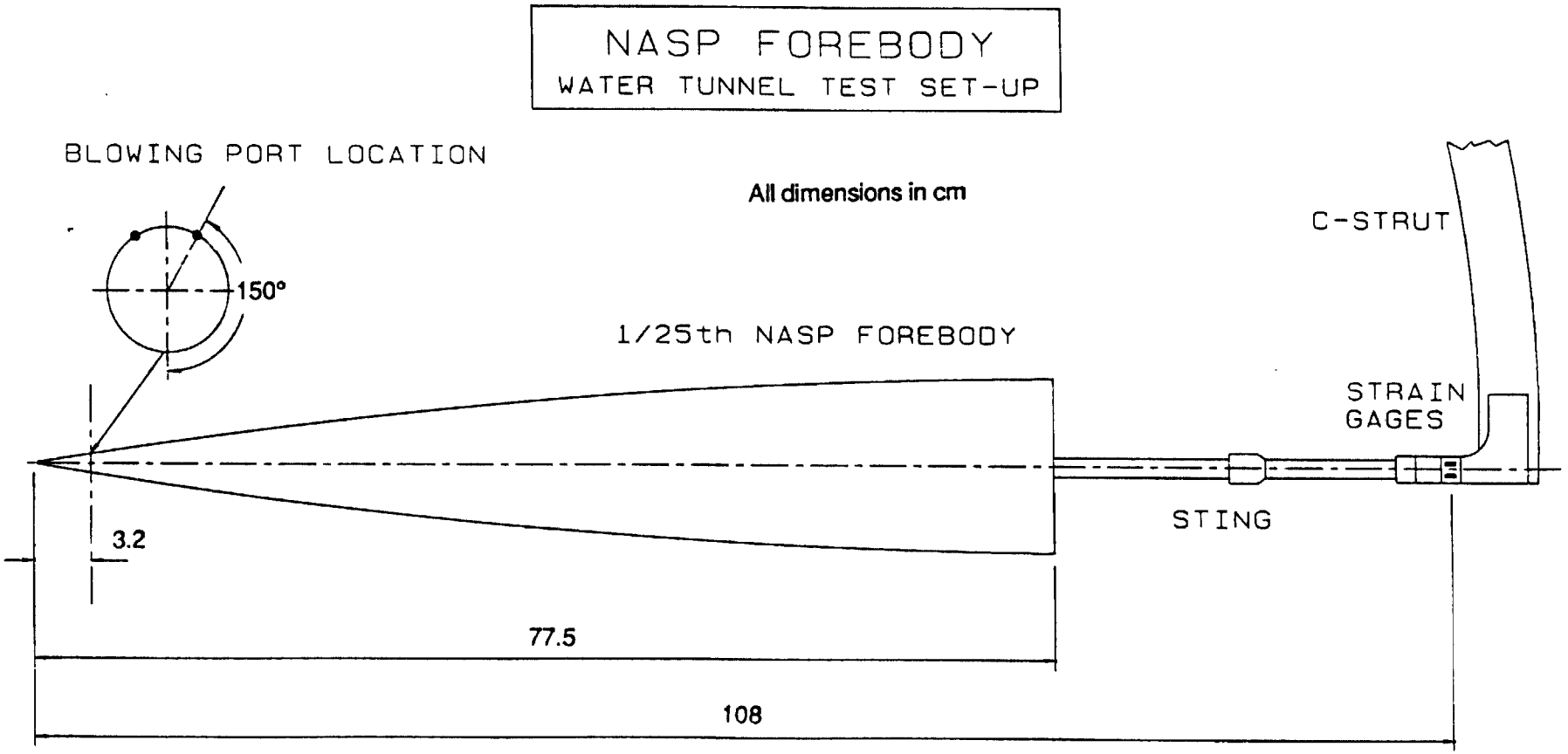

Figure 3 - 1/25th-scale Forebody Model # 1
General Dimensions and Setup

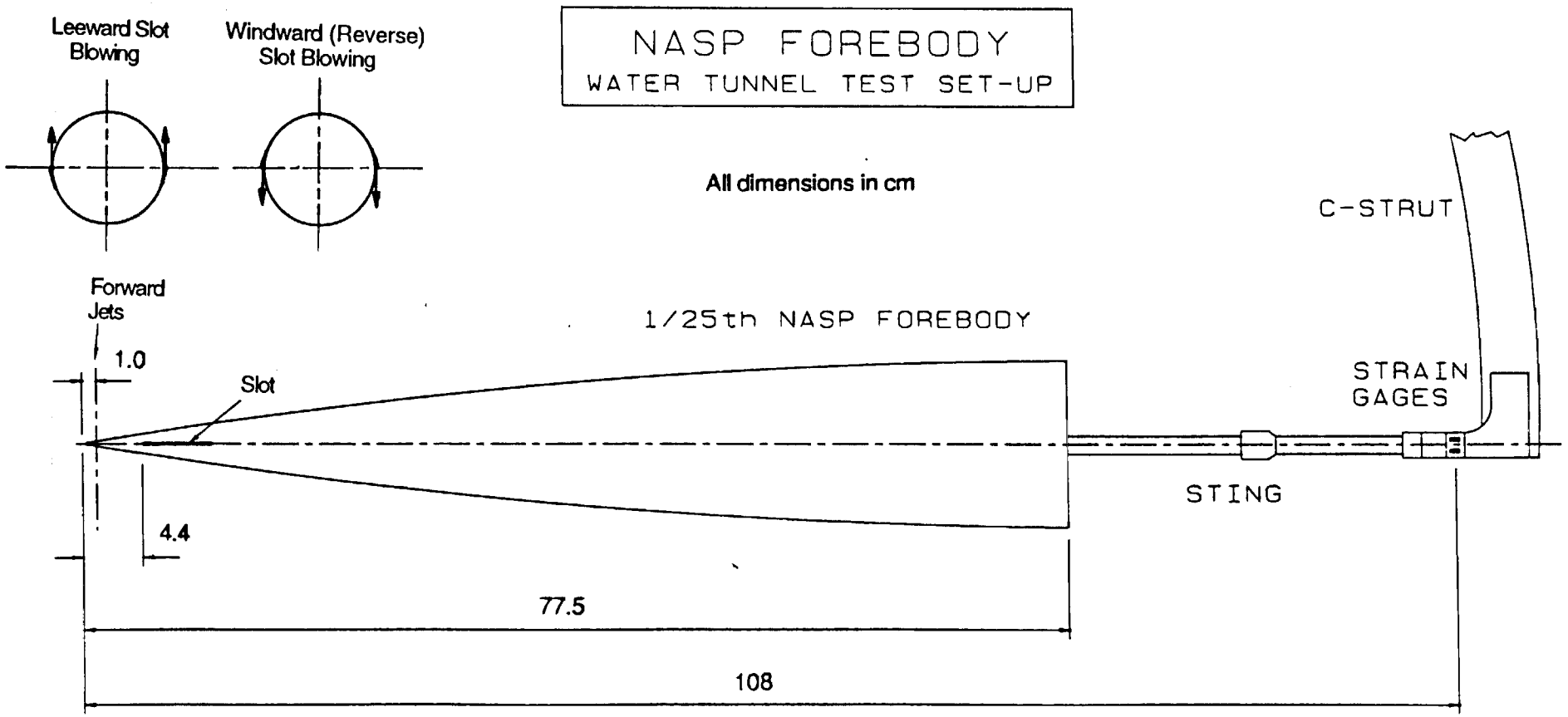

Figure 4 - 1/25th-scale Forebody Model # 2
General Dimensions and Setup

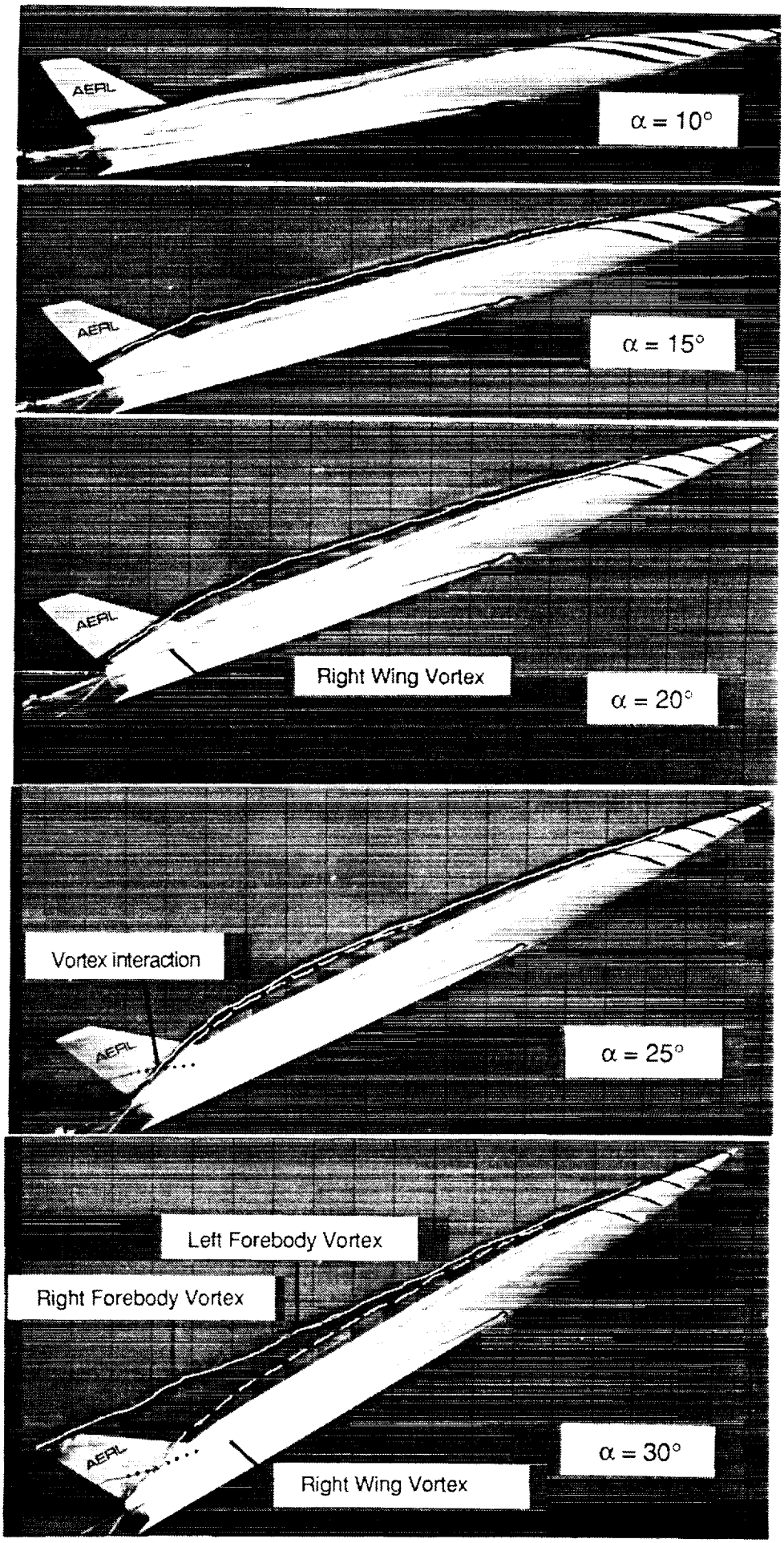

Figure 5 - Effect of Angle of Attack (1/50th-scale Model)

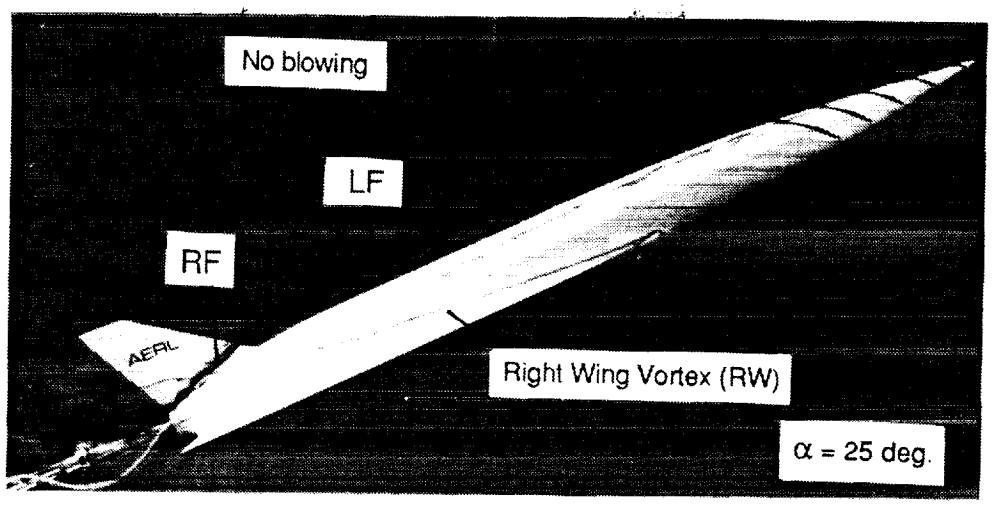

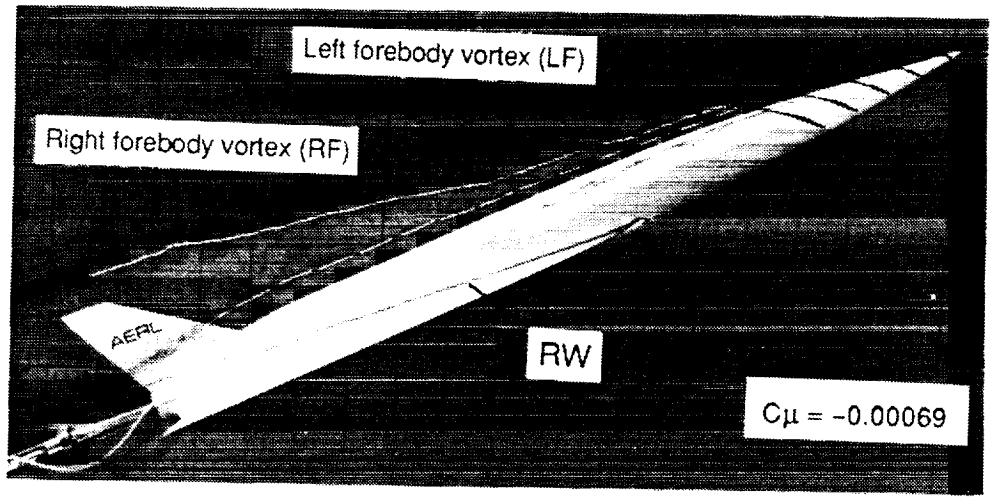

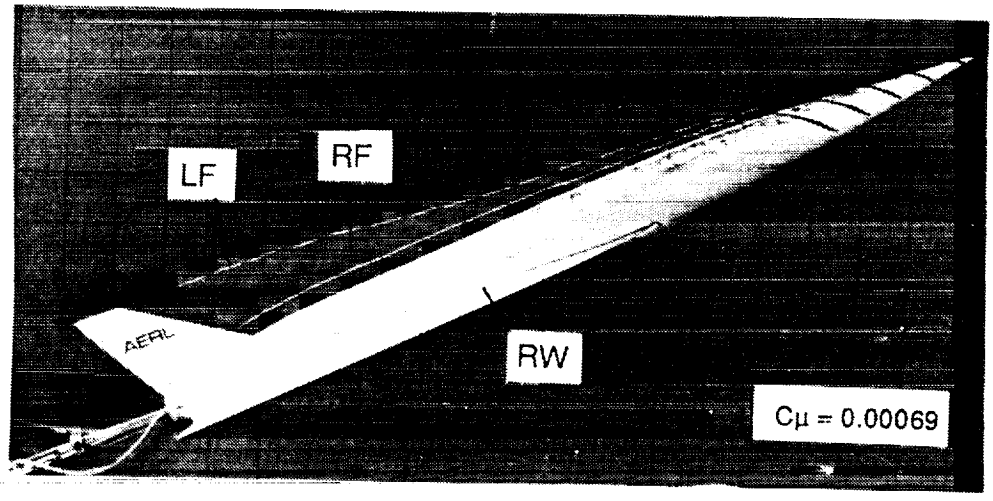

Figure 6 - Effect of Jet Blowing, $\alpha = 25^{\circ}$

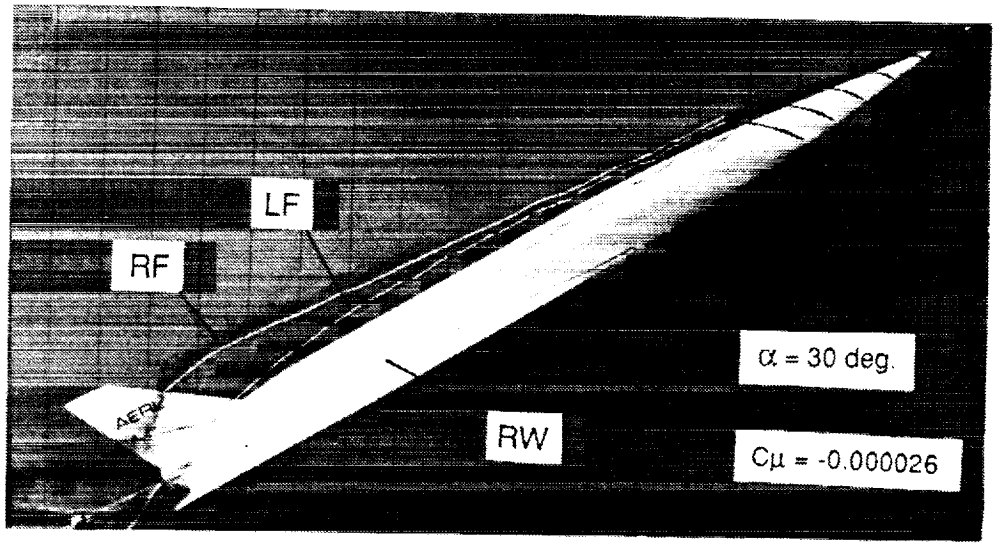

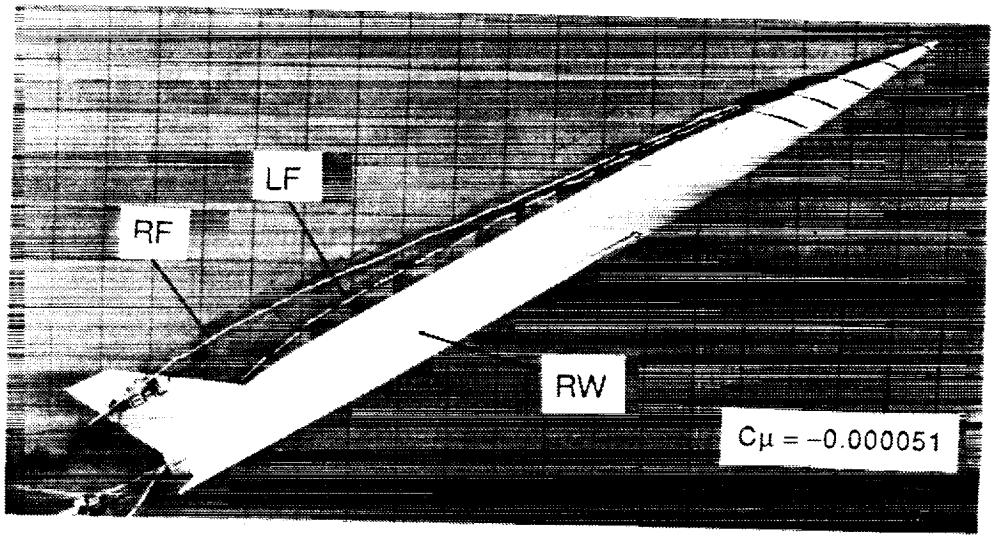

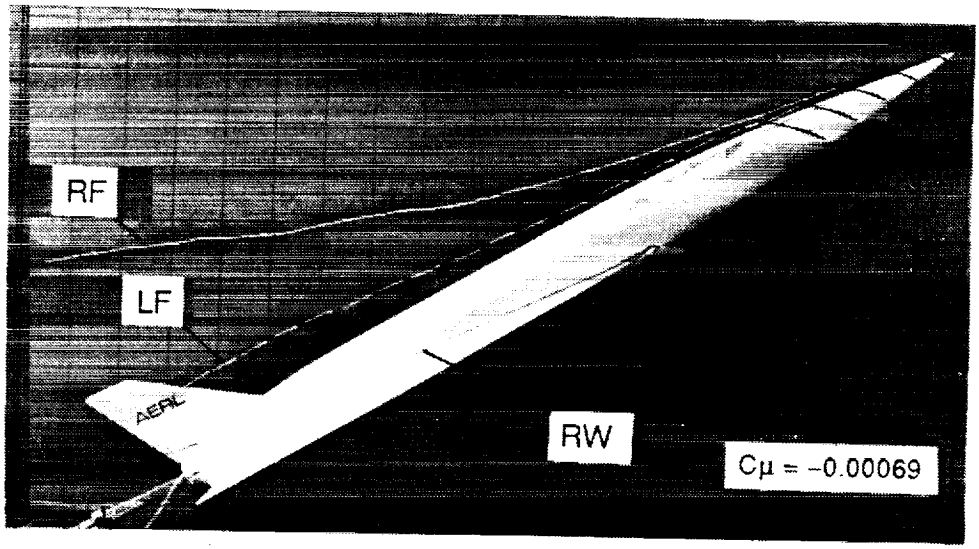

Figure 7 - Effect of Jet Blowing, Left Side, $\alpha = 30°$

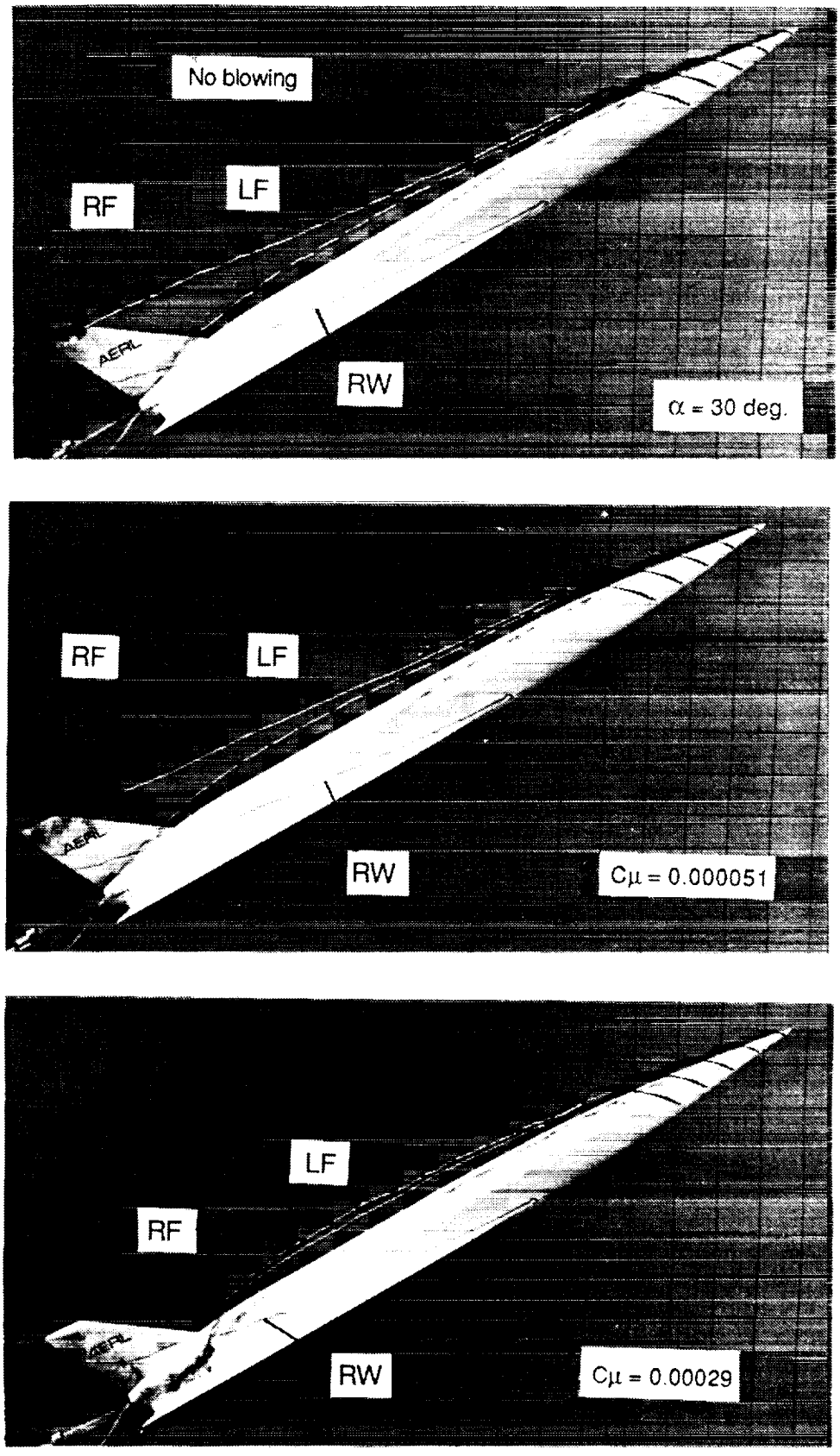

Figure 8 - Effect of Jet Blowing, Right Side, $\alpha = 30^{\circ}$

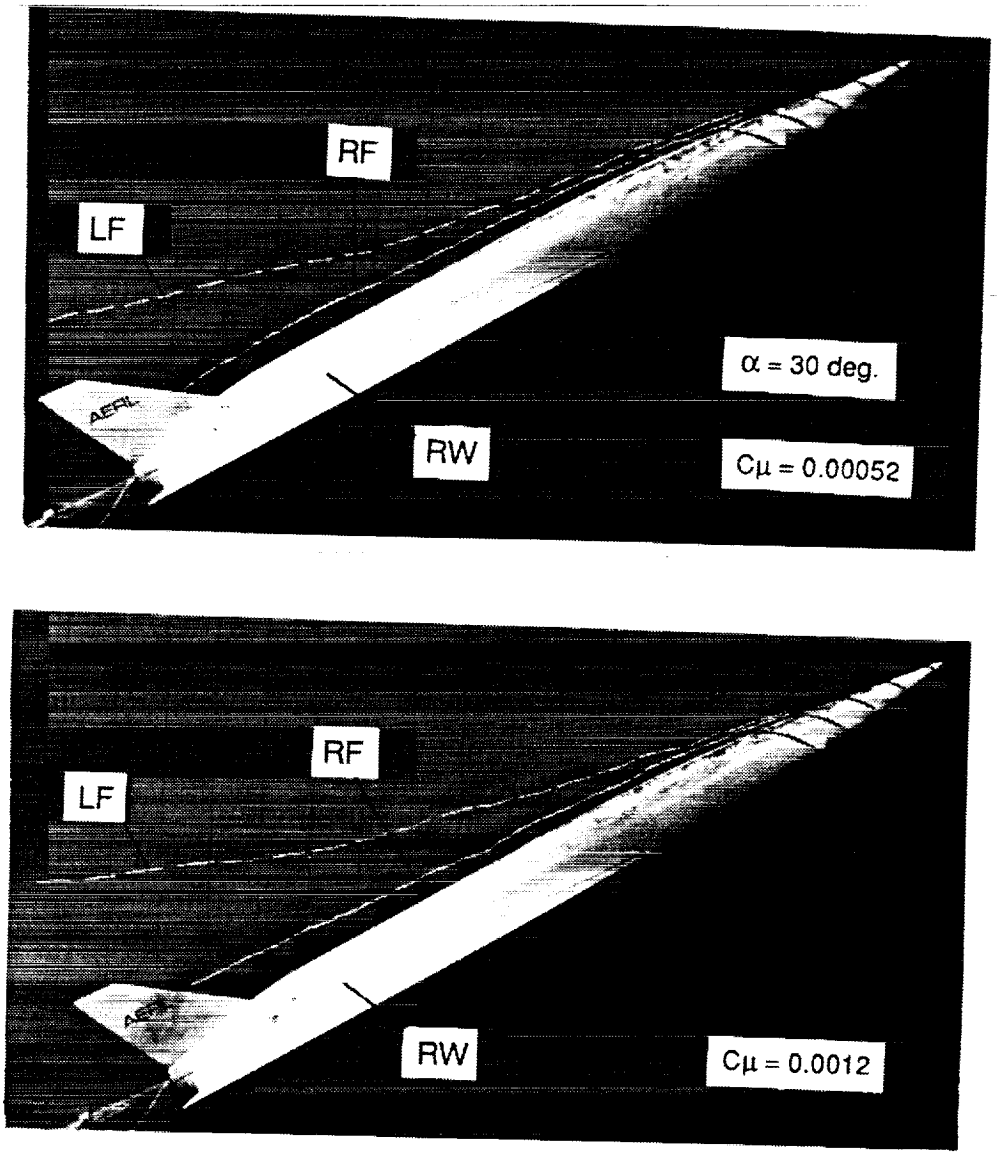

Figure 8 - Concluded

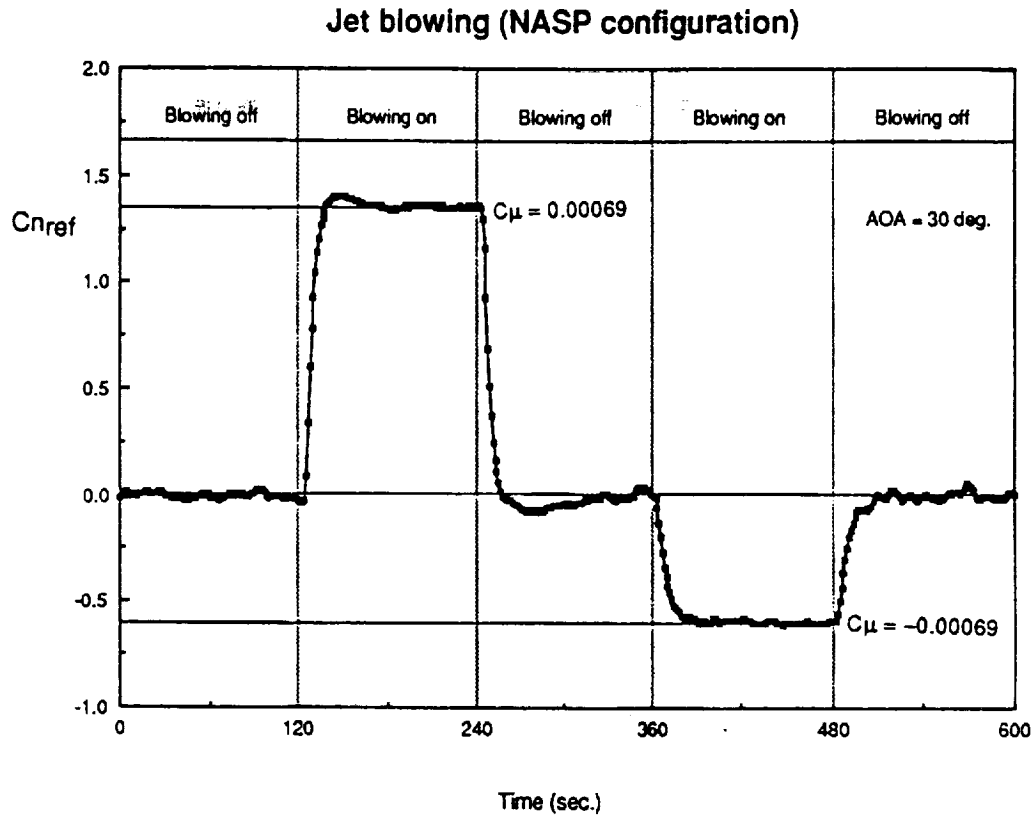

Figure 9 - Example of One-Component Water Tunnel Balance Output

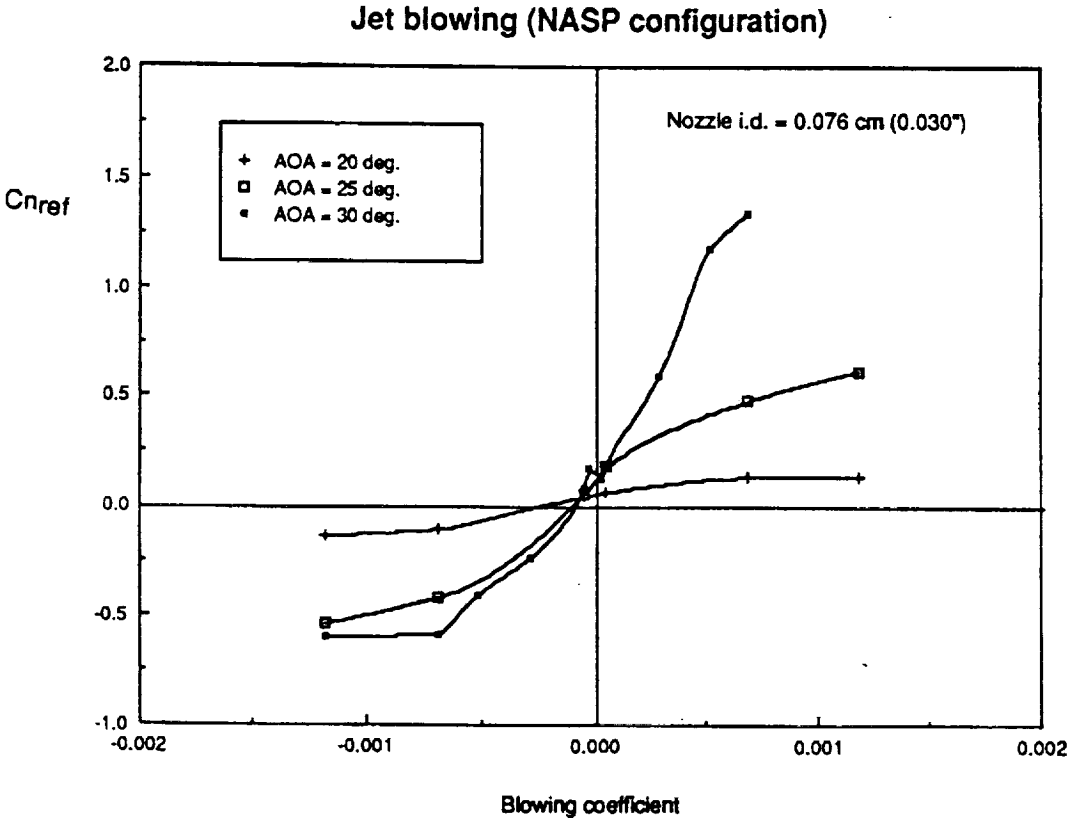

Figure 10 - Change in Reference Yawing Moment Produced by Jet Blowing, 1/50th-scale Model

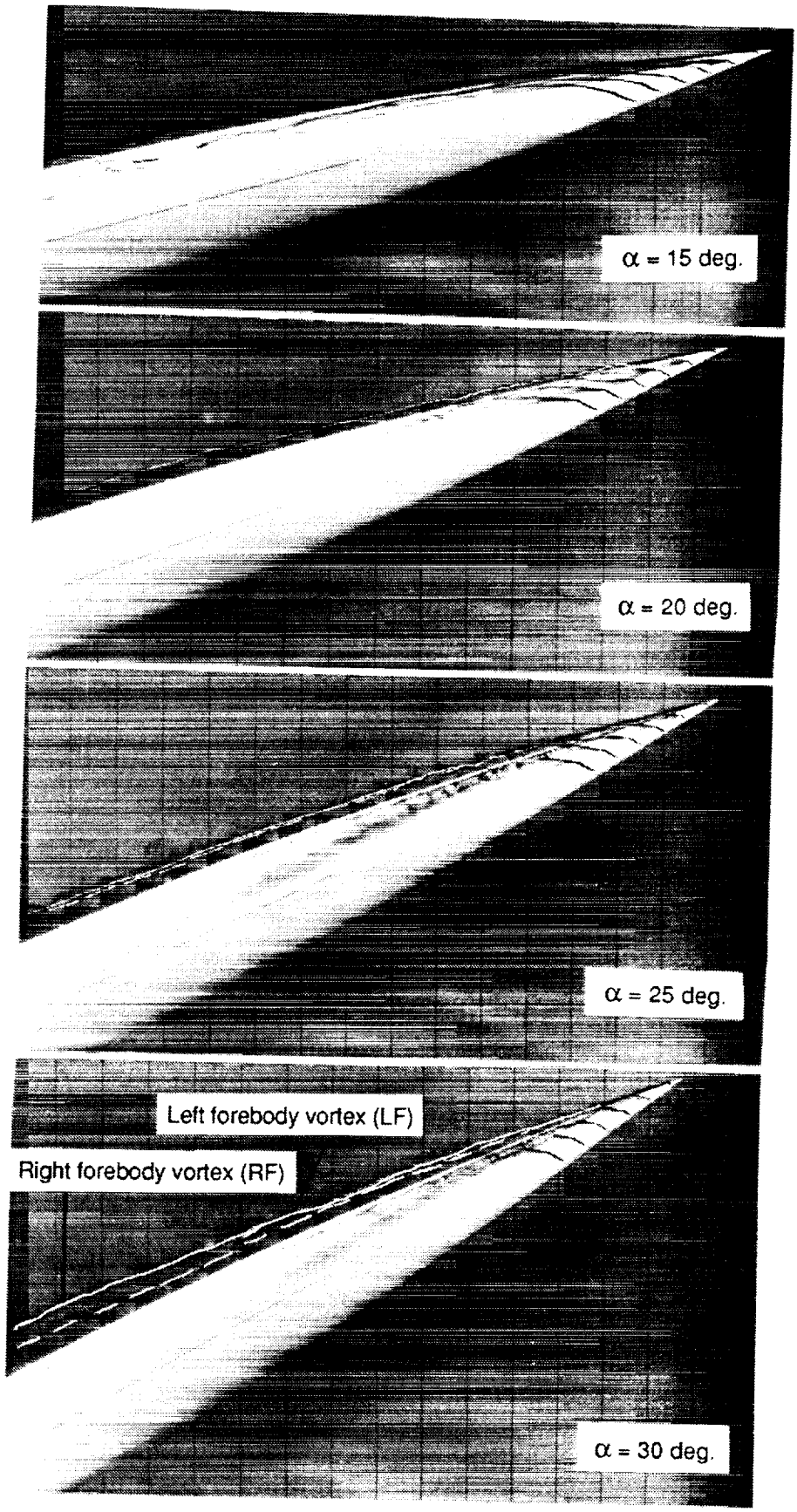

Figure 11 - Effect of Angle of Attack (1/25th-scale Forebody Model # 1)

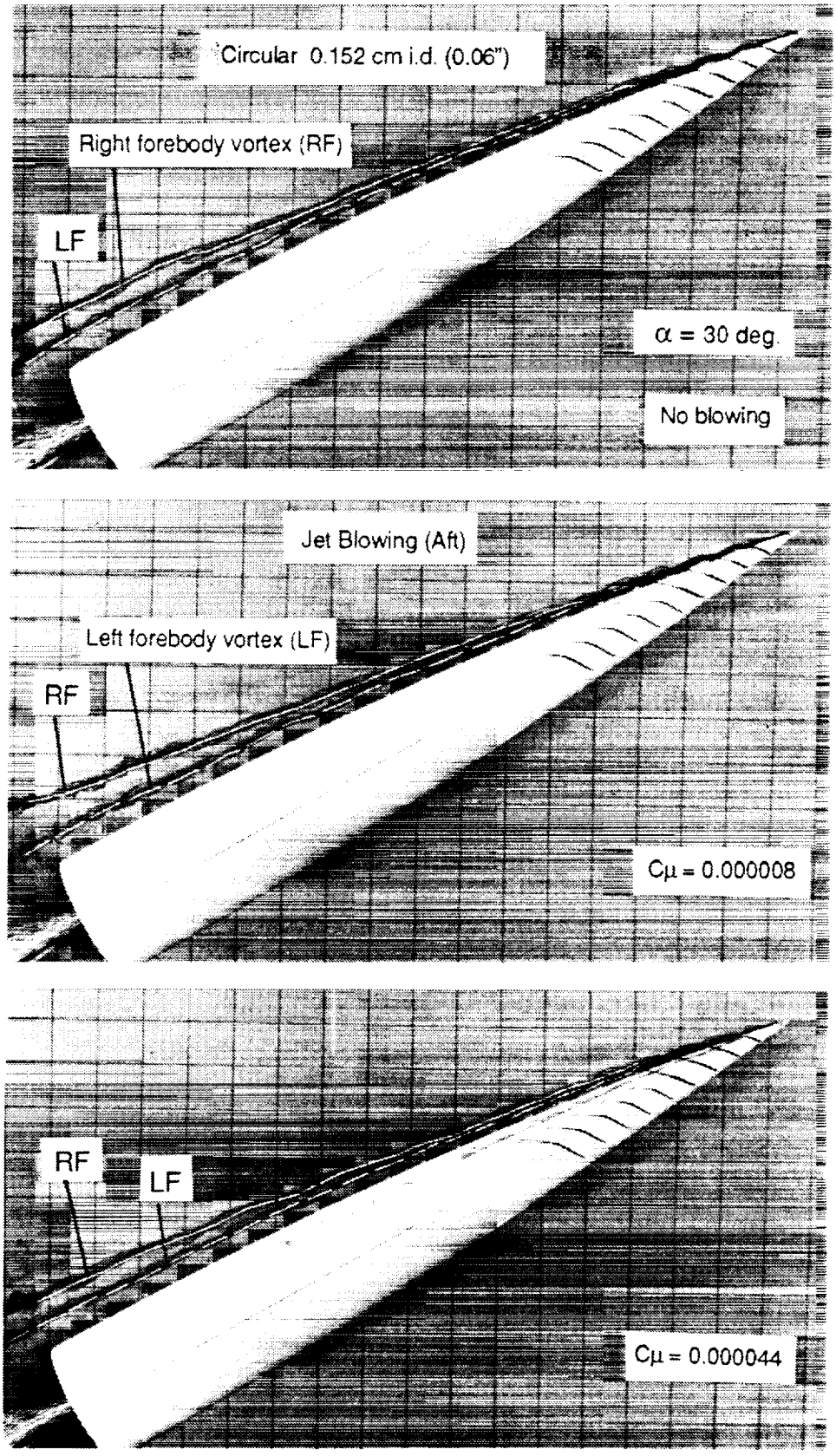

Figure 12 - Effect of Jet Blowing (Aft, Right Side, Forebody Model # 1) Circular Nozzle, 0.152 cm i.d., $\alpha = 30^{\circ}$

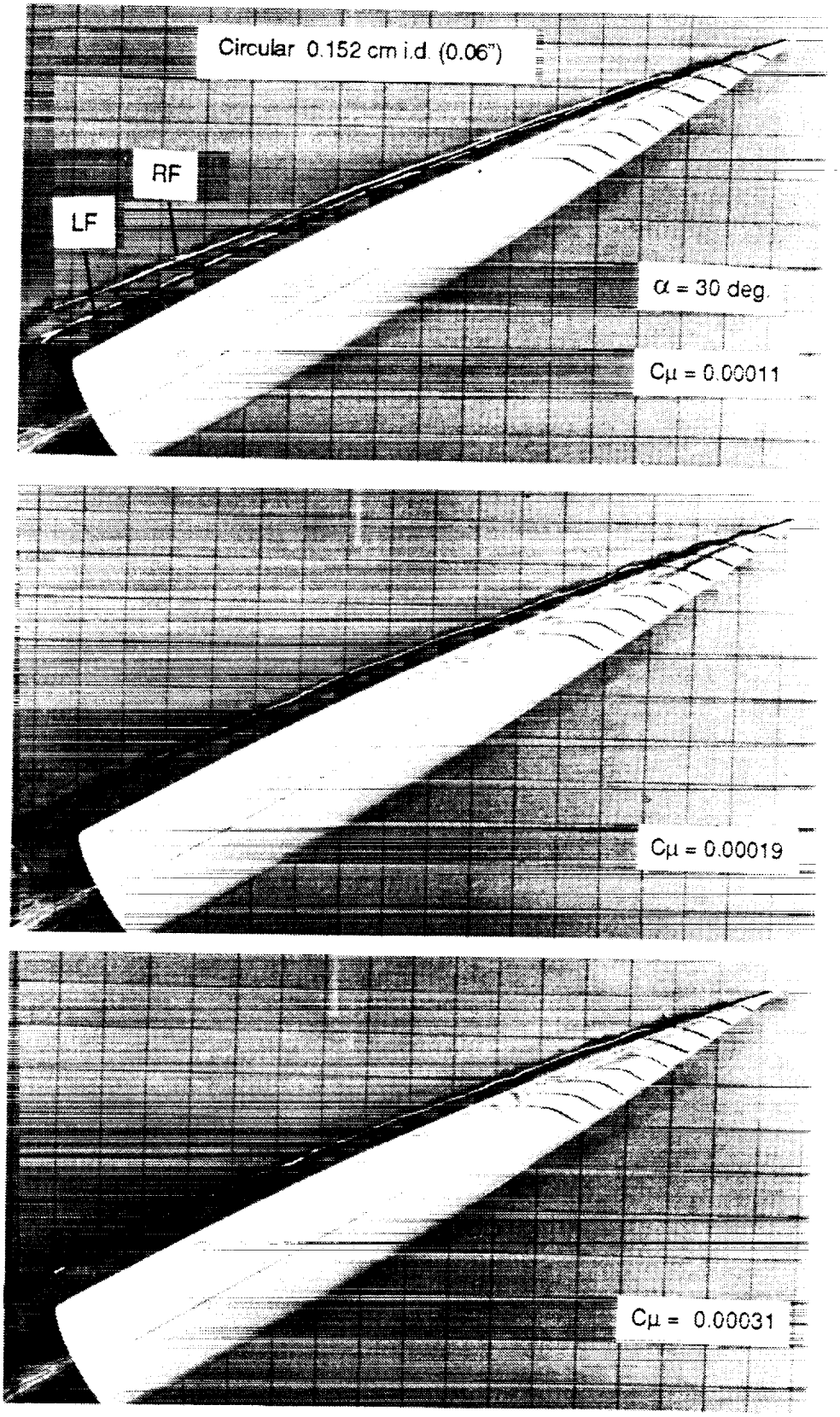

Figure 12 - Concluded

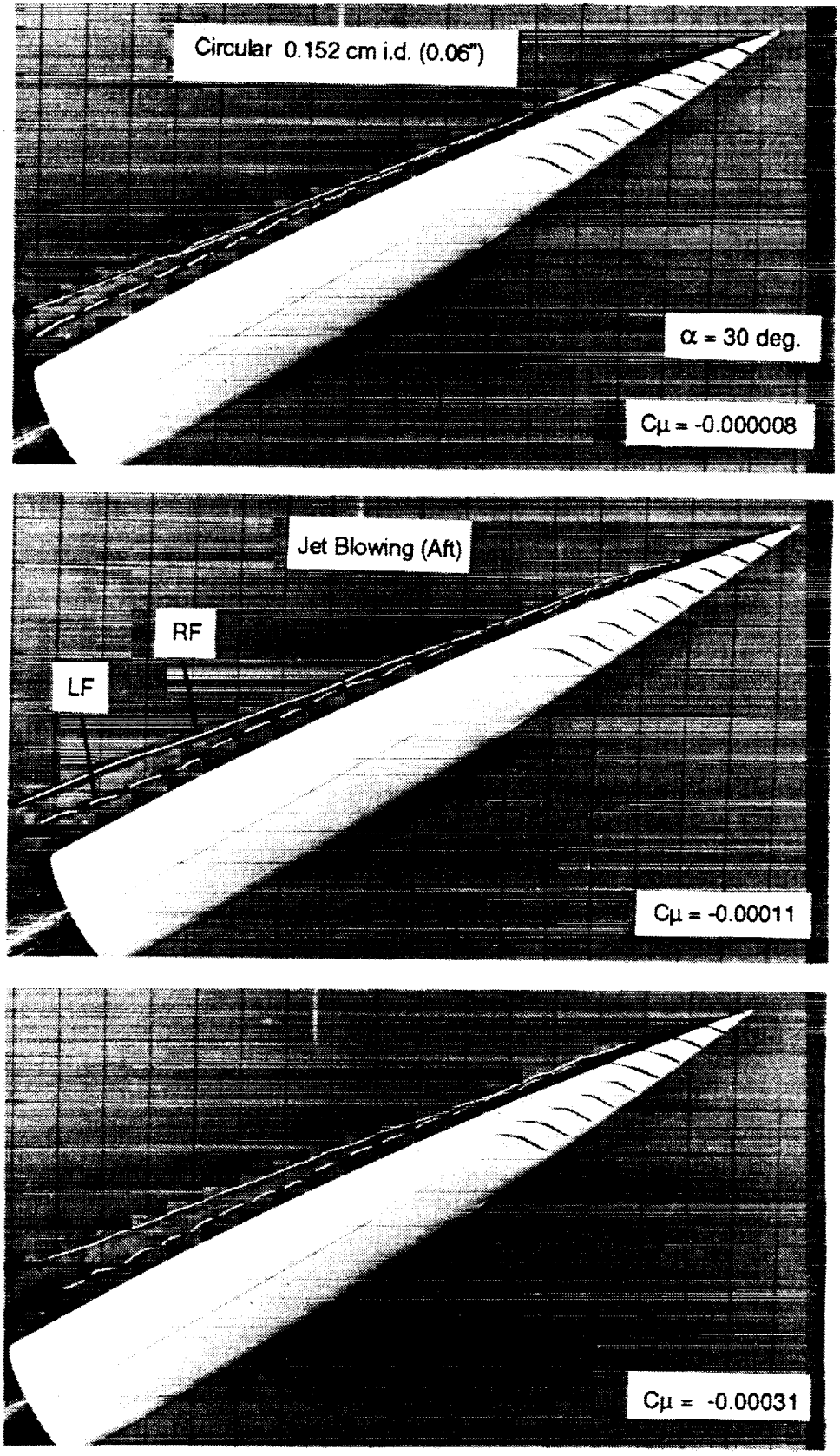

Figure 13 - Effect of Jet Blowing (Aft, Left Side, Forebody Model # 1) Circular Nozzle, 0.152 cm i.d., $\alpha = 30°$

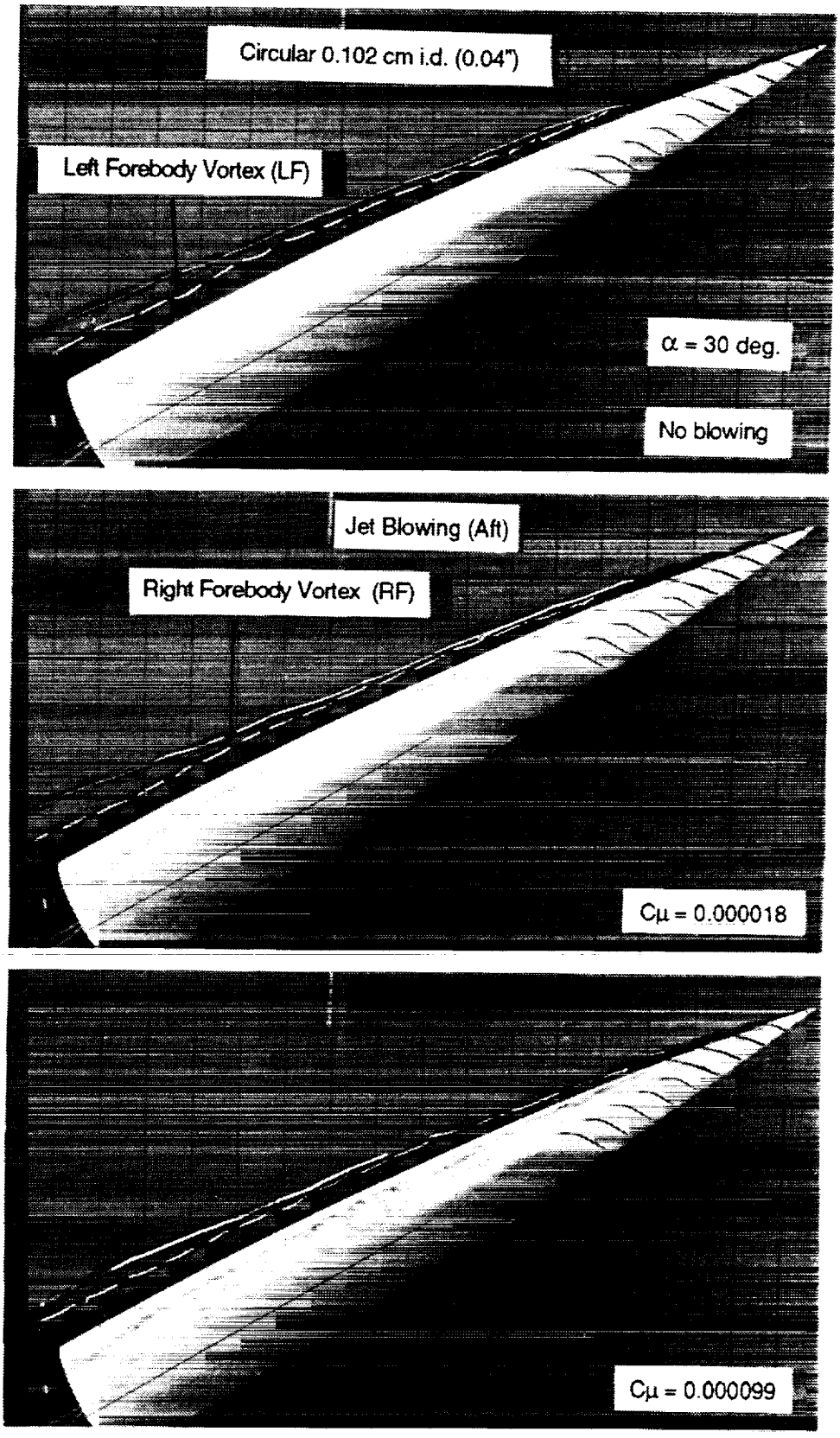

Figure 14 - Effect of Jet Blowing (Aft, Right Side, Forebody Model # 1) Circular Nozzle, 0.102 cm i.d., $\alpha = 30°$

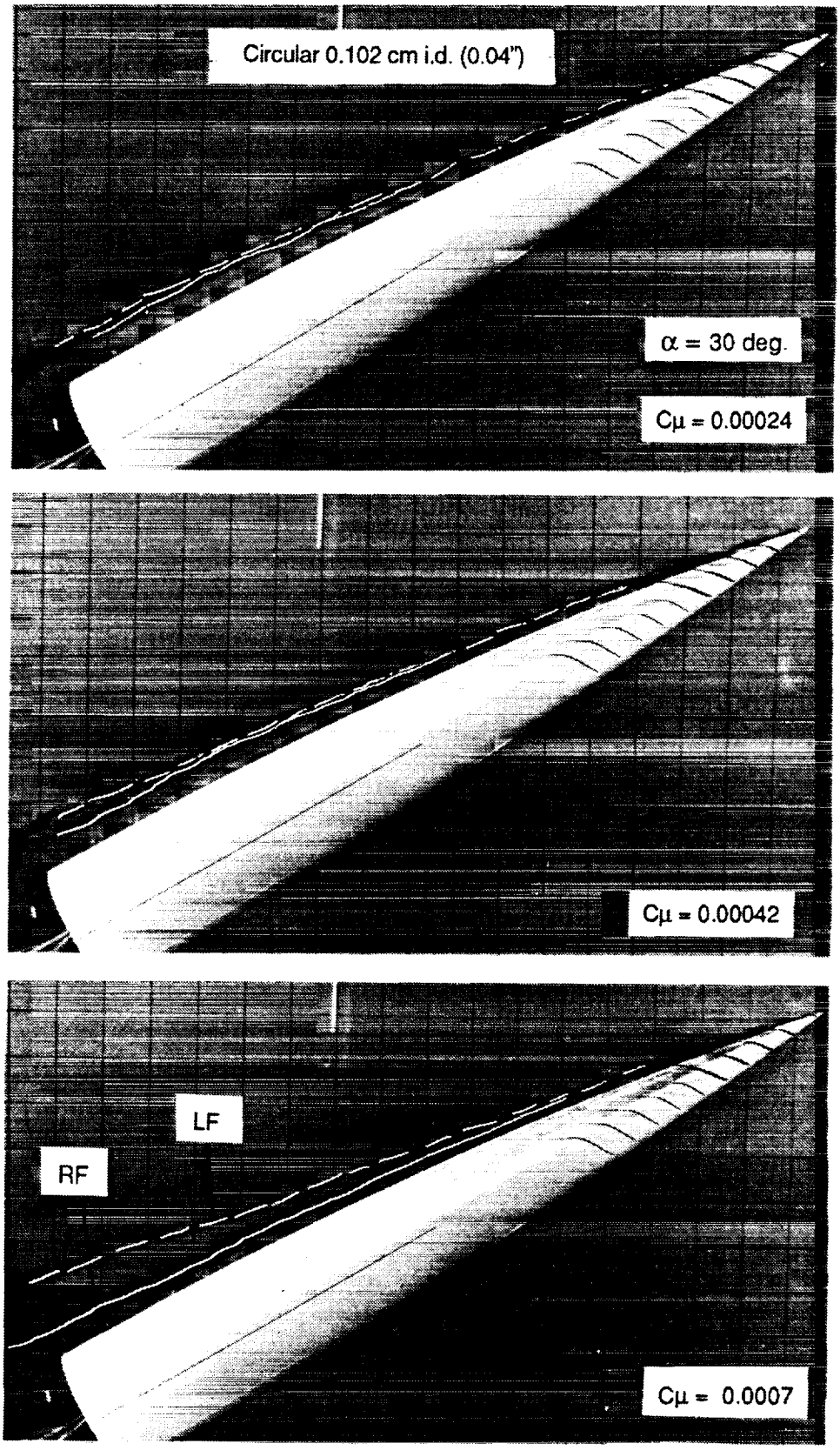

Figure 14 - Concluded

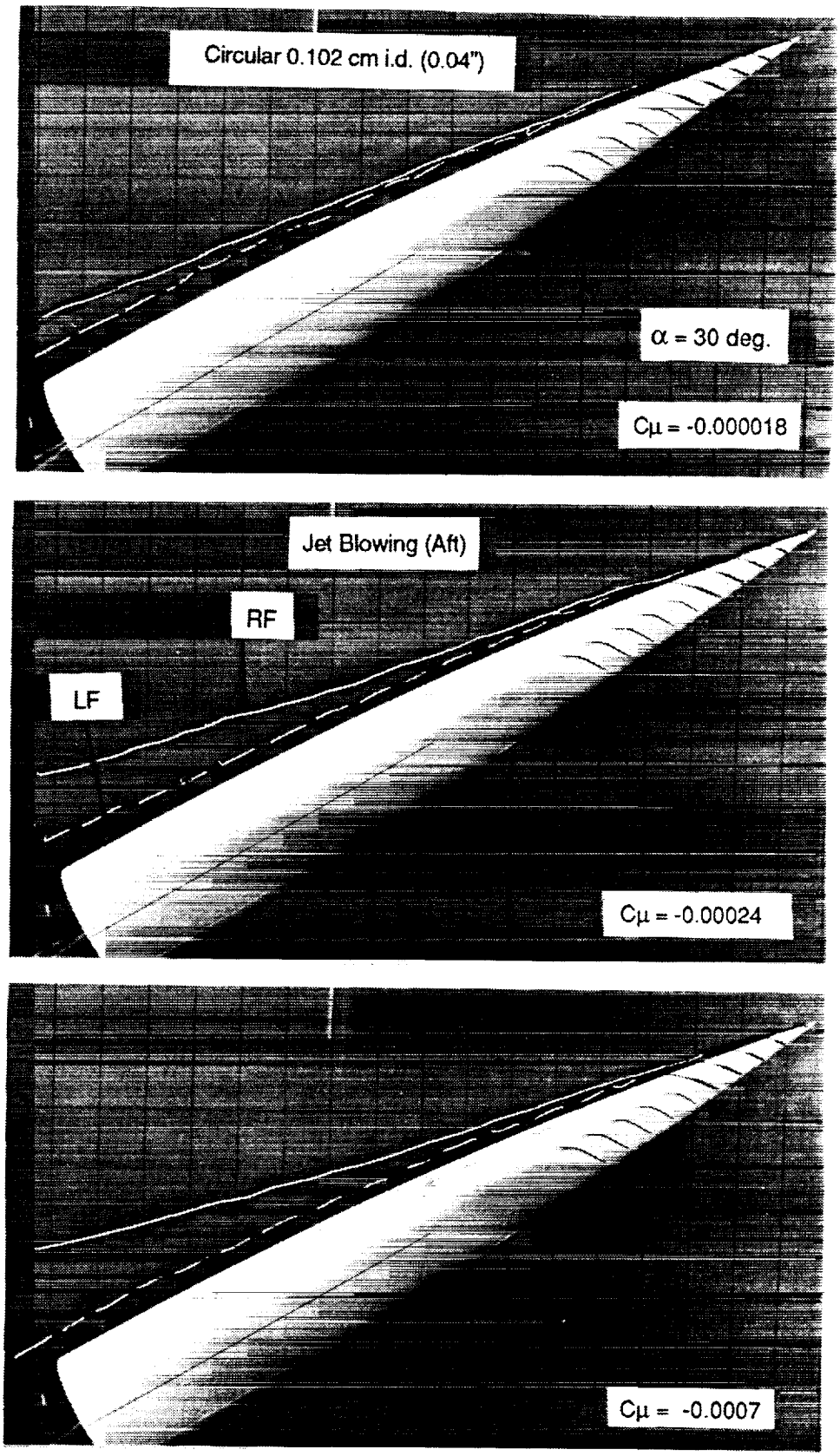

Figure 15 - Effect of Jet Blowing (Aft, Left Side, Forebody Model # 1) Circular Nozzle, 0.102 cm i.d., $\alpha = 30°$

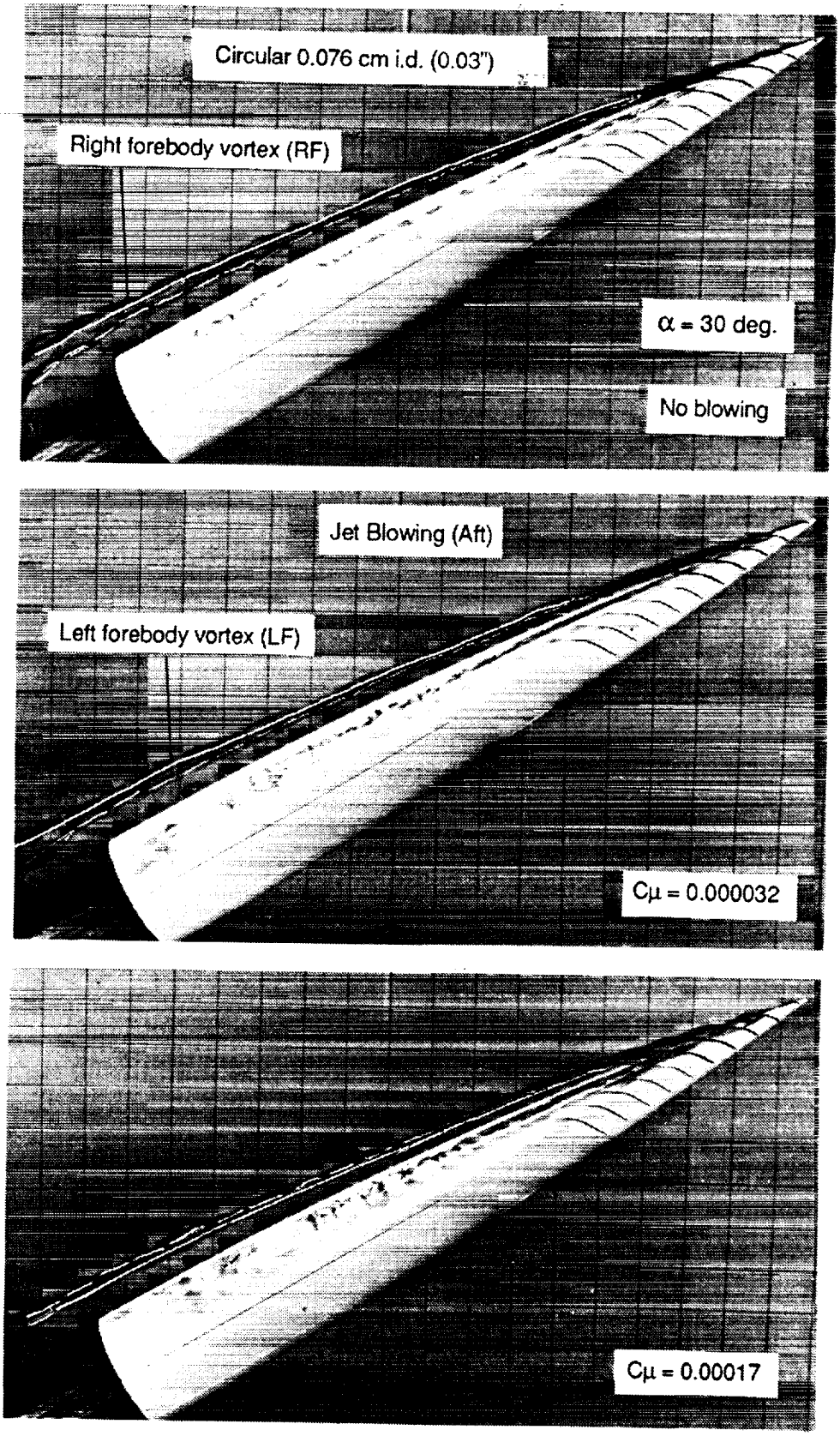

Figure 16 - Effect of Jet Blowing (Aft, Right Side, Forebody Model # 1) Circular Nozzle, 0.076 cm i.d., $\alpha = 30°$

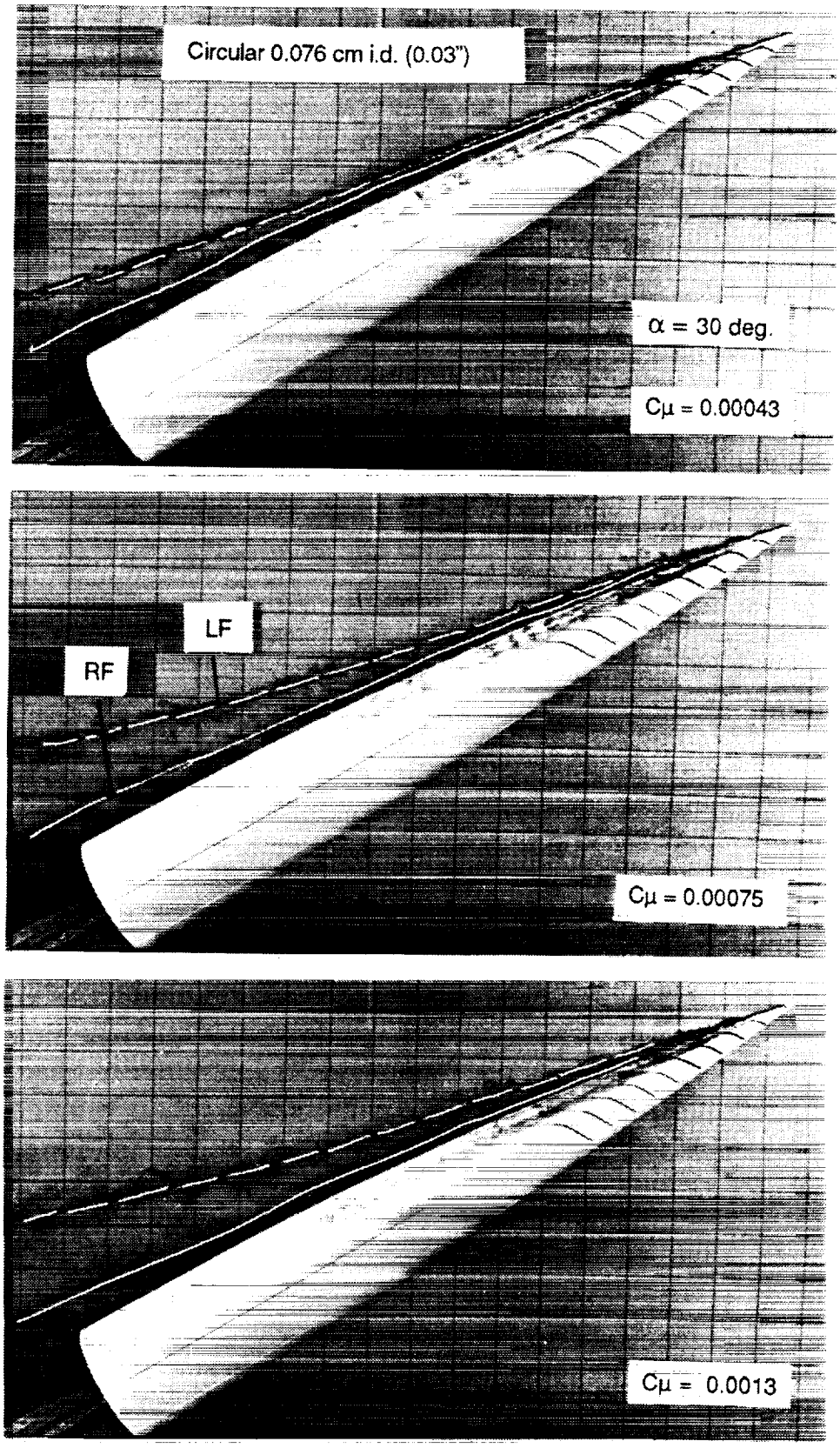

Figure 16 - Concluded

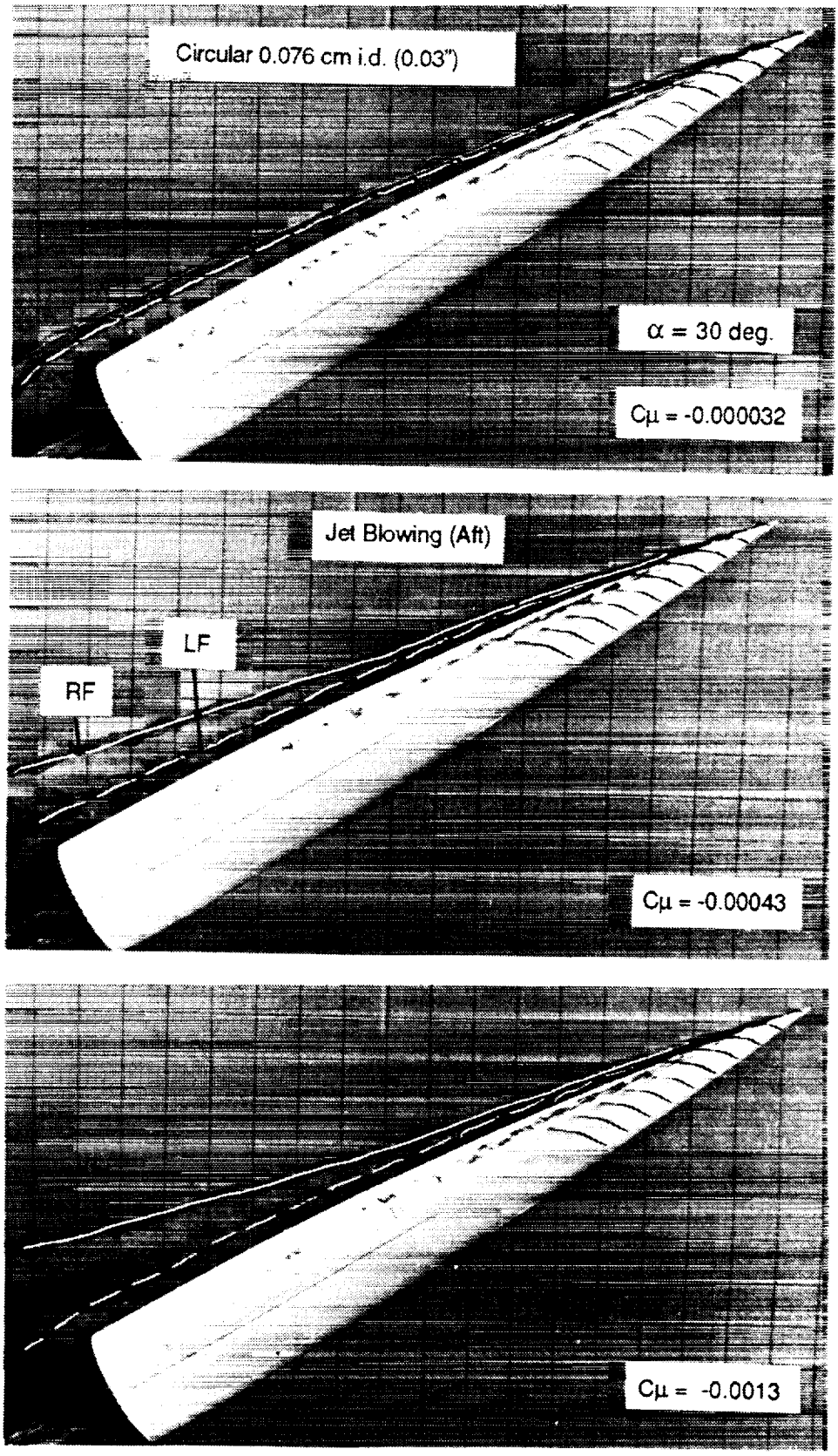

Figure 17 - Effect of Jet Blowing (Aft, Left Side, Forebody Model # 1) Circular Nozzle, 0.076 cm i.d., $\alpha = 30°$

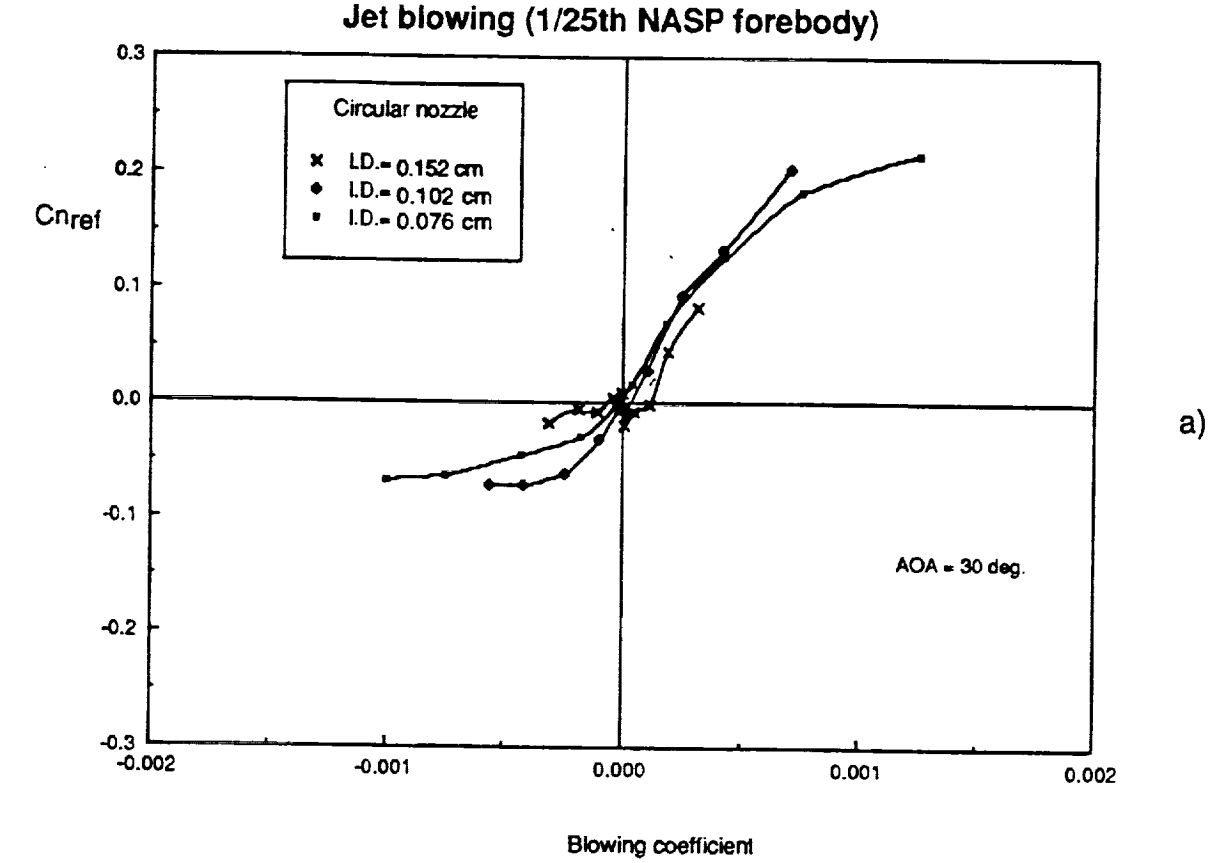

a)

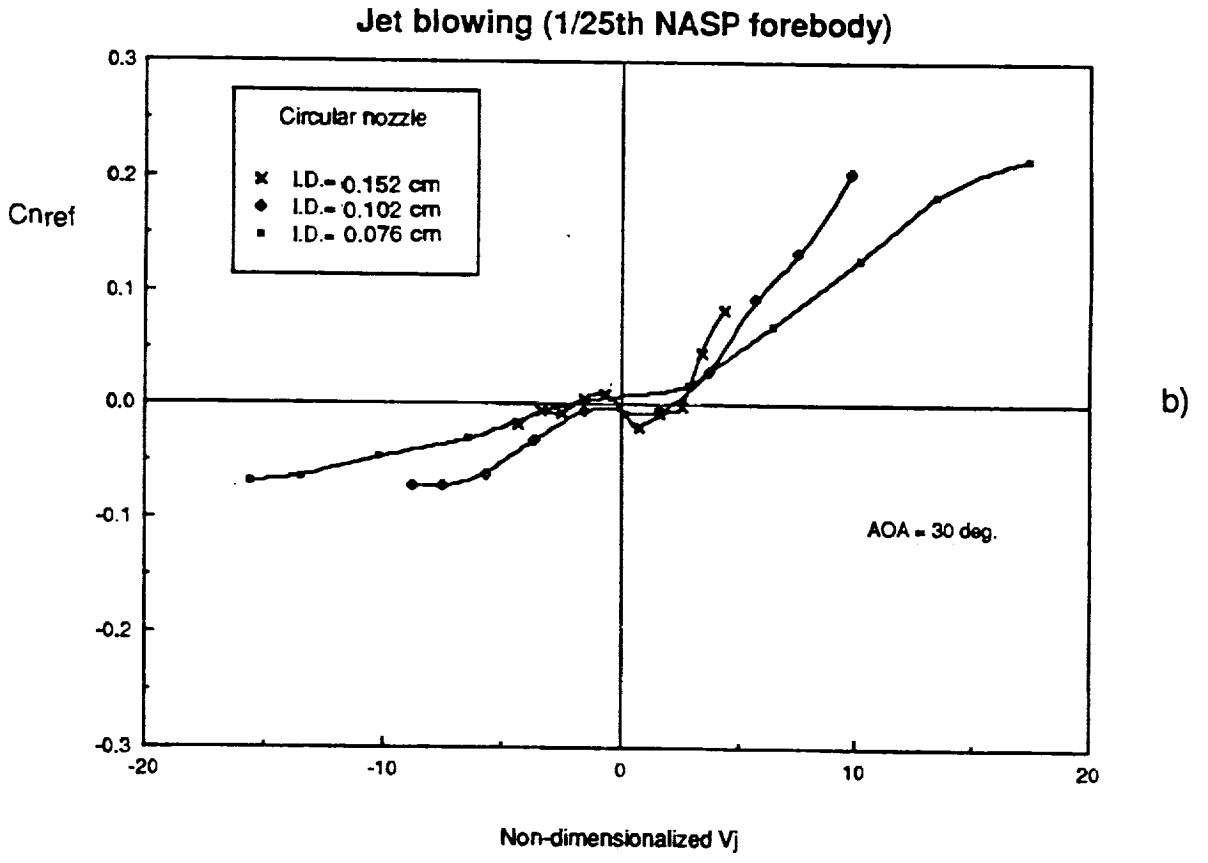

b)

Figure 18 - Change in Reference Yawing Moment as a function of a) Blowing Coefficient, b) Vj, c) Mass Flow Rate; $\alpha = 30°$

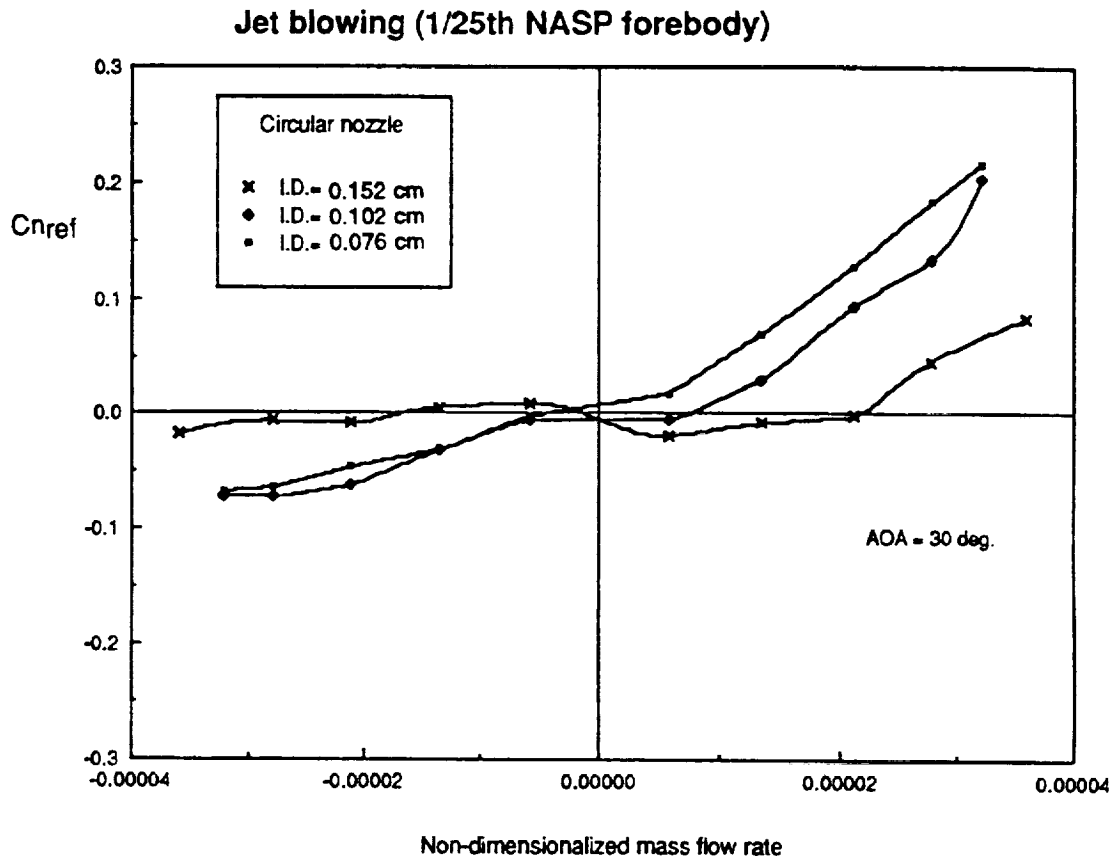

c)

Figure 18 - Concluded

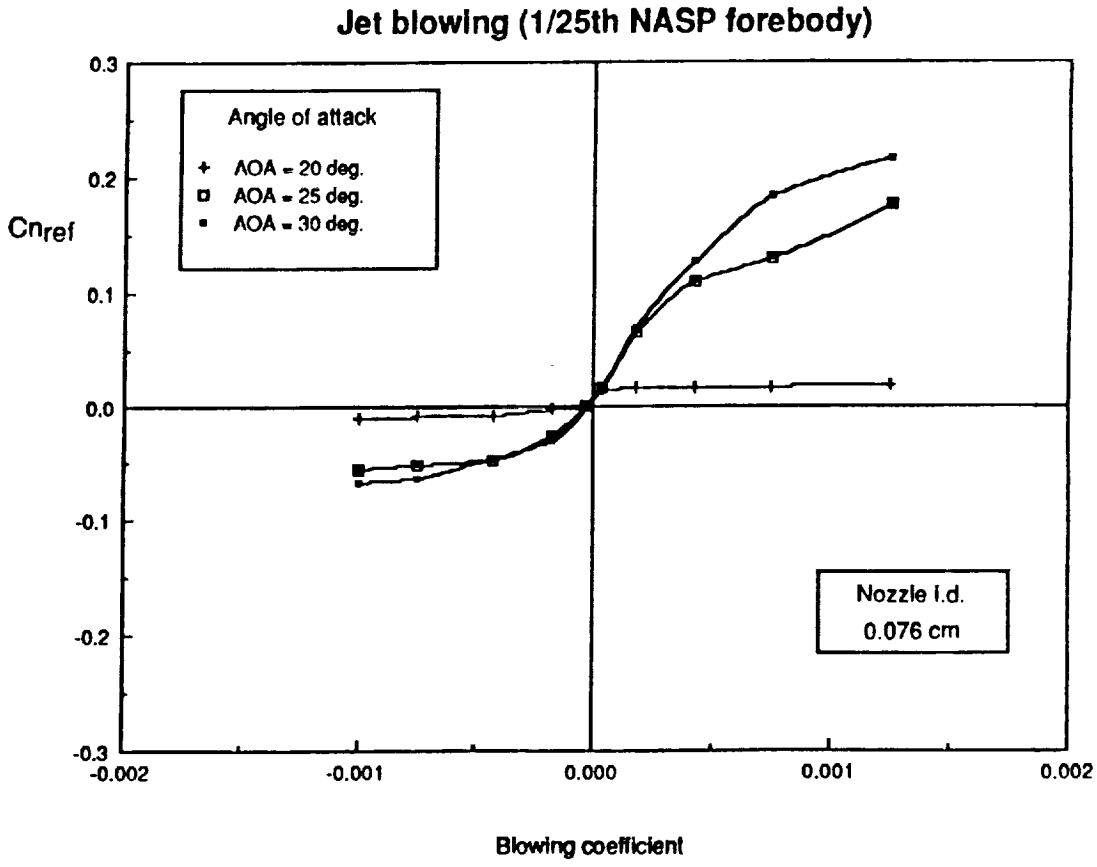

Figure 19 - Change in Reference Yawing Moment Produced by Jet Blowing Circular Nozzle, 0.076 cm i.d.

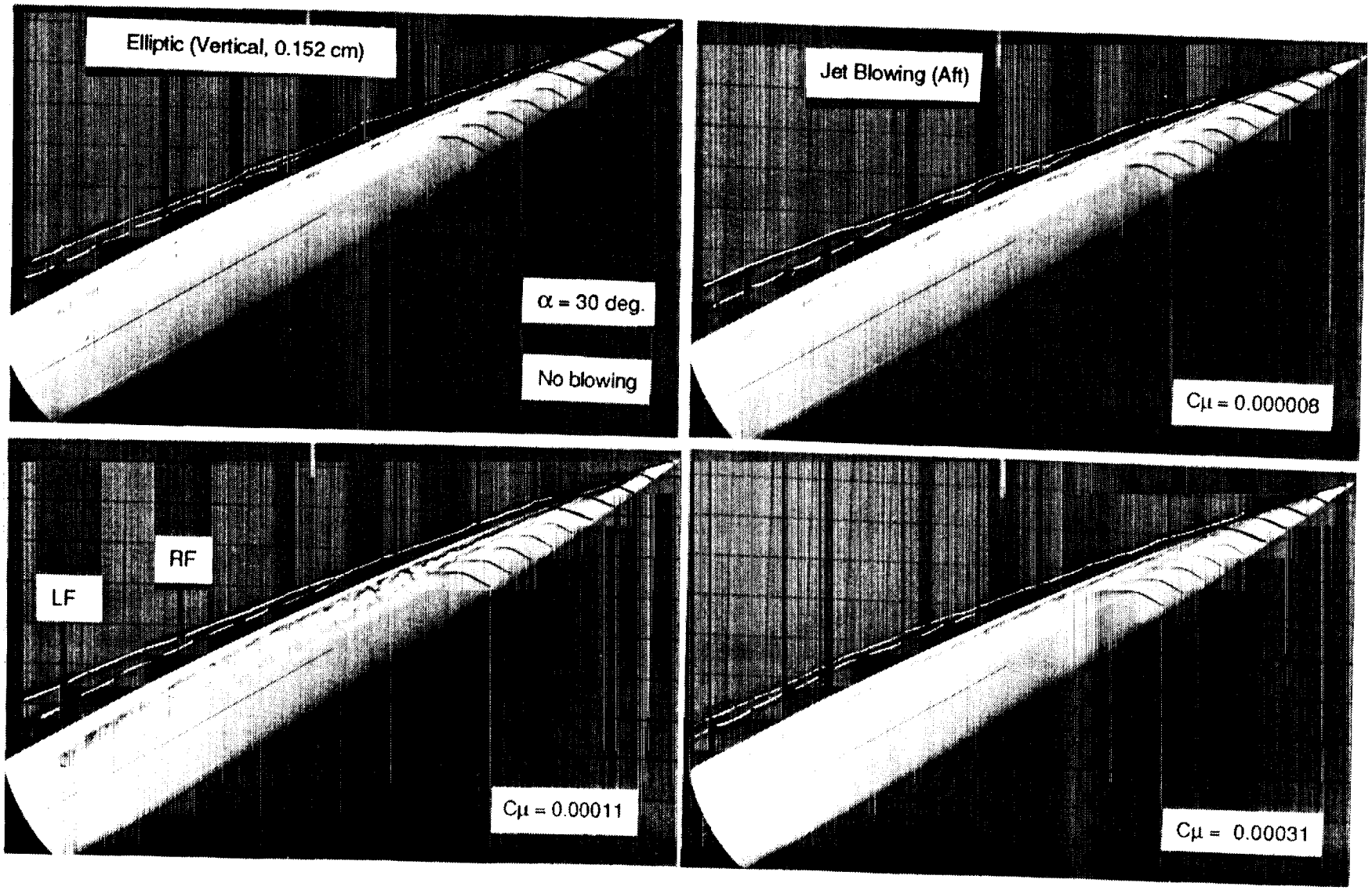

Figure 20 - Effect of Jet Blowing (Aft, Right Side, Forebody Model # 1)
Elliptic Vertical Nozzle, 0.152 cm i.d., $\alpha = 30°$

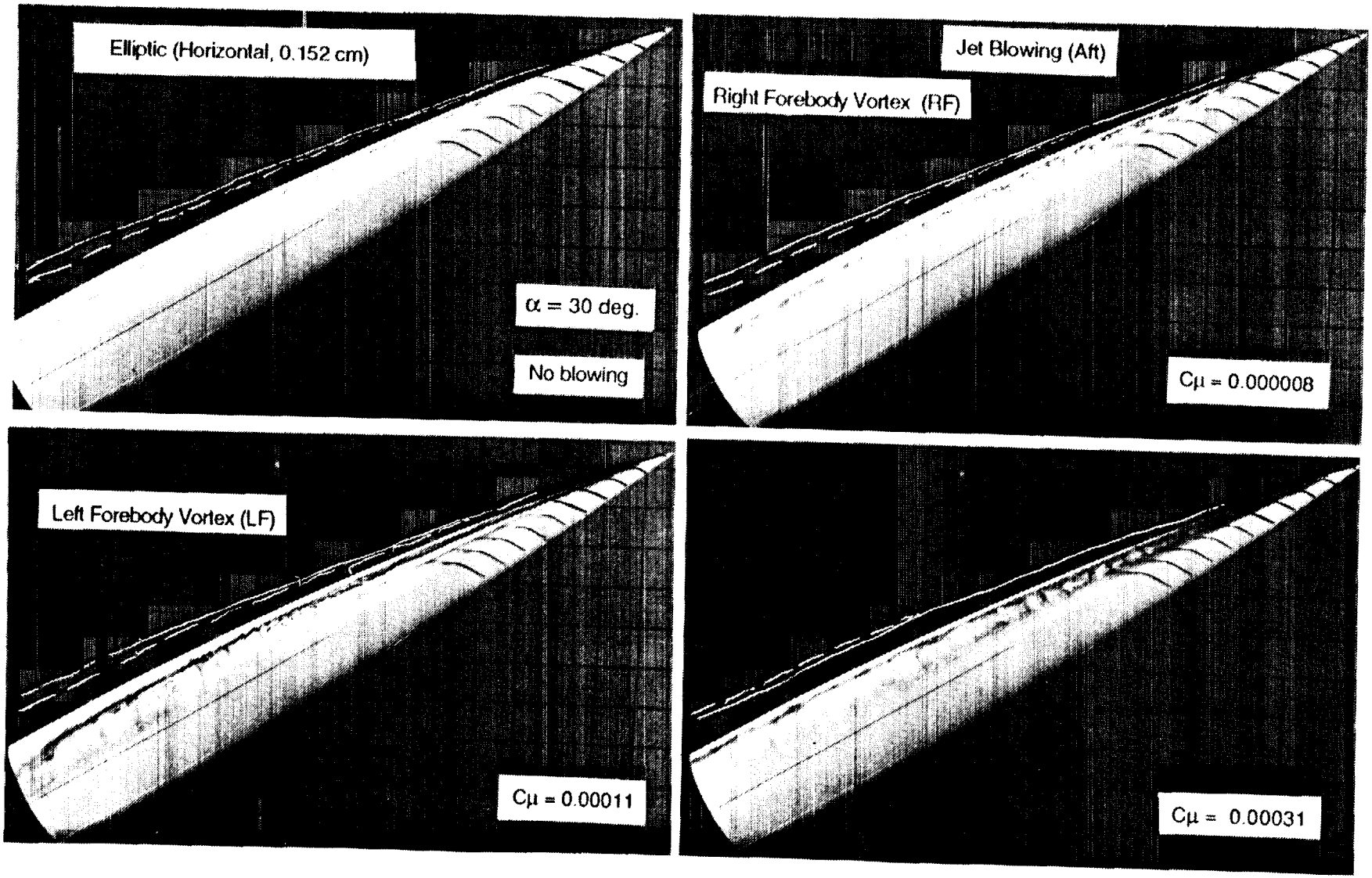

Figure 21 - Effect of Jet Blowing (Aft, Right Side, Forebody Model # 1)
Elliptic Horizontal Nozzle, 0.152 cm i.d., $\alpha = 30°$

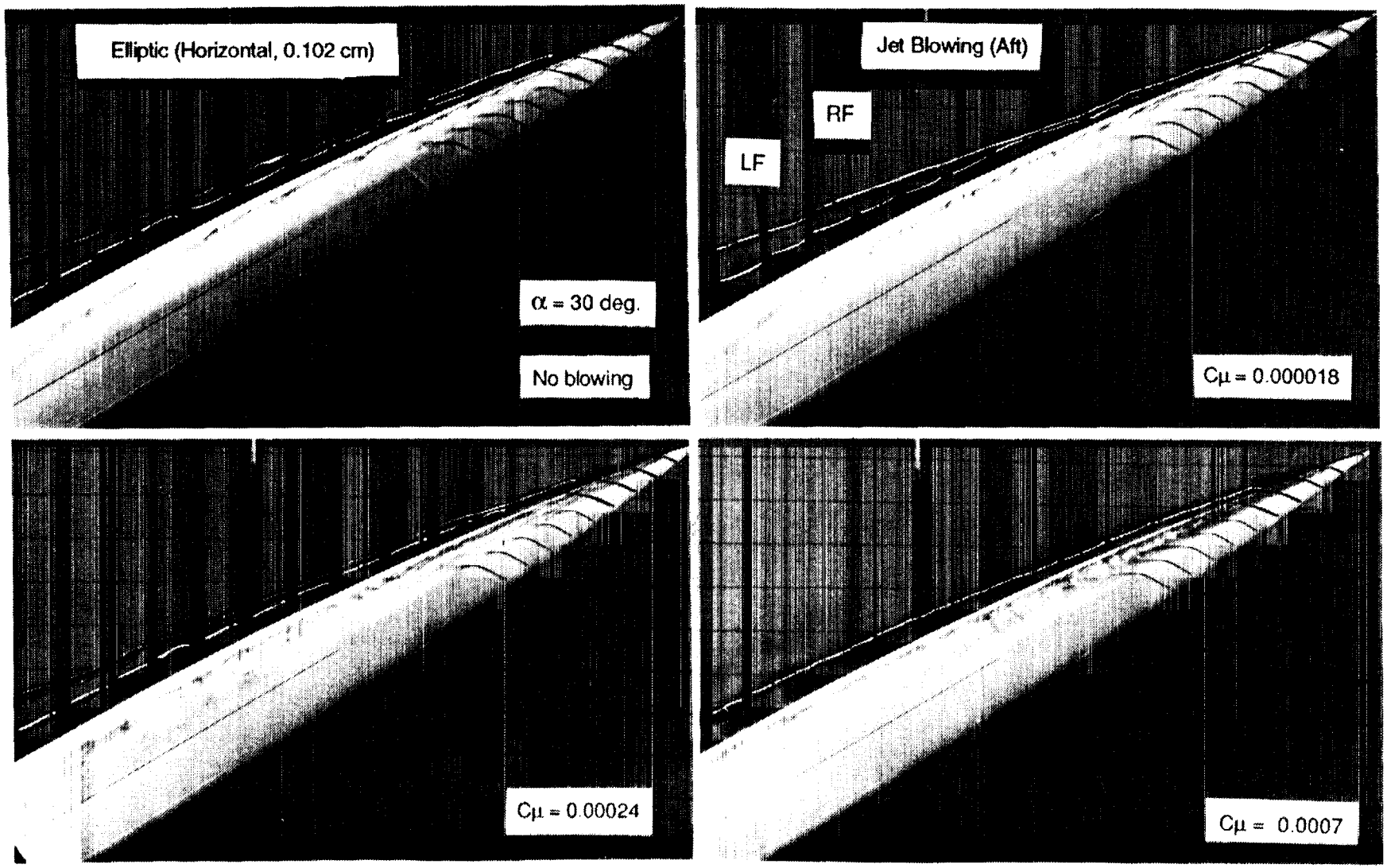

Figure 22 - Effect of Jet Blowing (Aft, Right Side, Forebody Model # 1)
Elliptic Horizontal Nozzle, 0.102 cm i.d., $\alpha = 30^{\circ}$

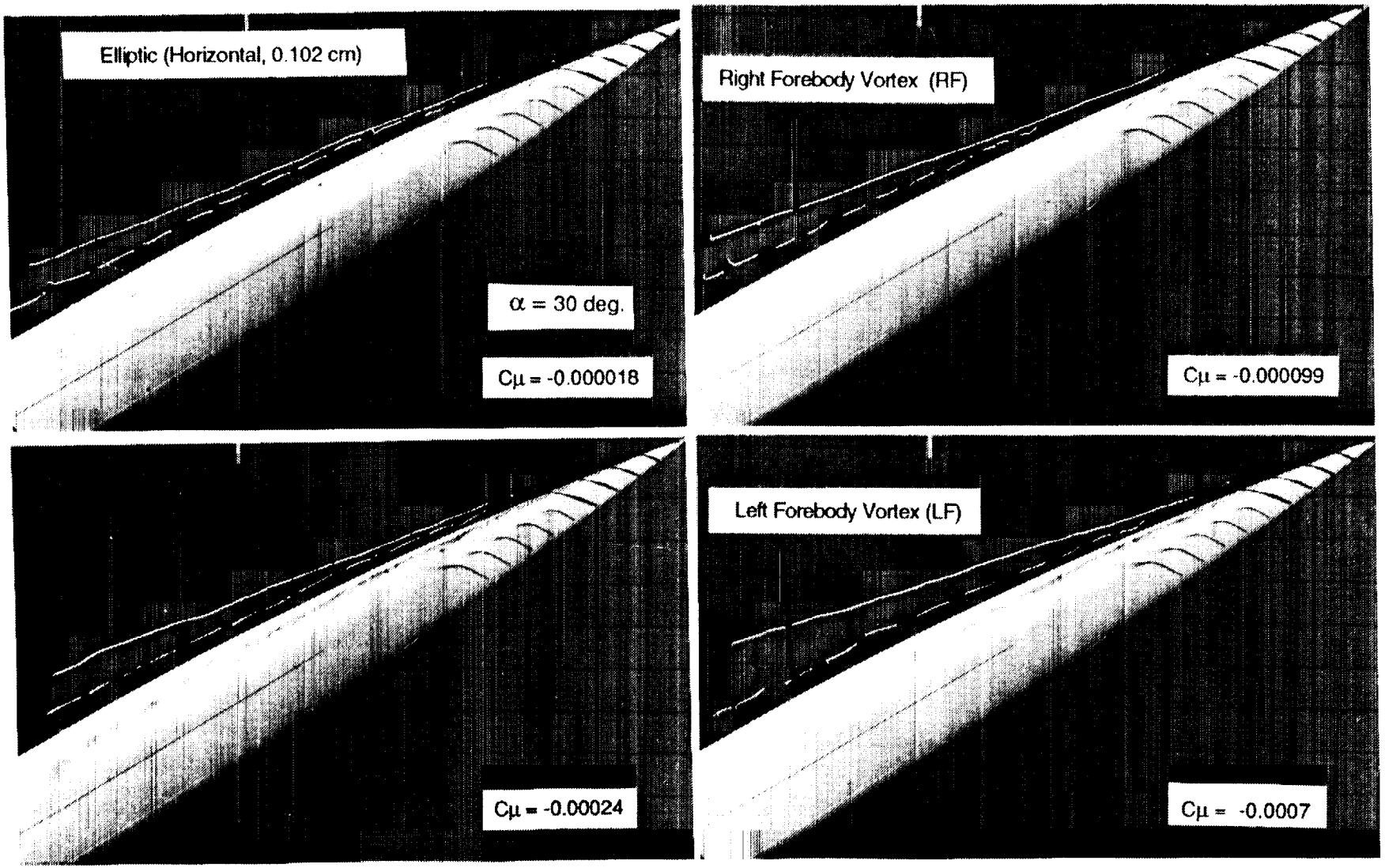

Figure 23 - Effect of Jet Blowing (Aft, Left Side, Forebody Model # 1)
Elliptic Horizontal Nozzle, 0.102 cm i.d., α = 30°

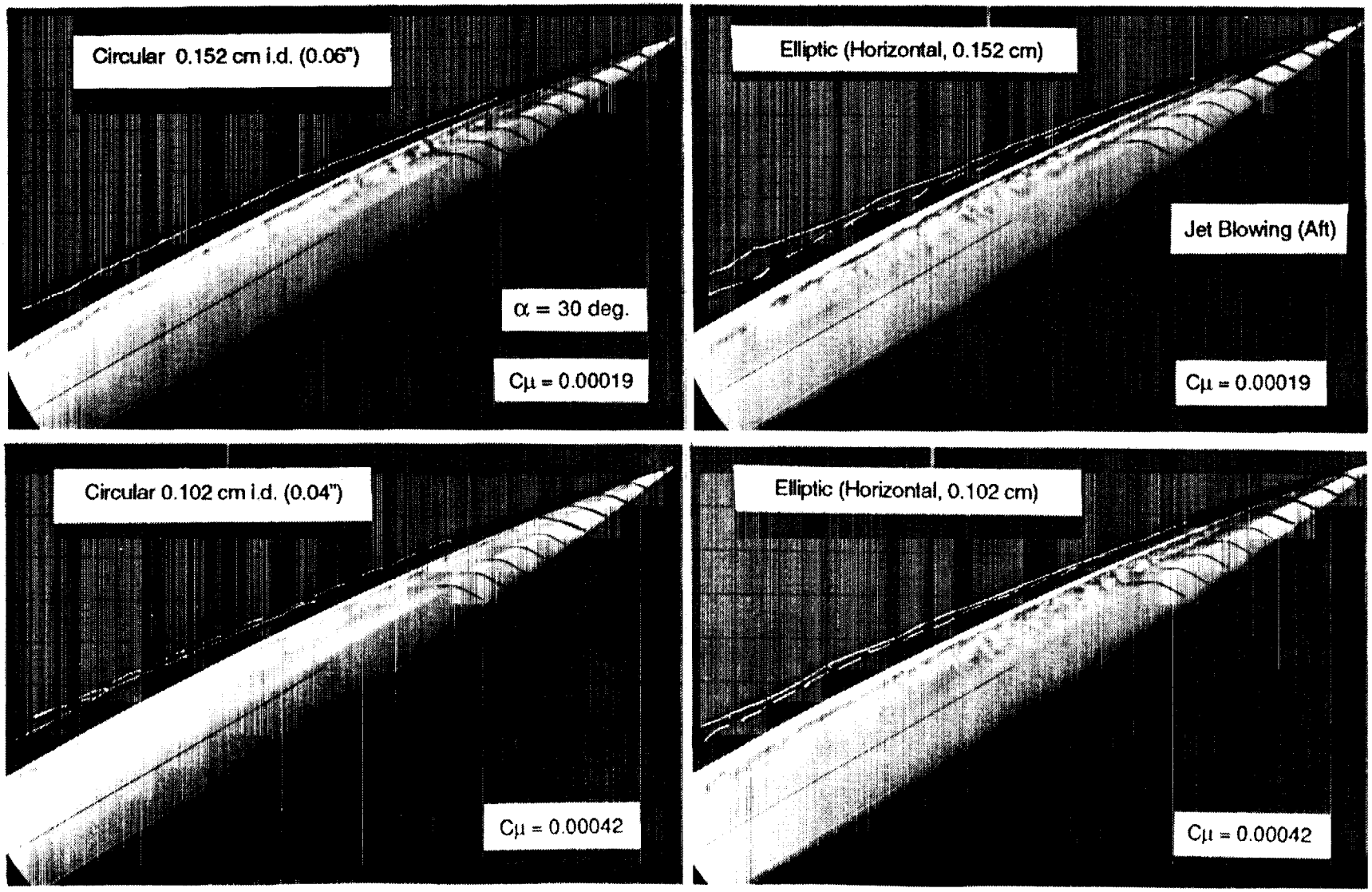

Figure 24 - Effect of Jet Blowing (Aft, Right Side, Forebody Model # 1)
Comparison Between Circular and Elliptic Nozzles, $\alpha = 30°$

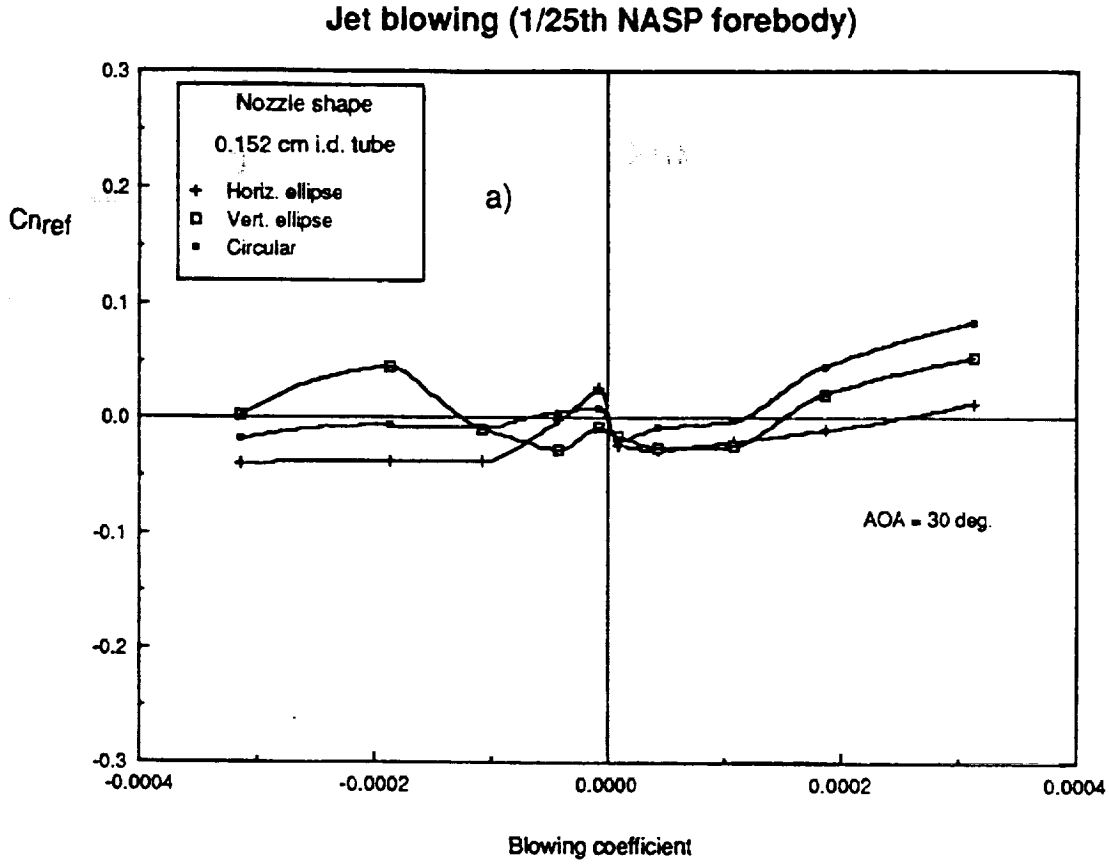

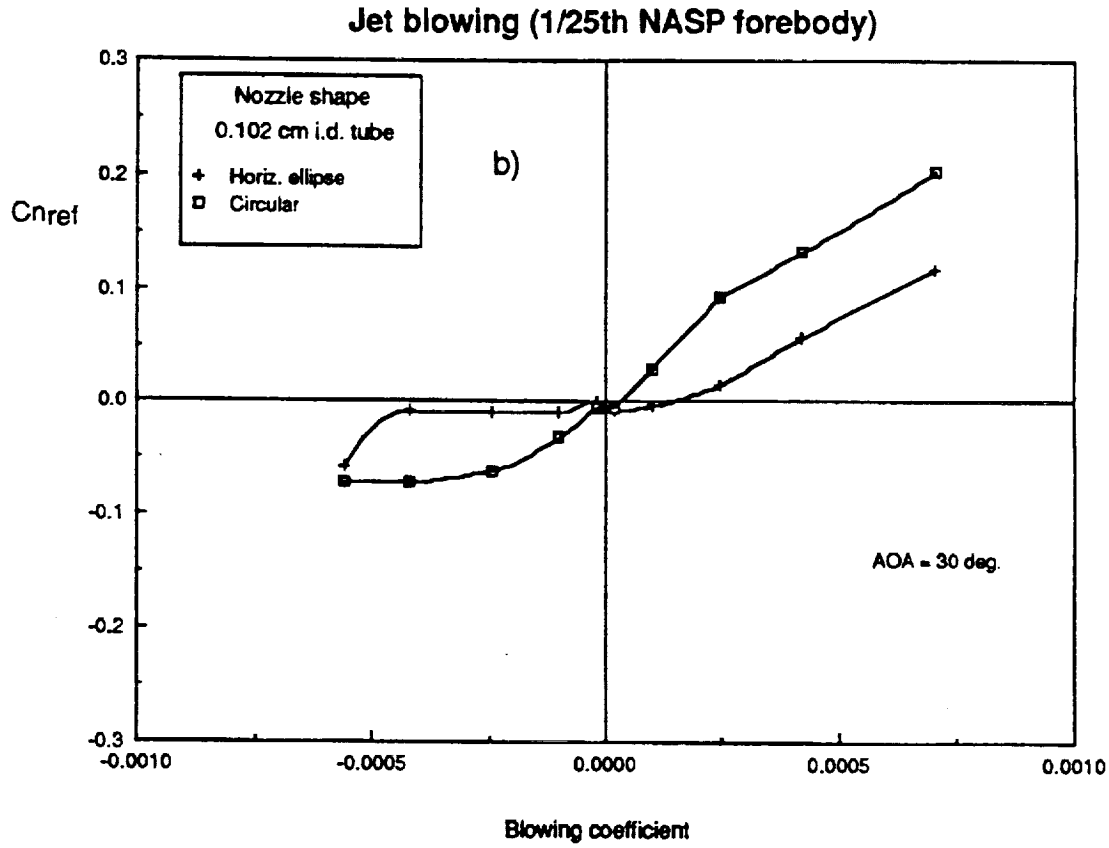

Figure 25 - Change in Reference Yawing Moment Produced by Jet Blowing Comparison Between Circular and Elliptic Nozzles, $\alpha = 30°$

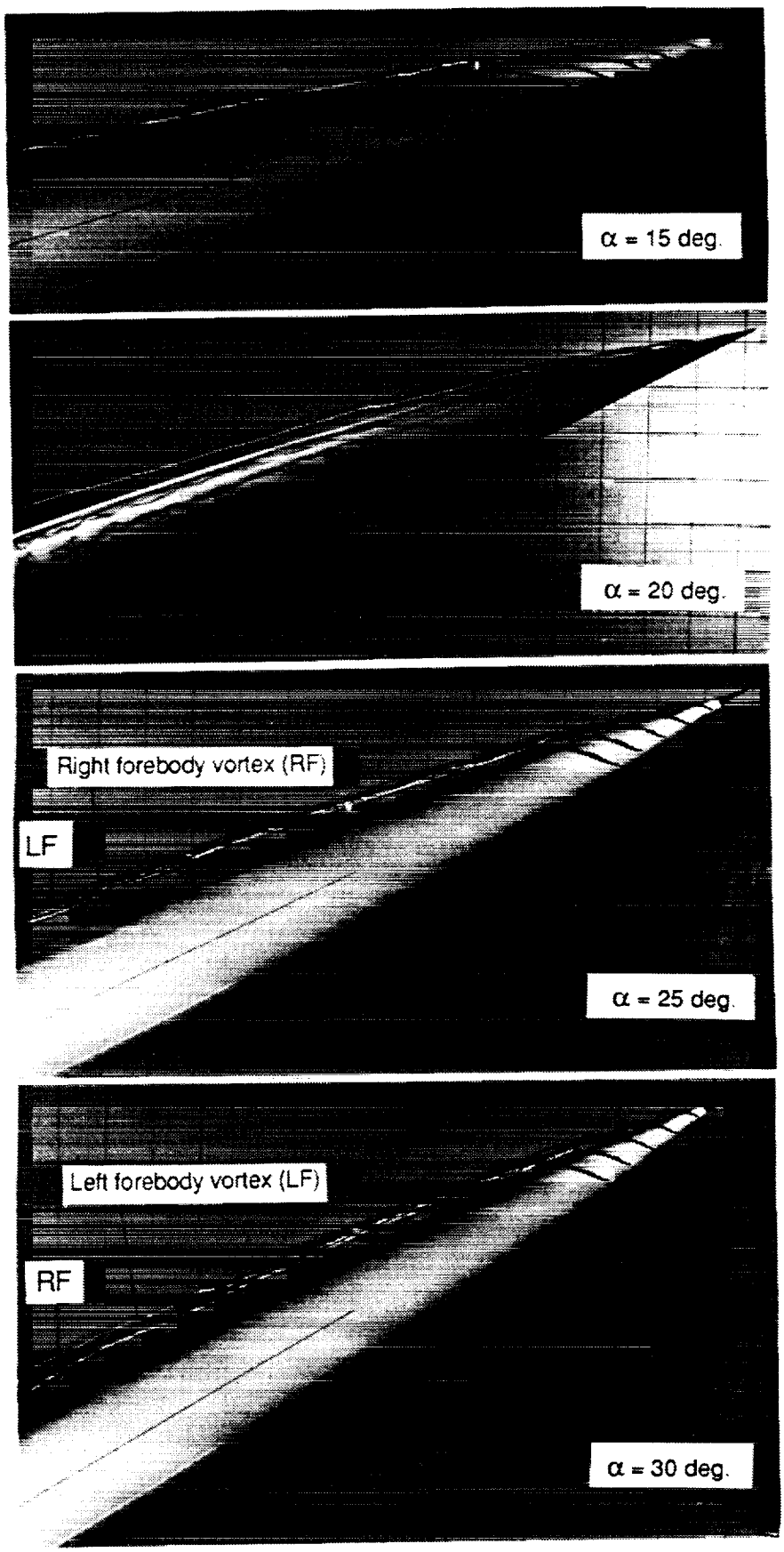

Figure 26 - Effect of Angle of Attack (1/25th-scale Forebody Model # 2)

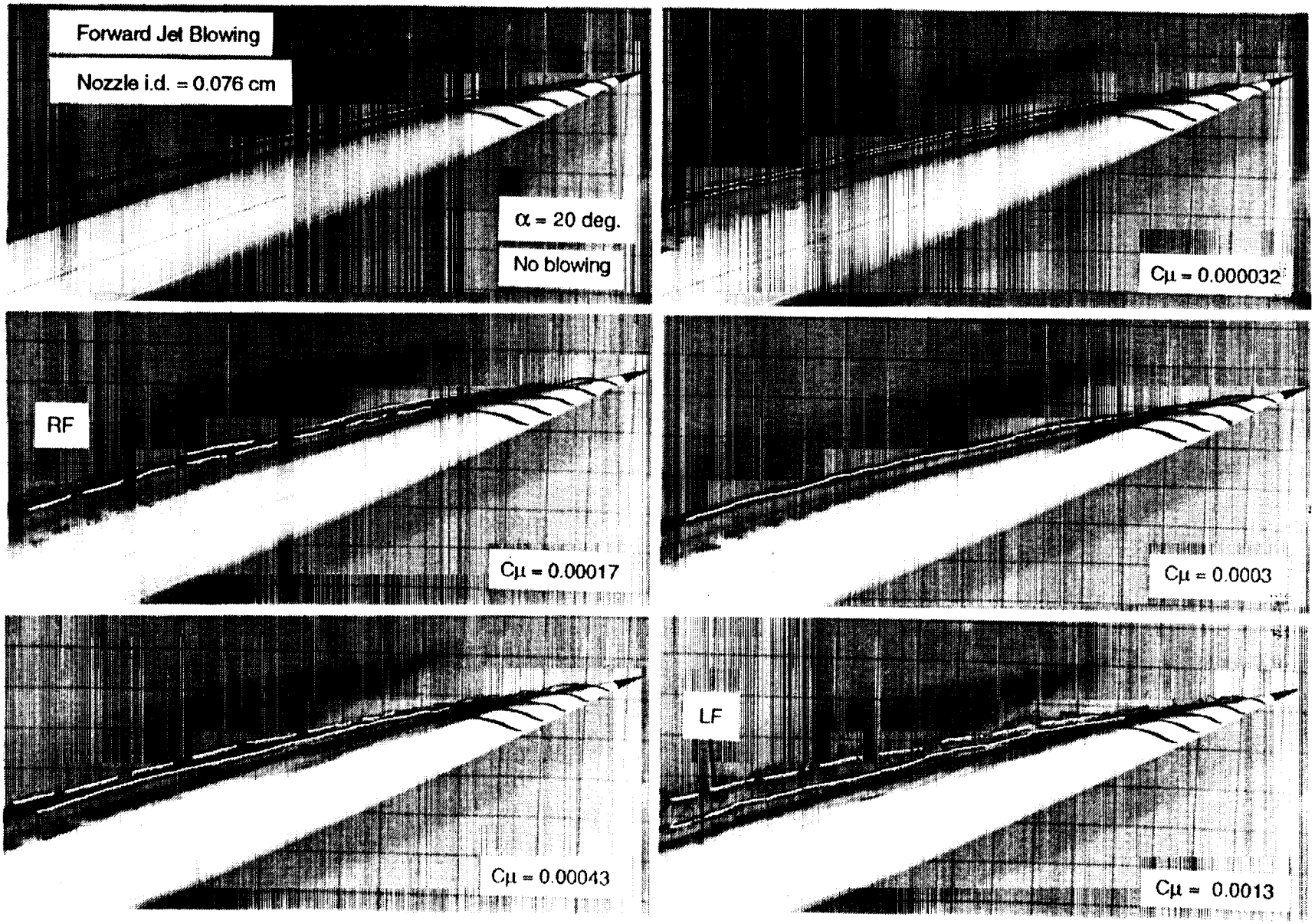

Figure 27 - Effect of Jet Blowing (Forward, Right Side, Forebody Model # 2) Circular Nozzle, 0.076 cm i.d., $\alpha = 20^{\circ}$

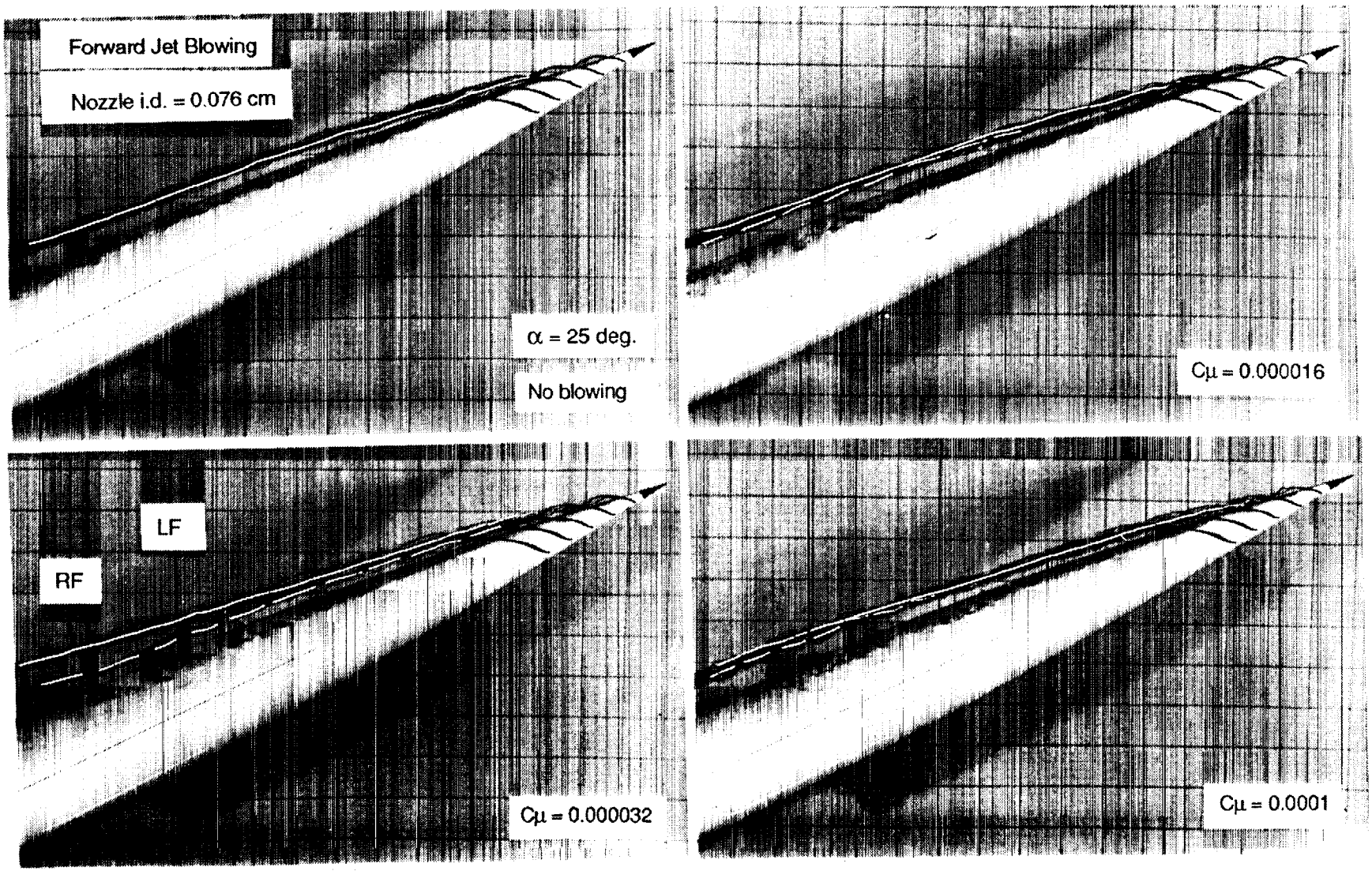

Figure 28 - Effect of Jet Blowing (Forward, Right Side, Forebody Model # 2)
Circular Nozzle, 0.076 cm i.d., $\alpha = 25°$

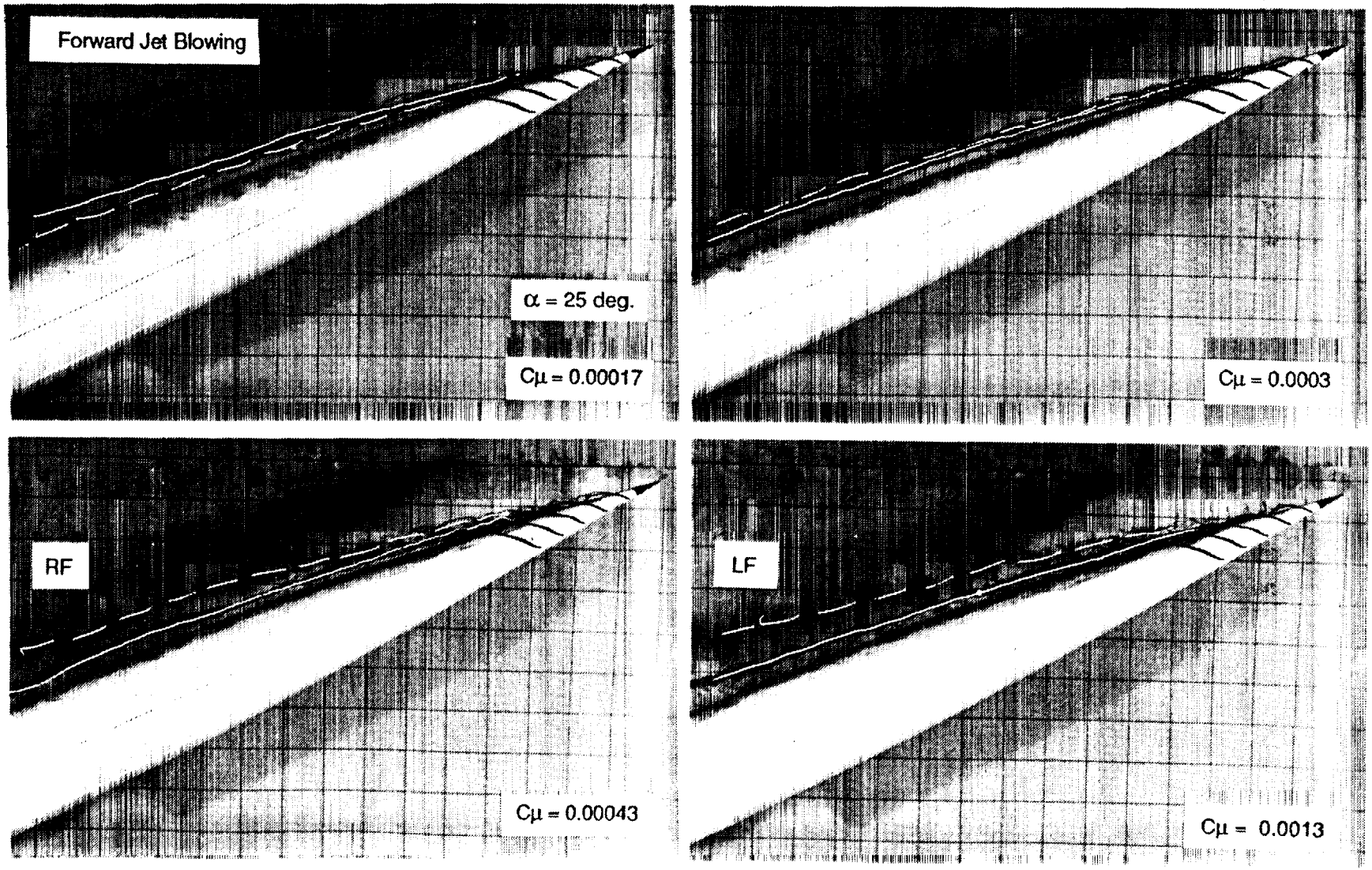

Figure 28 - Concluded

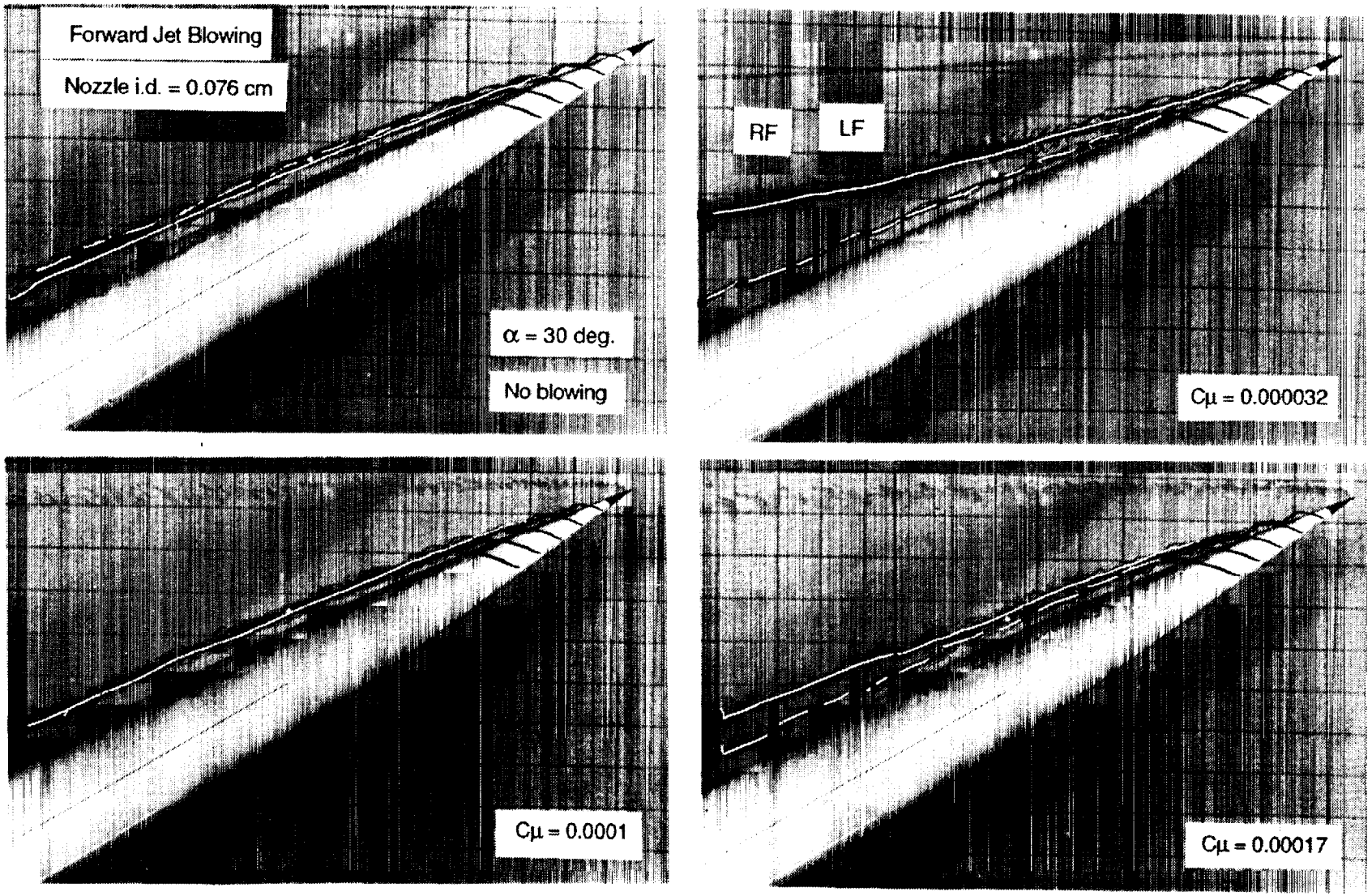

Figure 29 - Effect of Jet Blowing (Forward, Right Side, Forebody Model # 2)
Circular Nozzle, 0.076 cm i.d., α = 30°

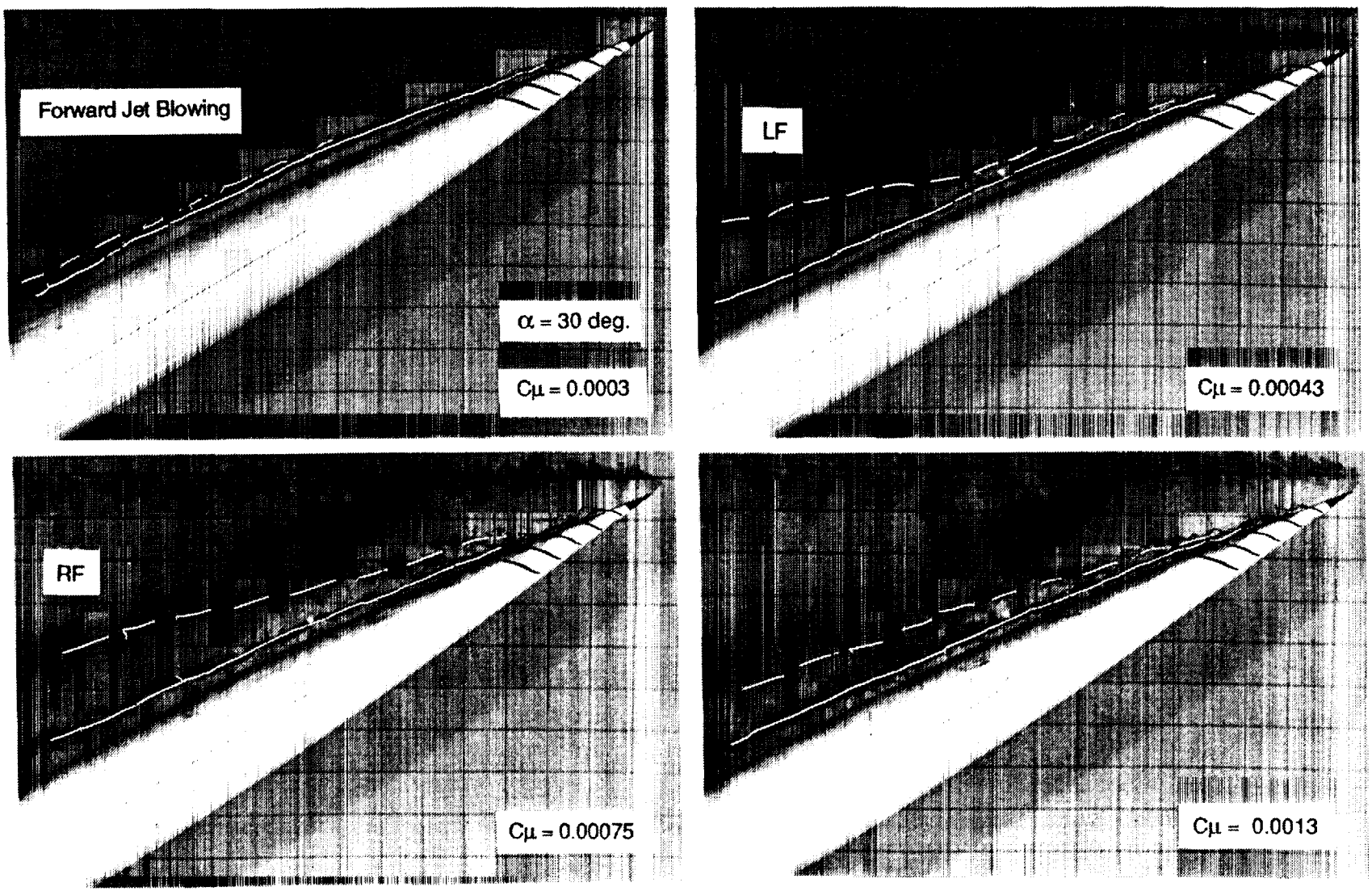

Figure 29 - Concluded

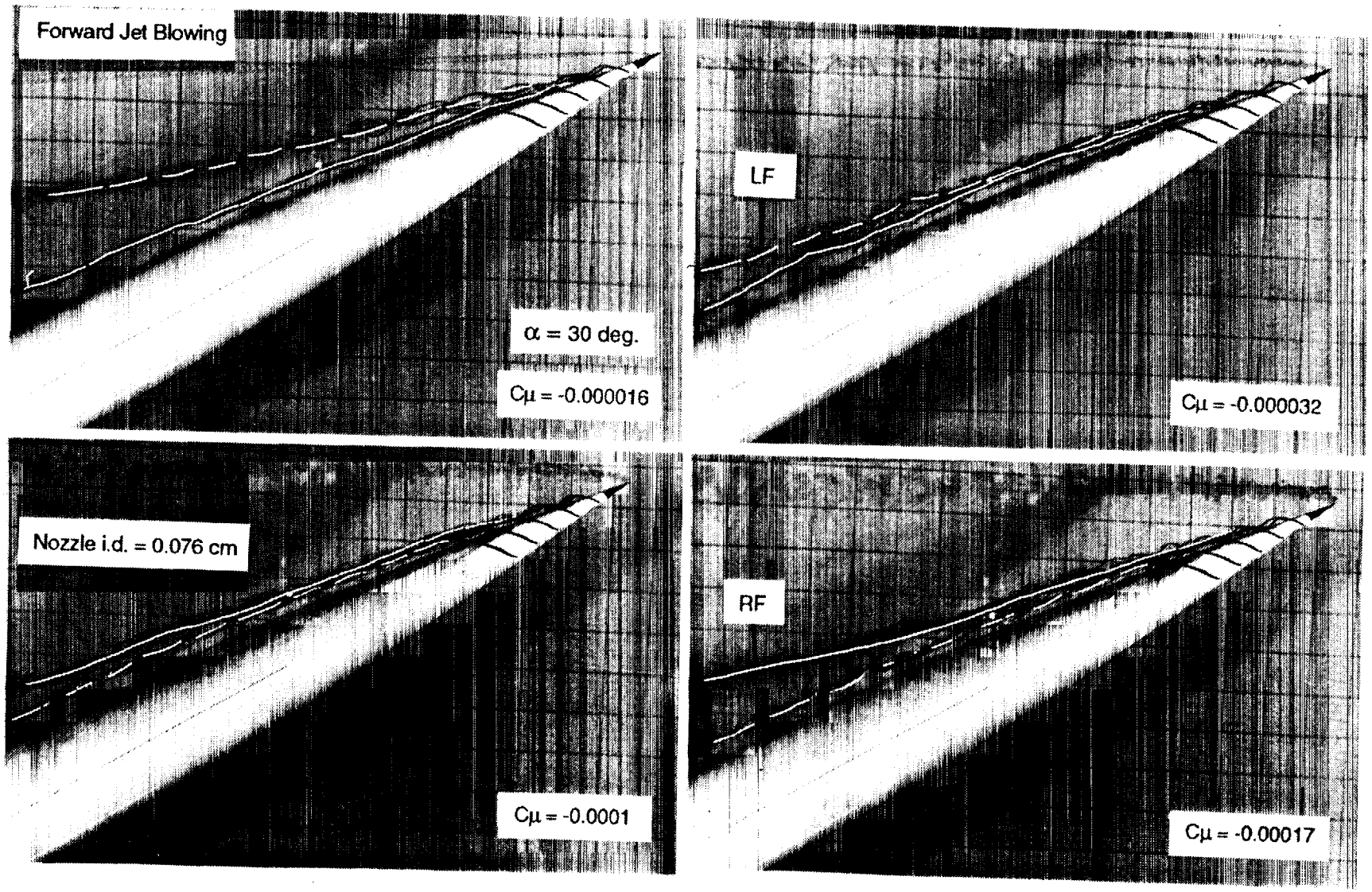

Figure 30 - Effect of Jet Blowing (Forward, Left Side, Forebody Model # 2)
Circular Nozzle, 0.076 cm i.d., $\alpha = 30°$

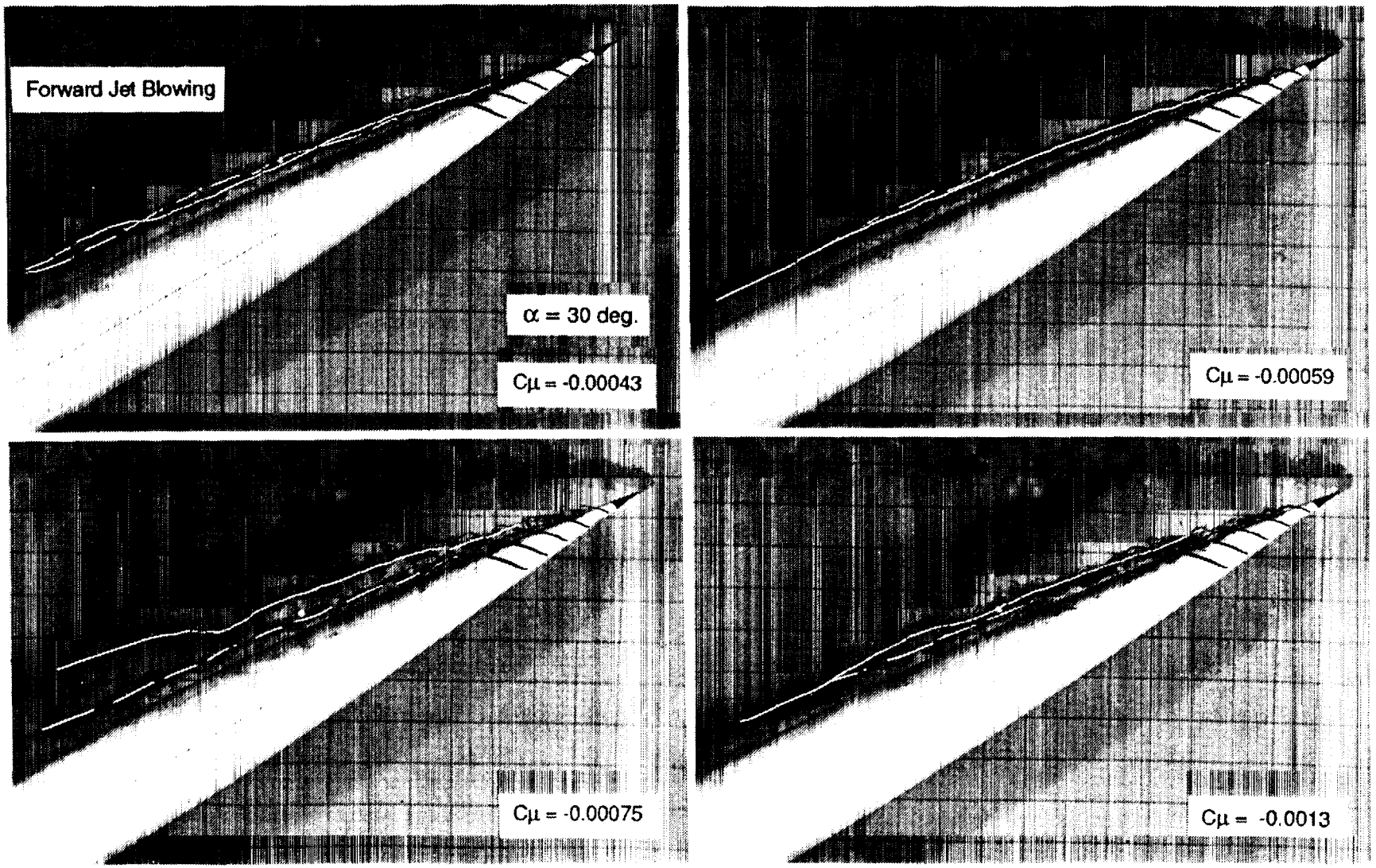

Figure 30 - Concluded

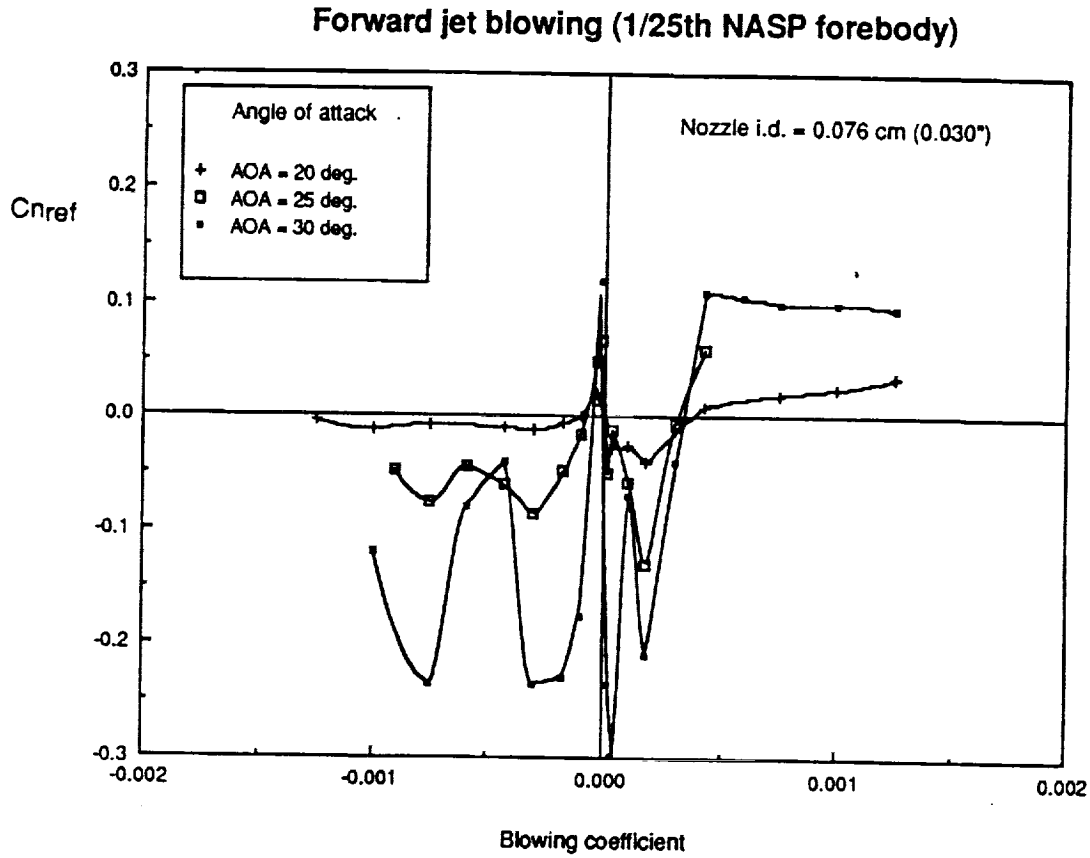

Figure 31 - Change in Reference Yawing Moment Produced By Forward Jet Blowing, Circular Nozzle, 0.076 cm i.d.

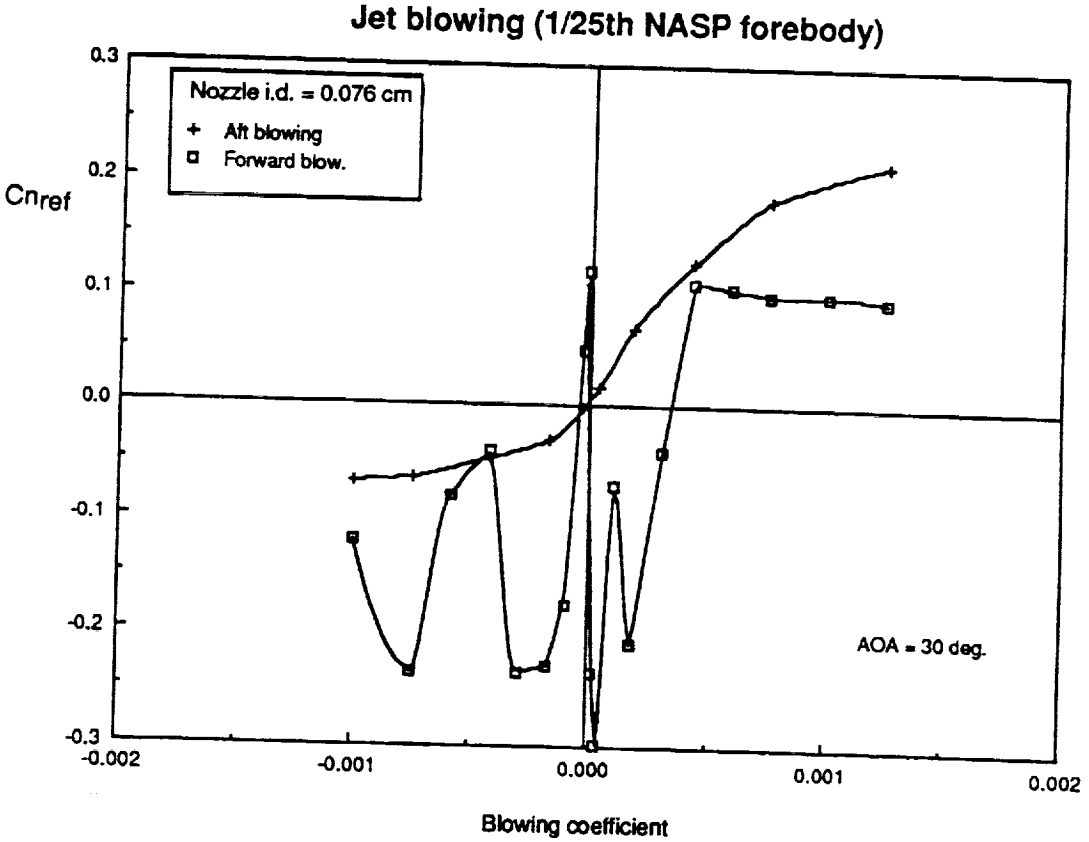

Figure 32 - Comparison Between Aft and Forward Jet Blowing Circular Nozzle, 0.076 cm i.d., $\alpha = 30°$

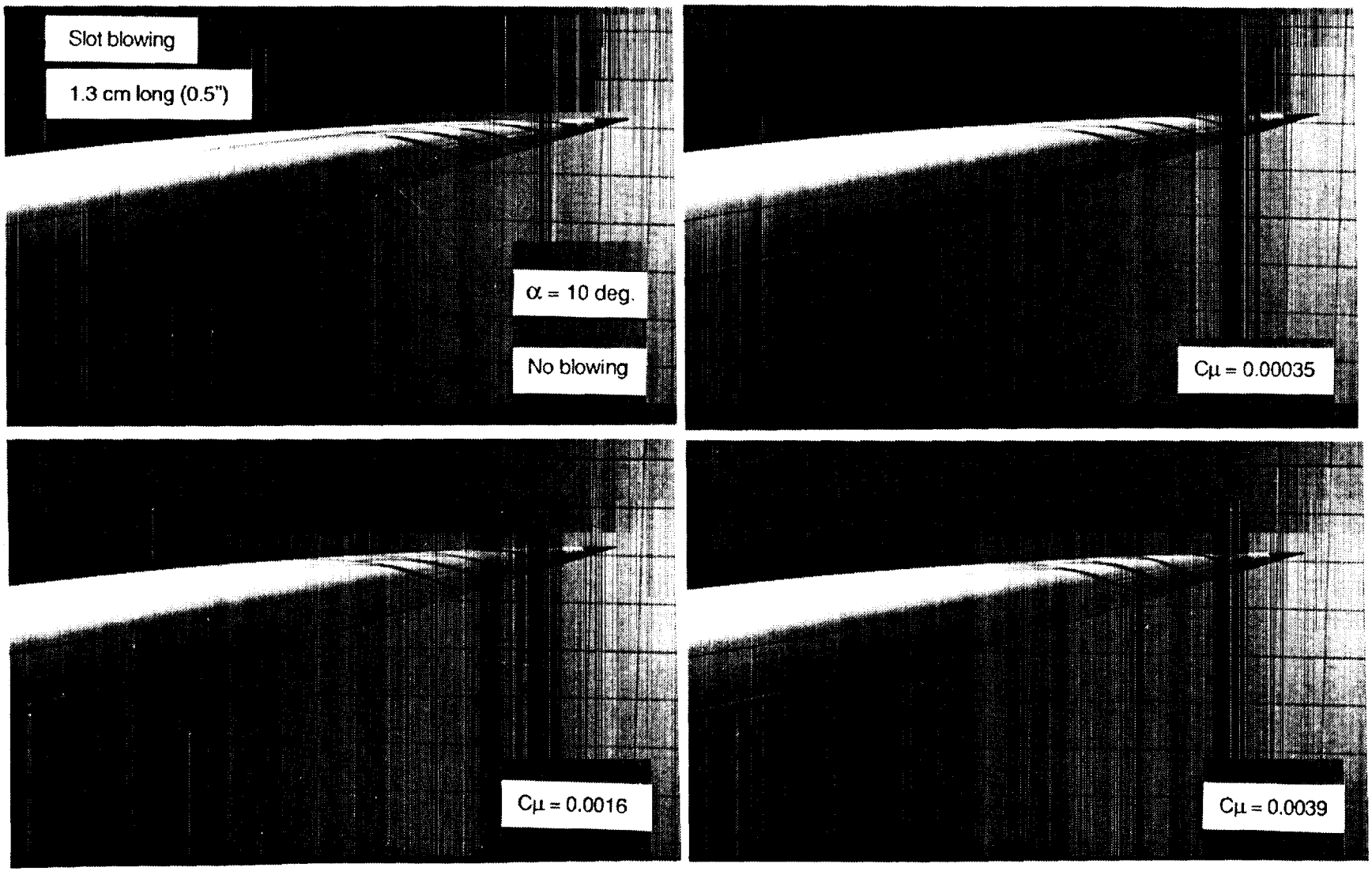

Figure 33 - Effect of Slot Blowing (Right Side, Forebody Model # 2)
1.3 cm long, $\alpha = 10°$

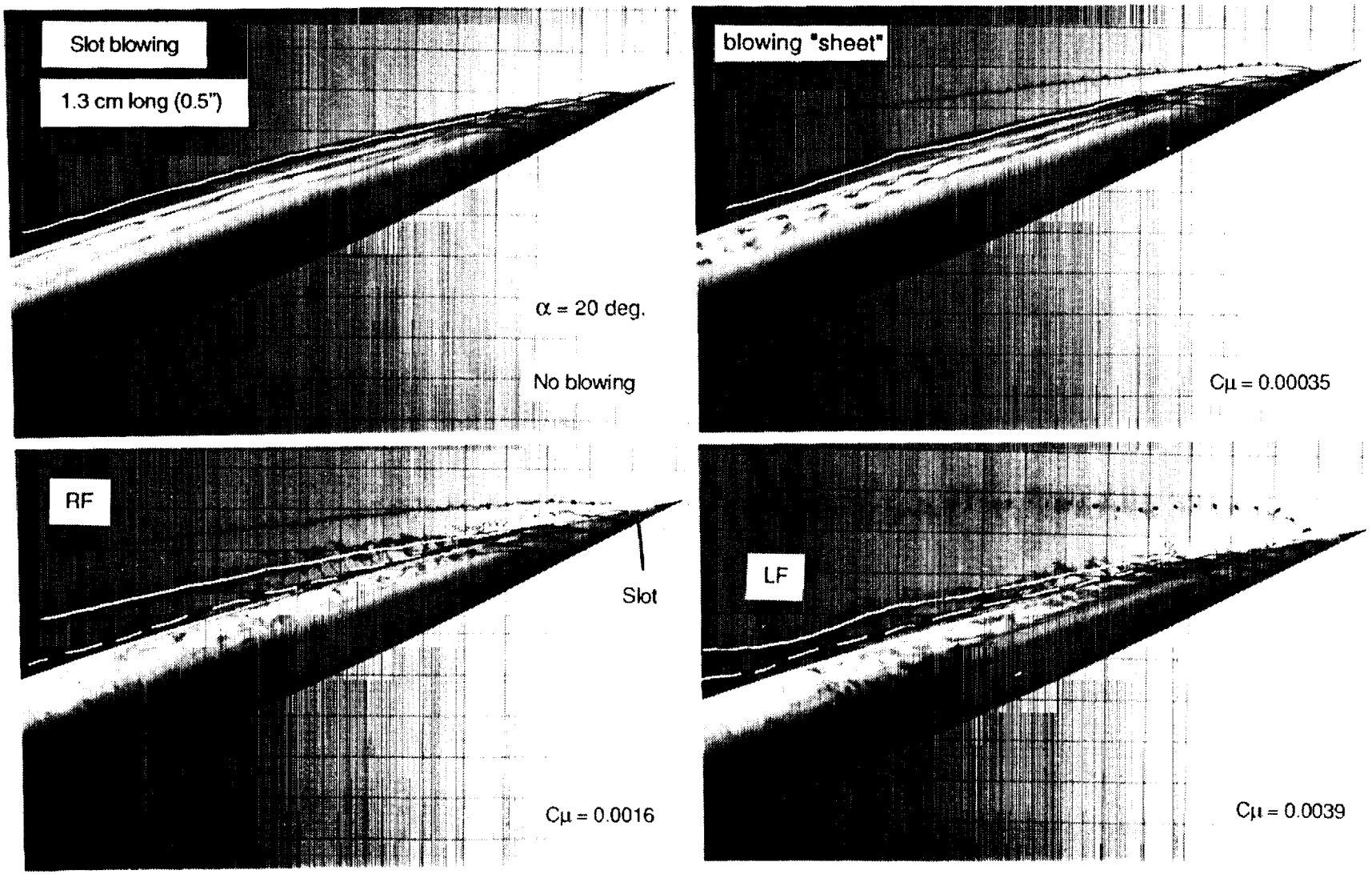

Figure 34 - Effect of Slot Blowing (Right Side, Forebody Model # 2)
1.3 cm long, $\alpha = 20°$

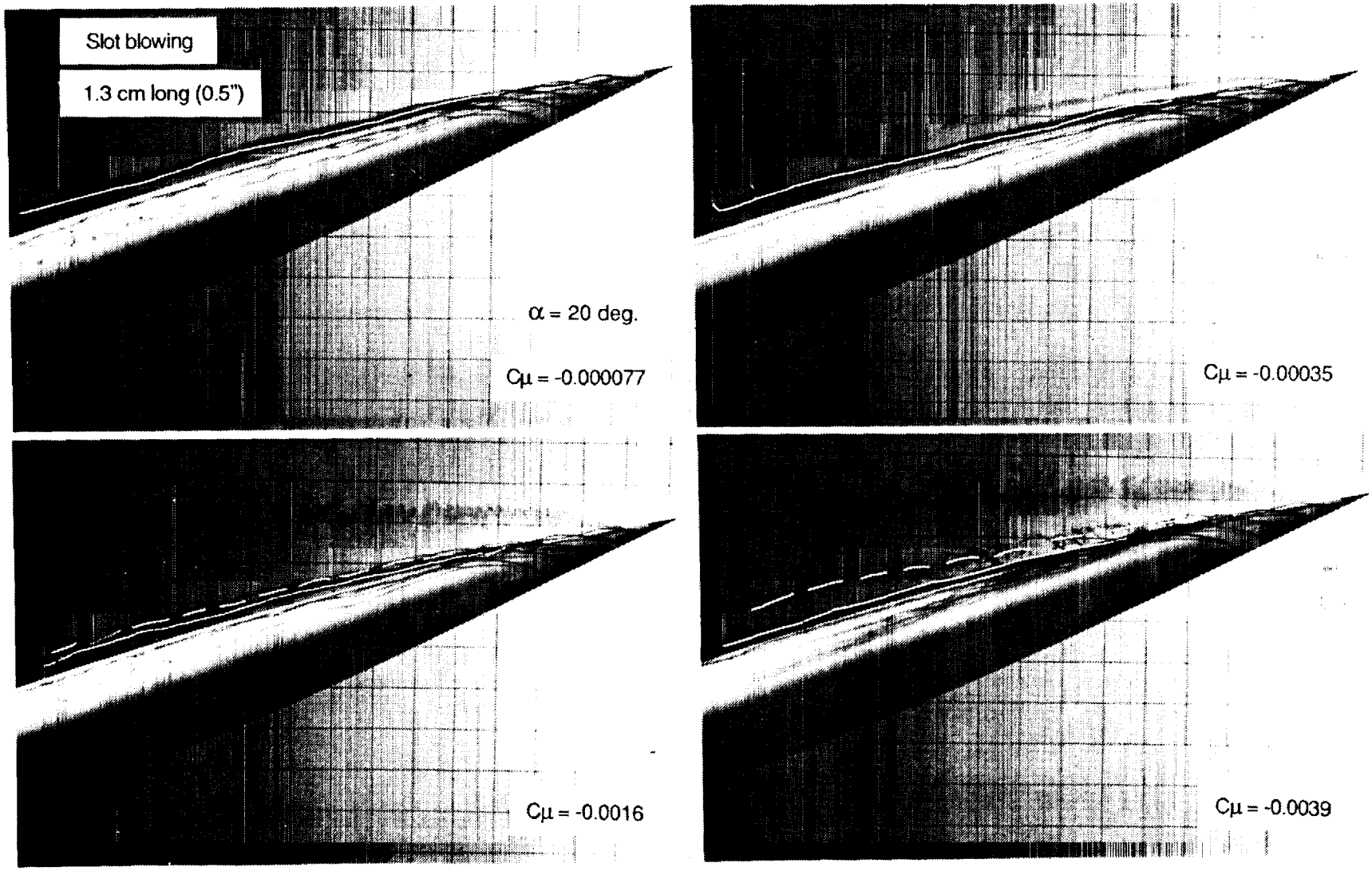

Figure 35 - Effect of Slot Blowing (Left Side, Forebody Model # 2)
1.3 cm long, $\alpha = 20°$

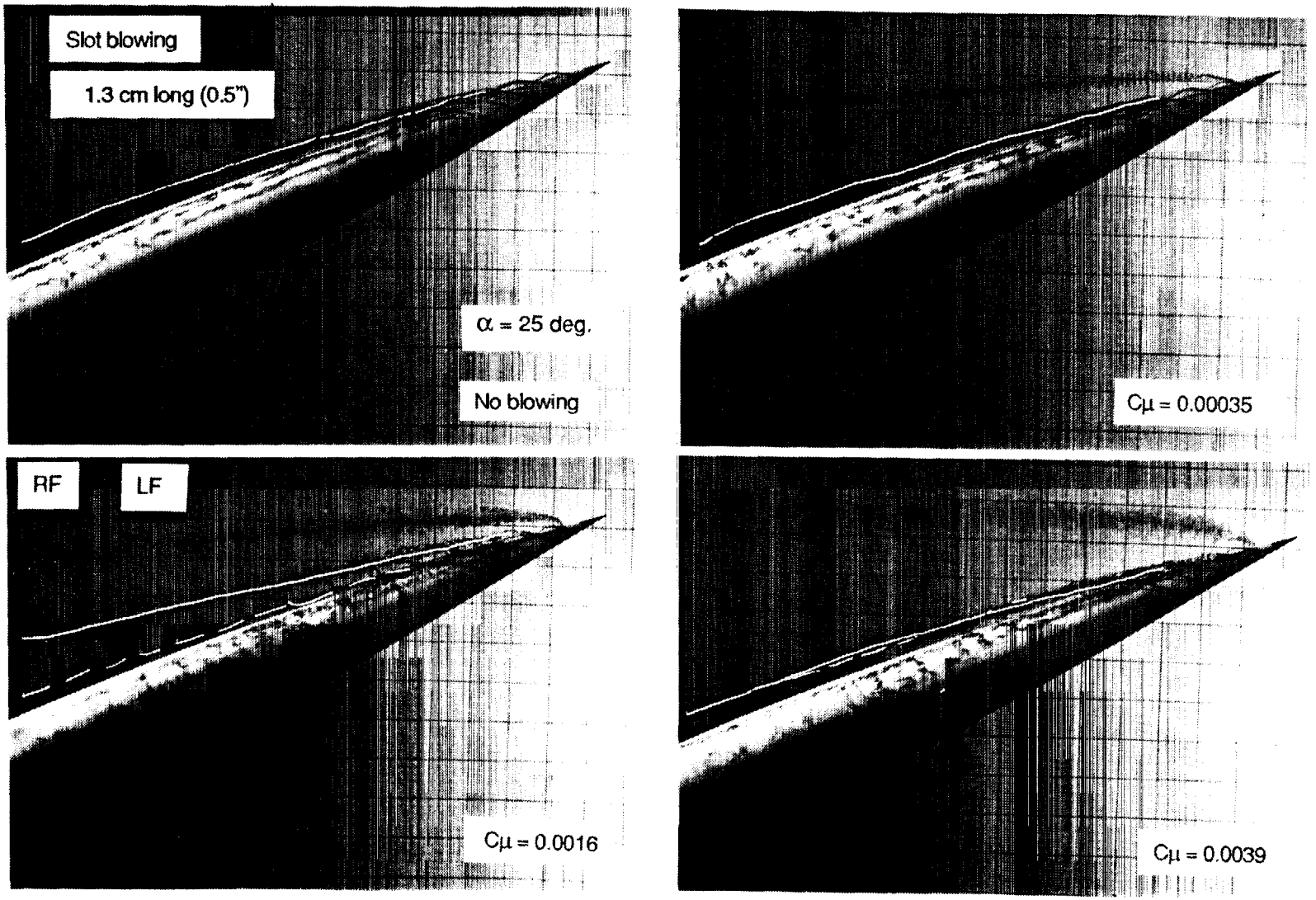

Figure 36 - Effect of Slot Blowing (Right Side, Forebody Model # 2)
1.3 cm long, $\alpha = 25°$

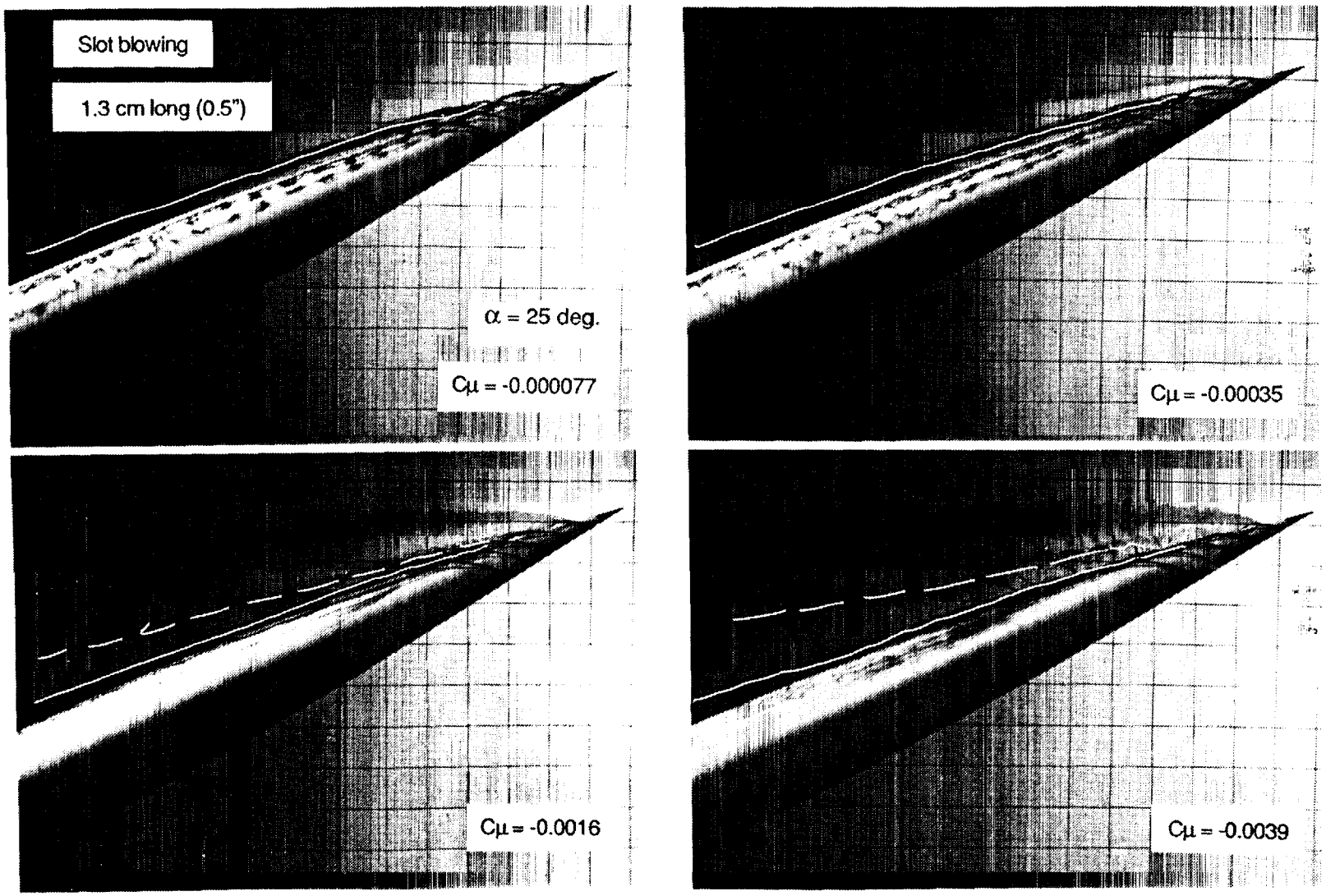

Figure 37 - Effect of Slot Blowing (Left Side, Forebody Model # 2)
1.3 cm long, $\alpha = 25°$

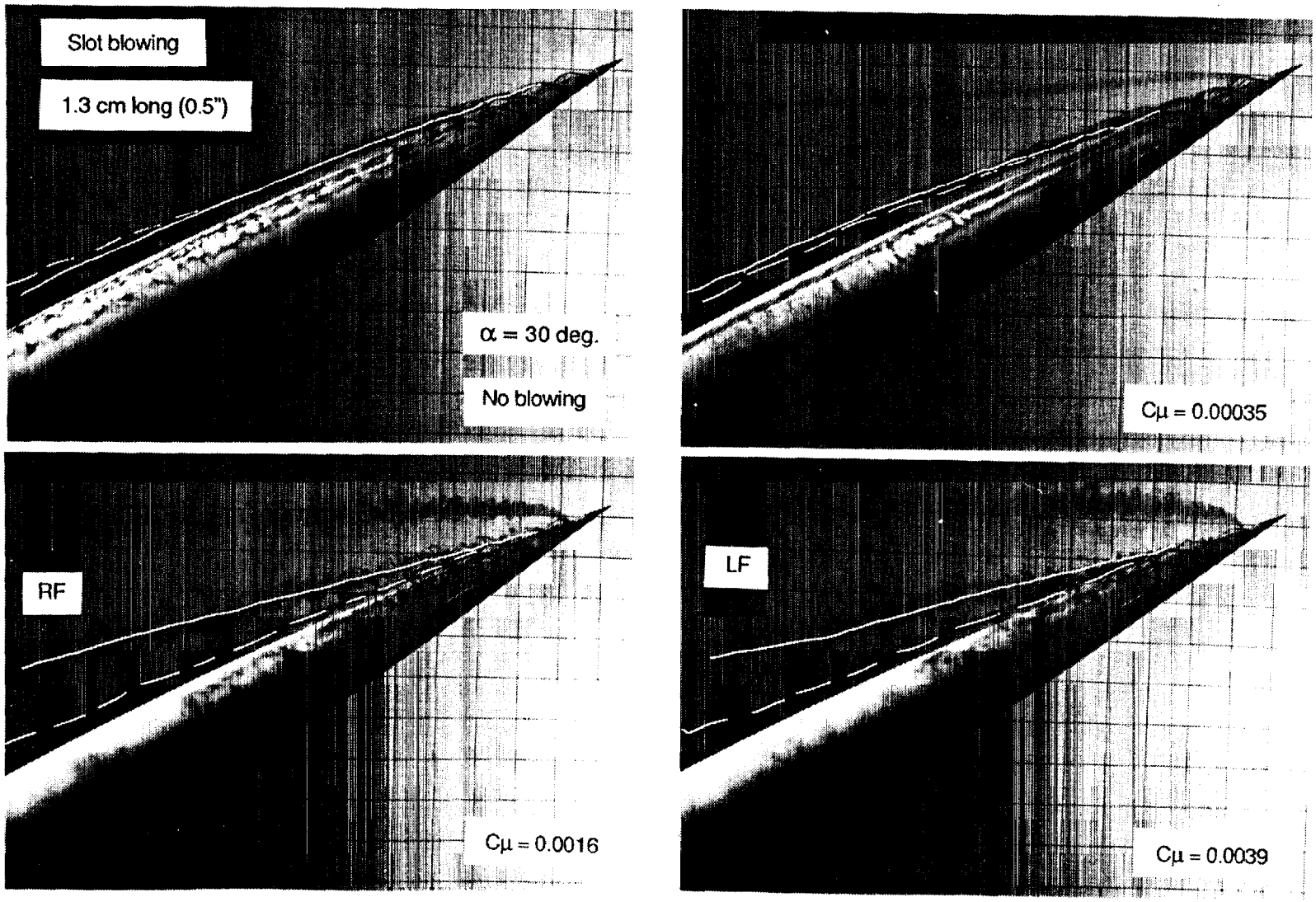

Figure 38 - Effect of Slot Blowing (Right Side, Forebody Model # 2)
1.3 cm long, $\alpha = 30°$

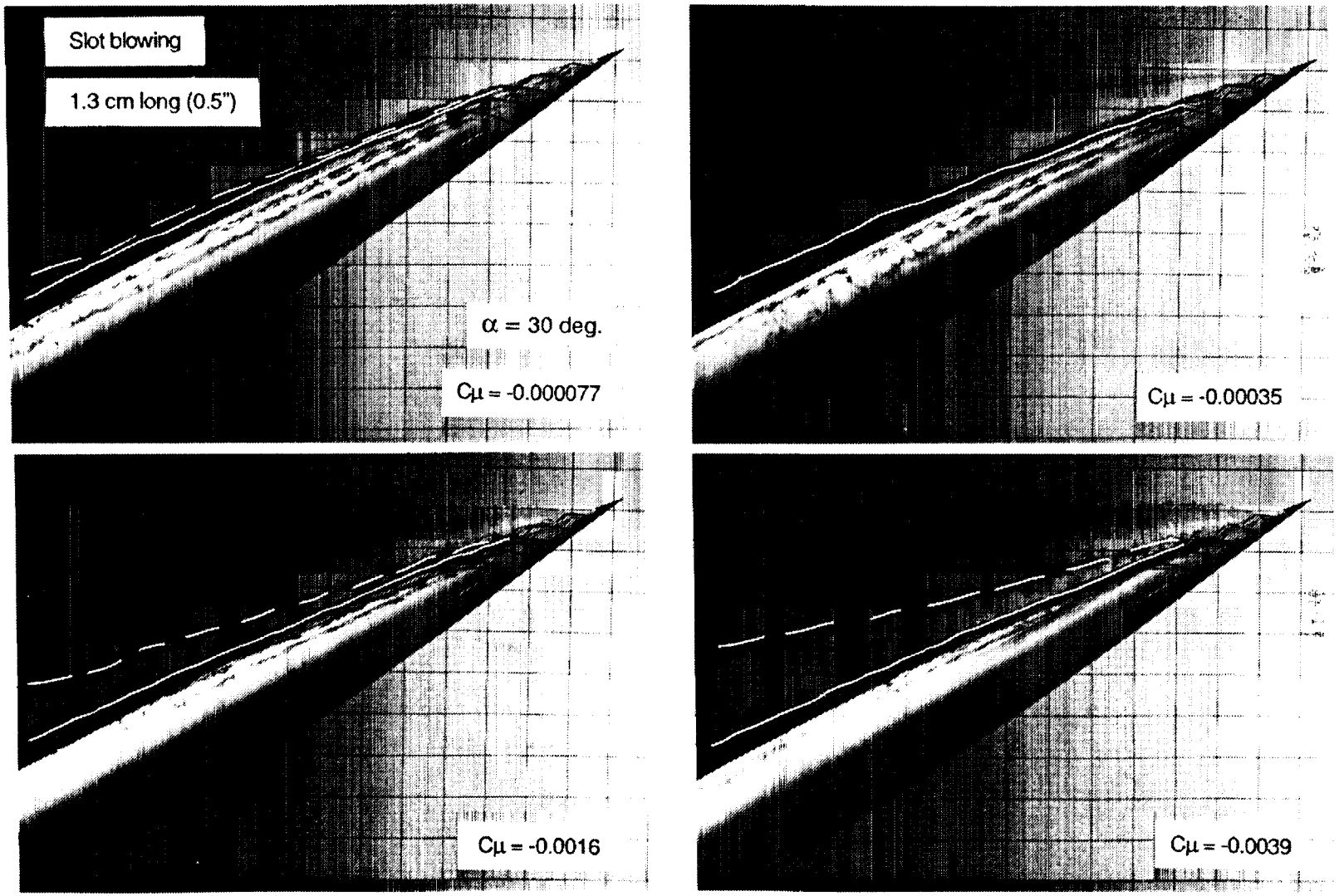

Figure 39 - Effect of Slot Blowing (Left Side, Forebody Model # 2)
1.3 cm long, $\alpha = 30°$

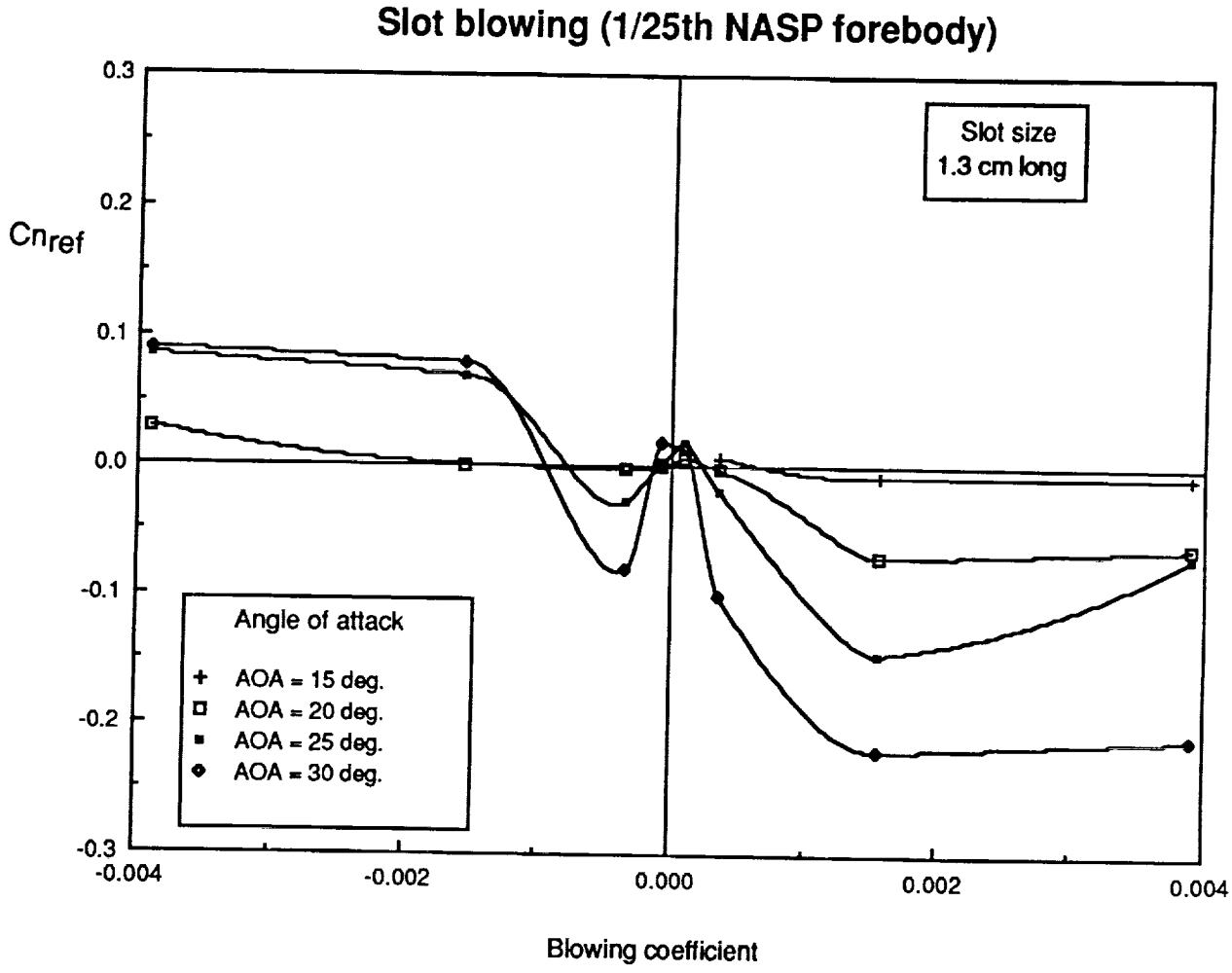

Figure 40 - Change in Reference Yawing Moment Produced by Slot Blowing 1.3 cm long, Forebody Model # 2

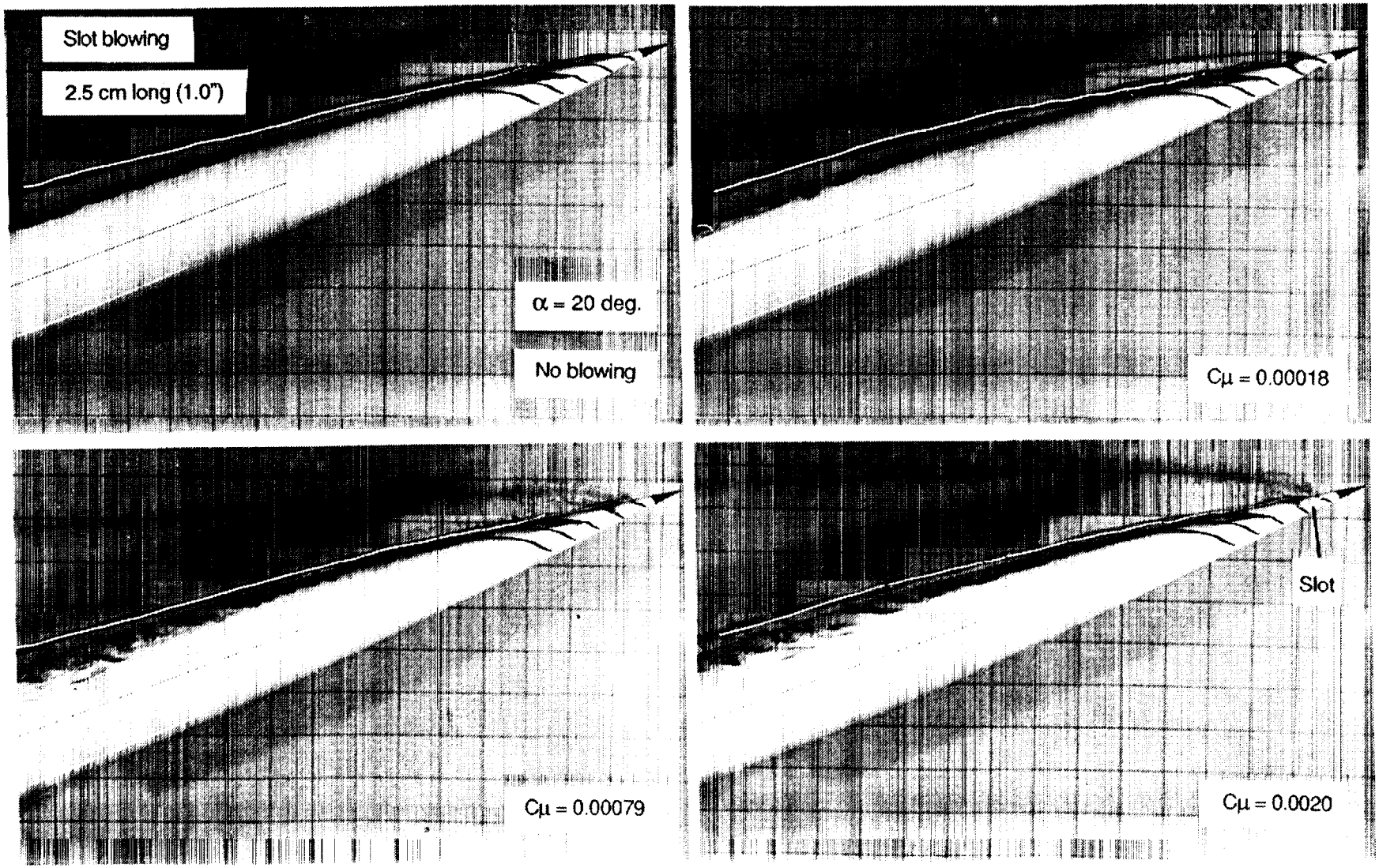

Figure 41 - Effect of Slot Blowing (Right Side, Forebody Model # 2)
2.5 cm long, $\alpha = 20°$

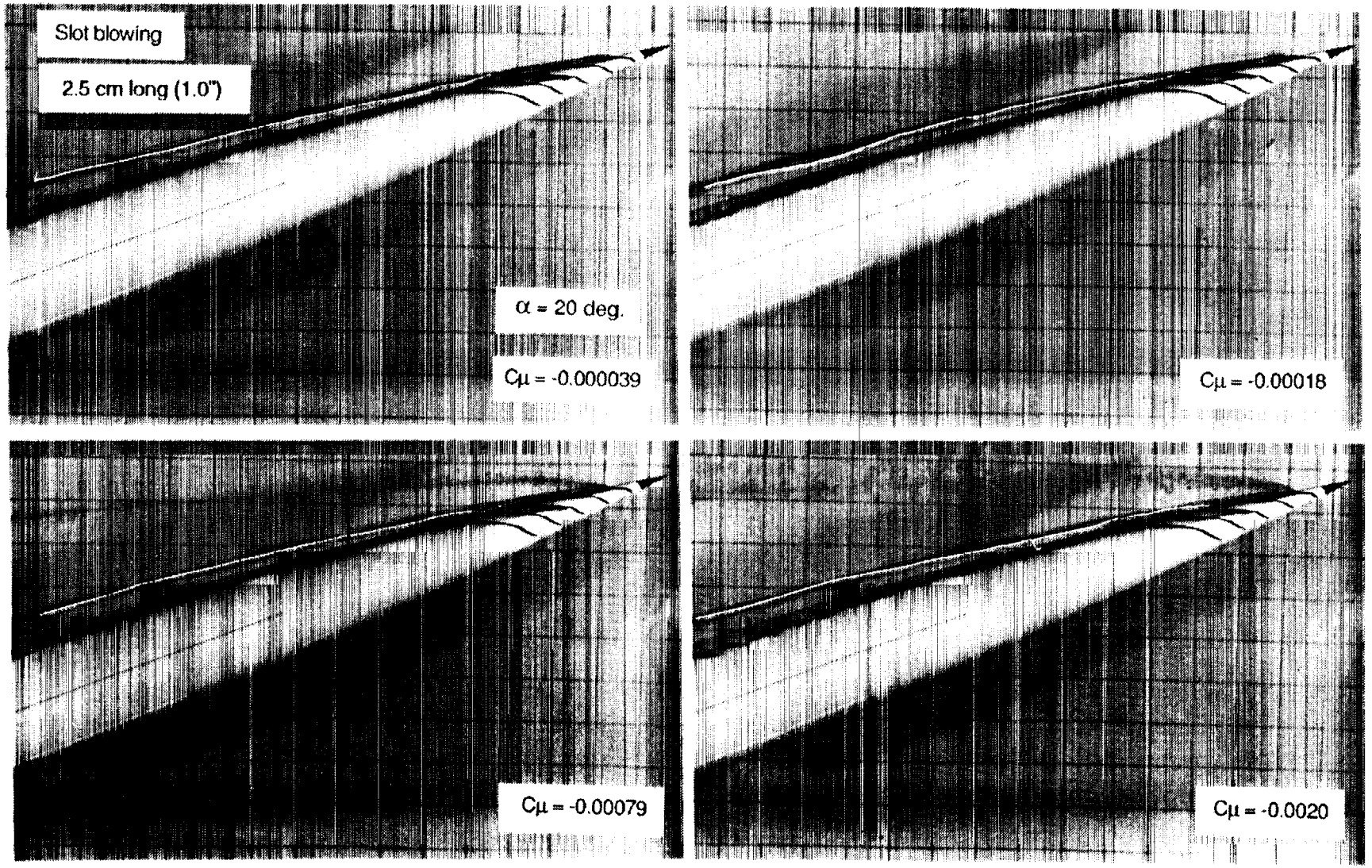

Figure 42 - Effect of Slot Blowing (Left Side, Forebody Model # 2)
2.5 cm long, $\alpha = 20^{\circ}$

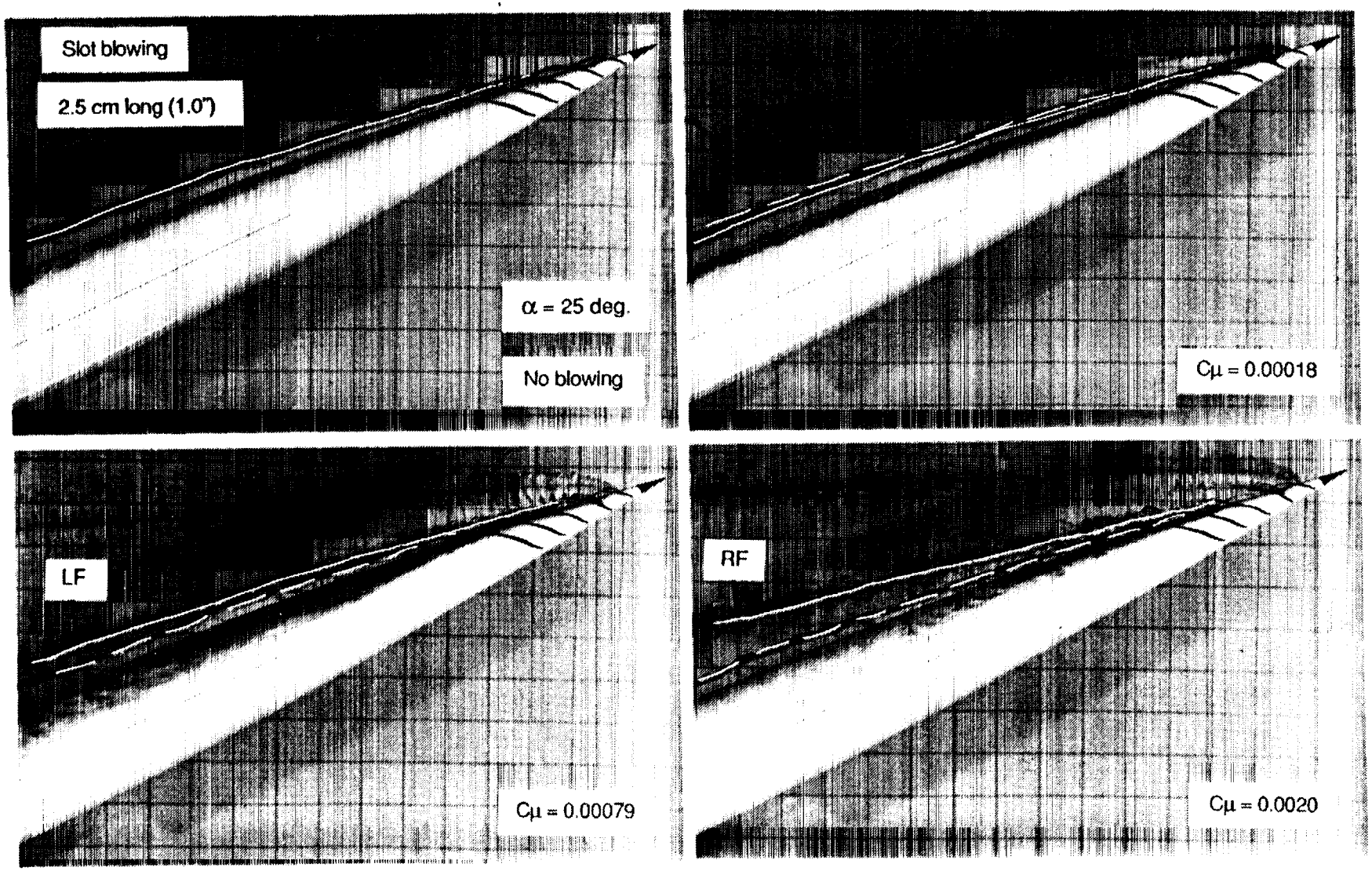

Figure 43 - Effect of Slot Blowing (Right Side, Forebody Model # 2)
2.5 cm long, $\alpha = 25^{\circ}$

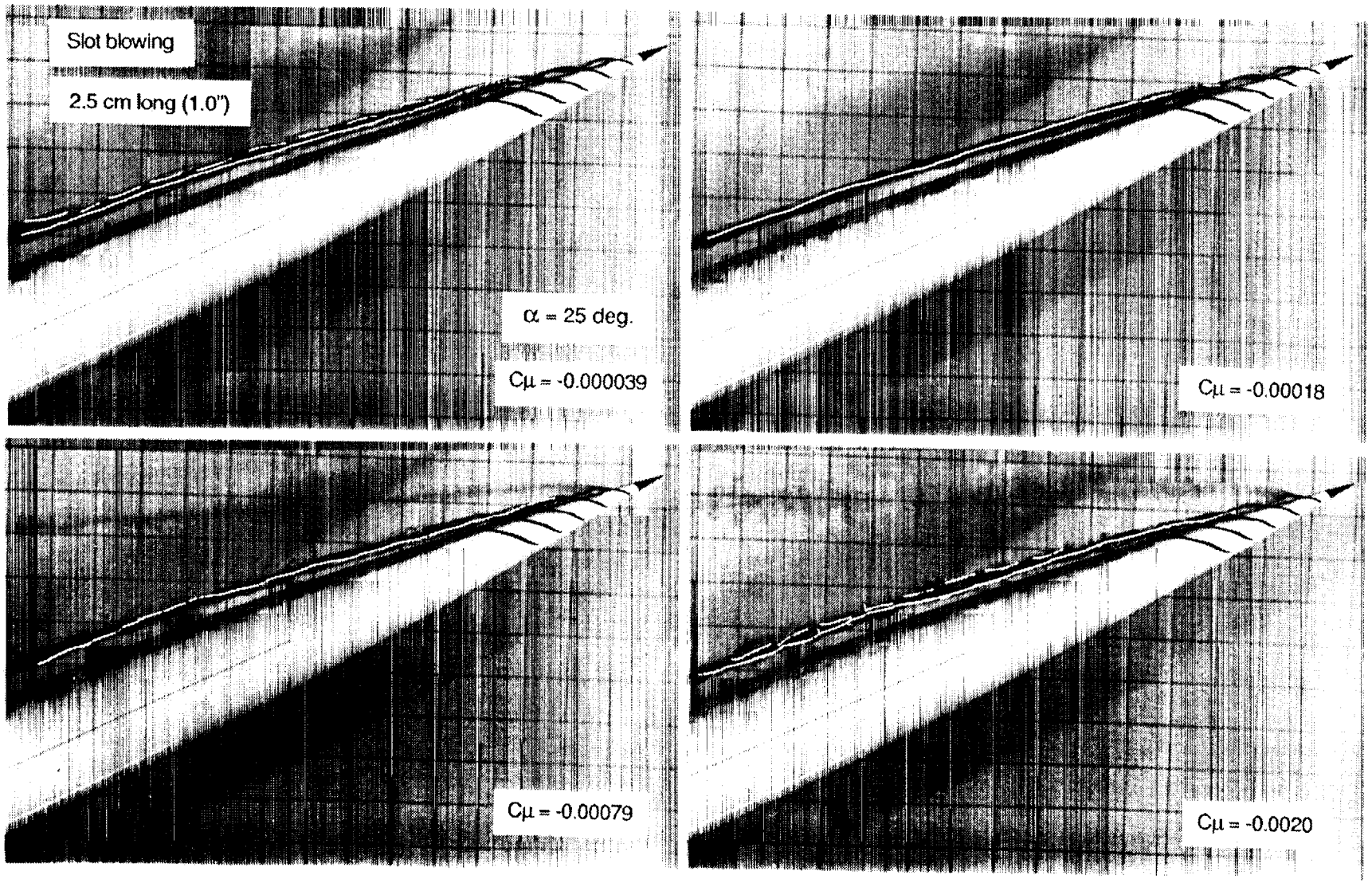

Figure 44 - Effect of Slot Blowing (Left Side, Forebody Model # 2)
2.5 cm long, $\alpha = 25°$

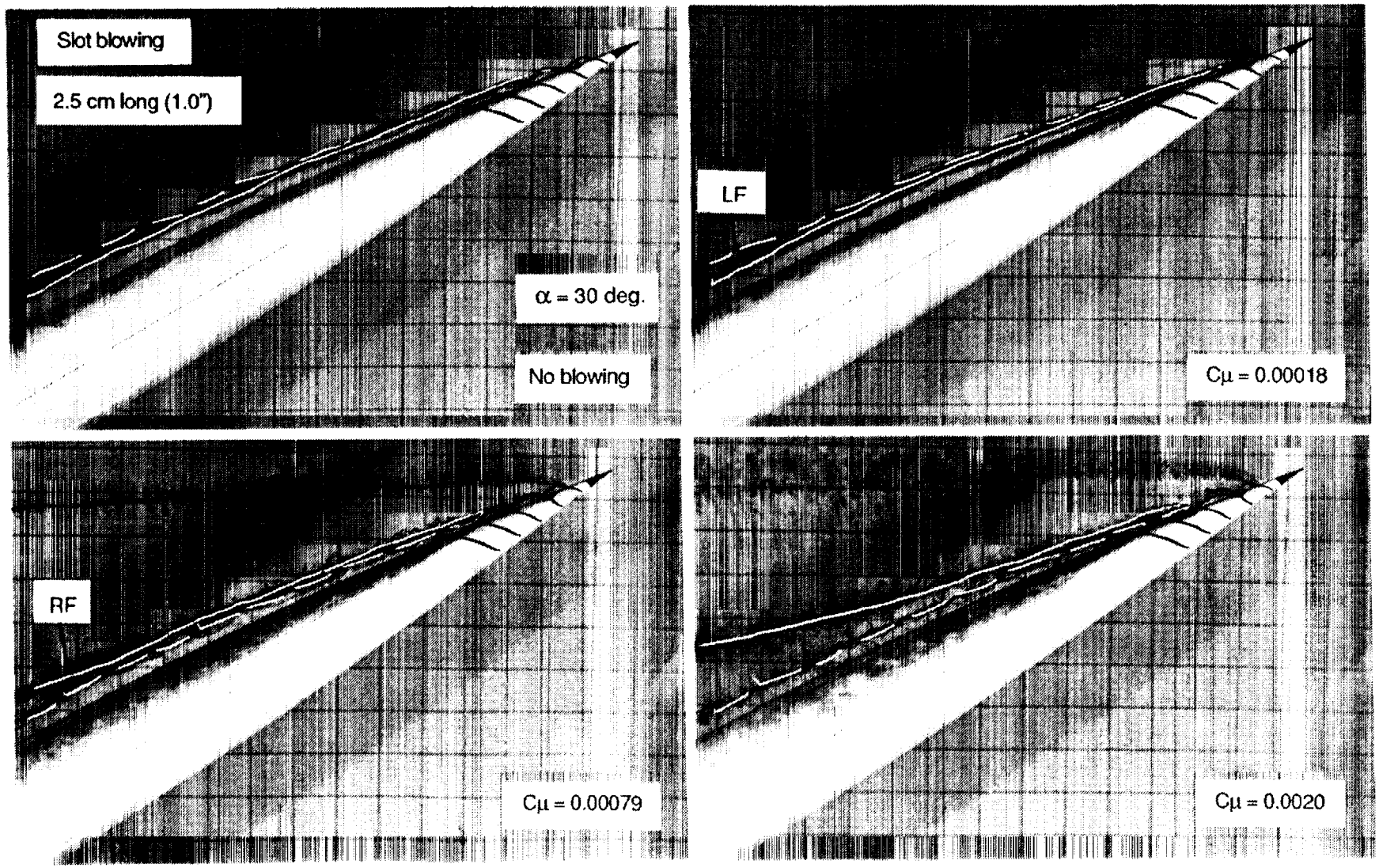

Figure 45 - Effect of Slot Blowing (Right Side, Forebody Model # 2)
2.5 cm long, $\alpha = 30^{o}$

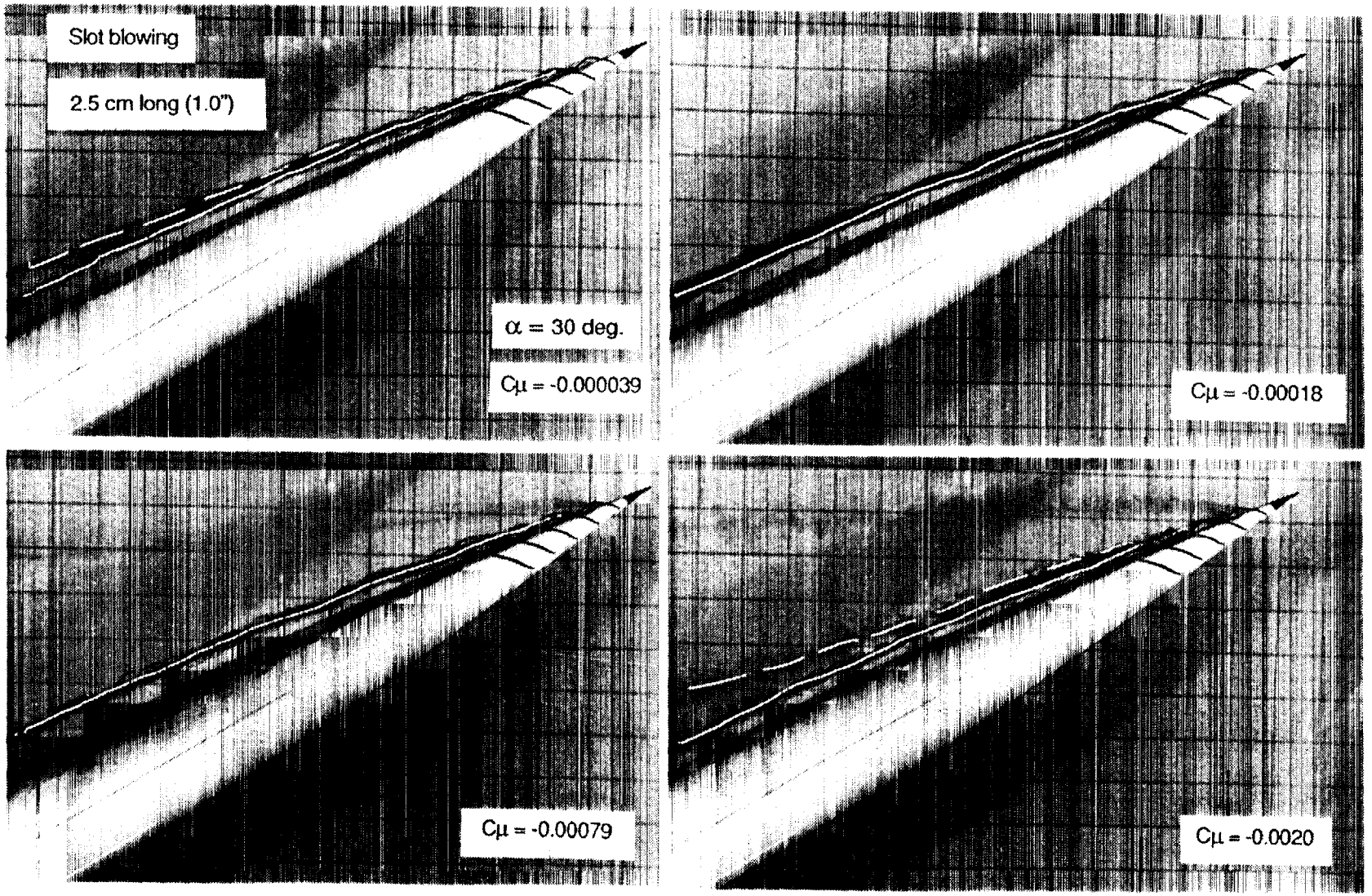

Figure 46 - Effect of Slot Blowing (Left Side, Forebody Model # 2)
2.5 cm long, $\alpha = 30°$

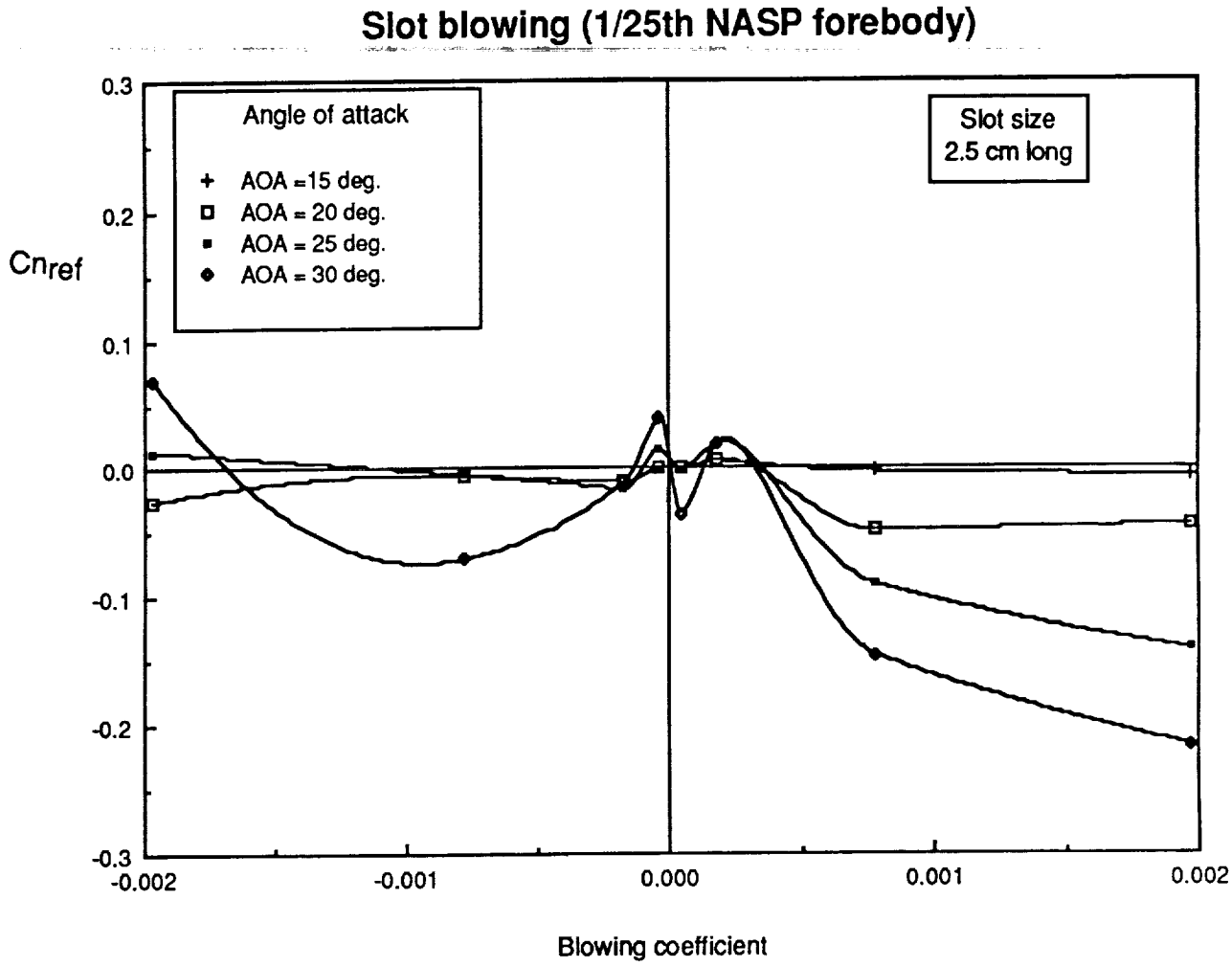

Figure 47 - Change in Reference Yawing Moment Produced by Slot Blowing 2.5 cm long, Forebody Model # 2

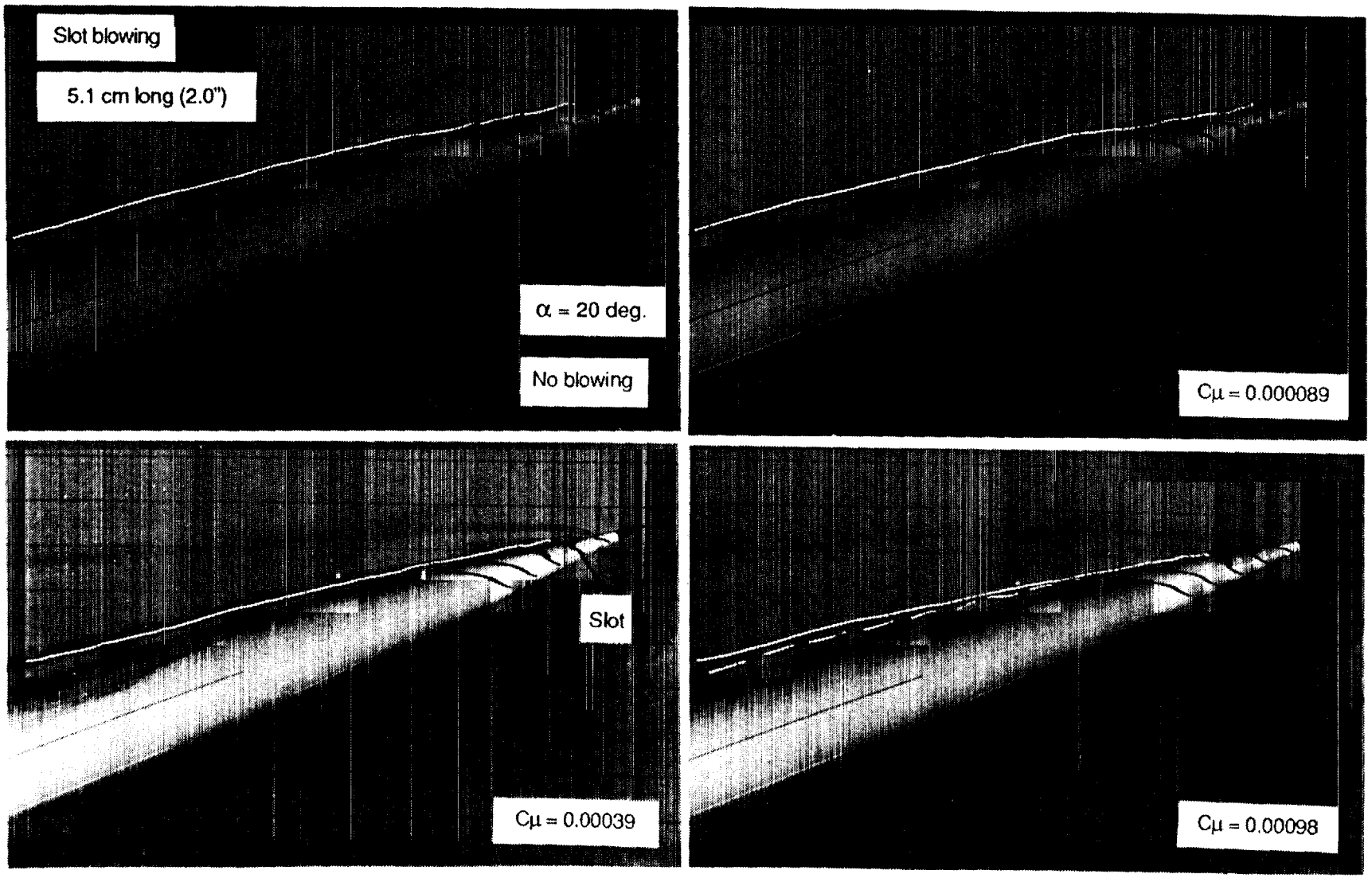

Figure 48 - Effect of Slot Blowing (Right Side, Forebody Model # 2)
5.1 cm long, $\alpha = 20^{\circ}$

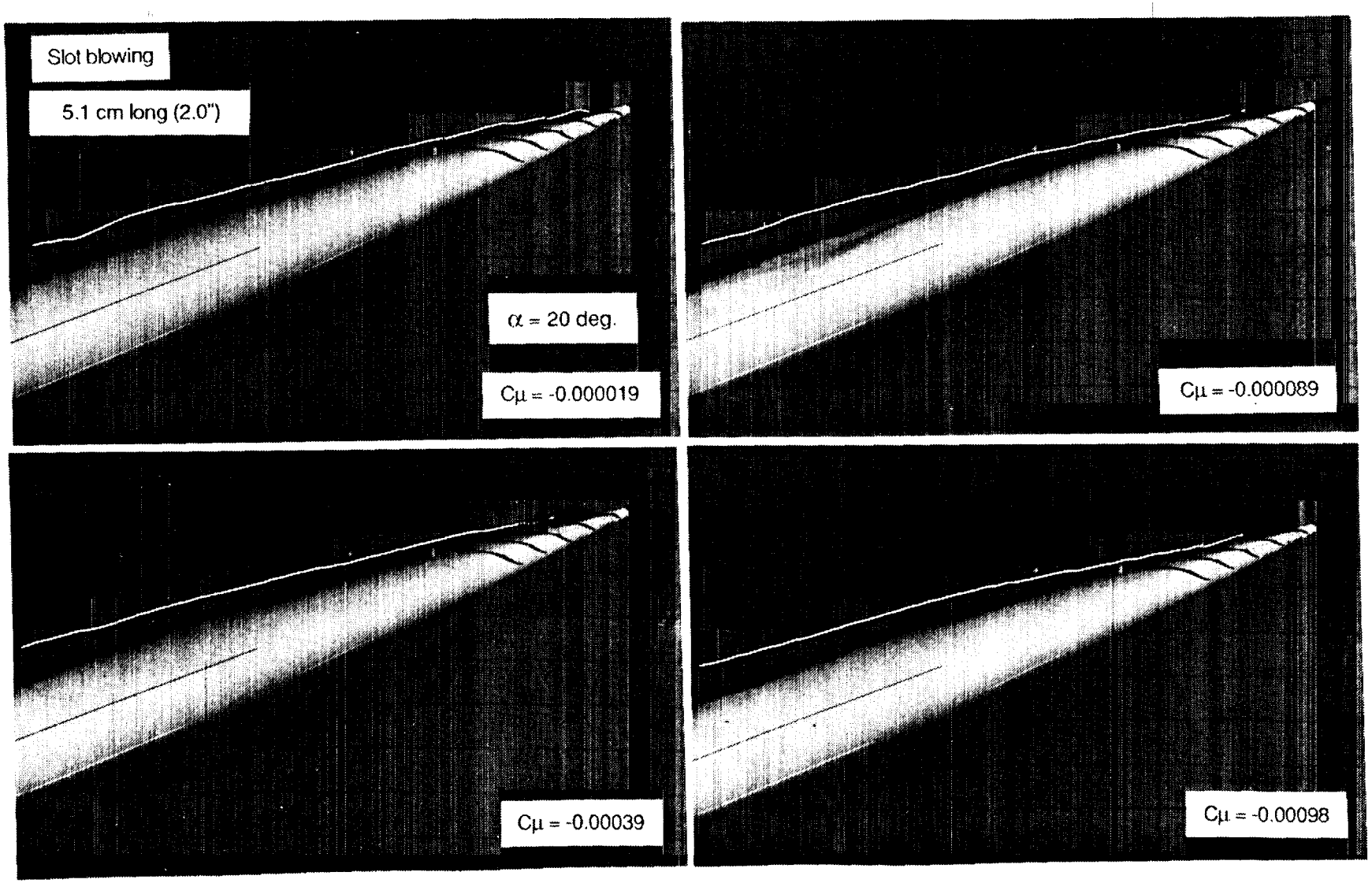

Figure 49 - Effect of Slot Blowing (Left Side, Forebody Model # 2)
5.1 cm long, $\alpha = 20°$

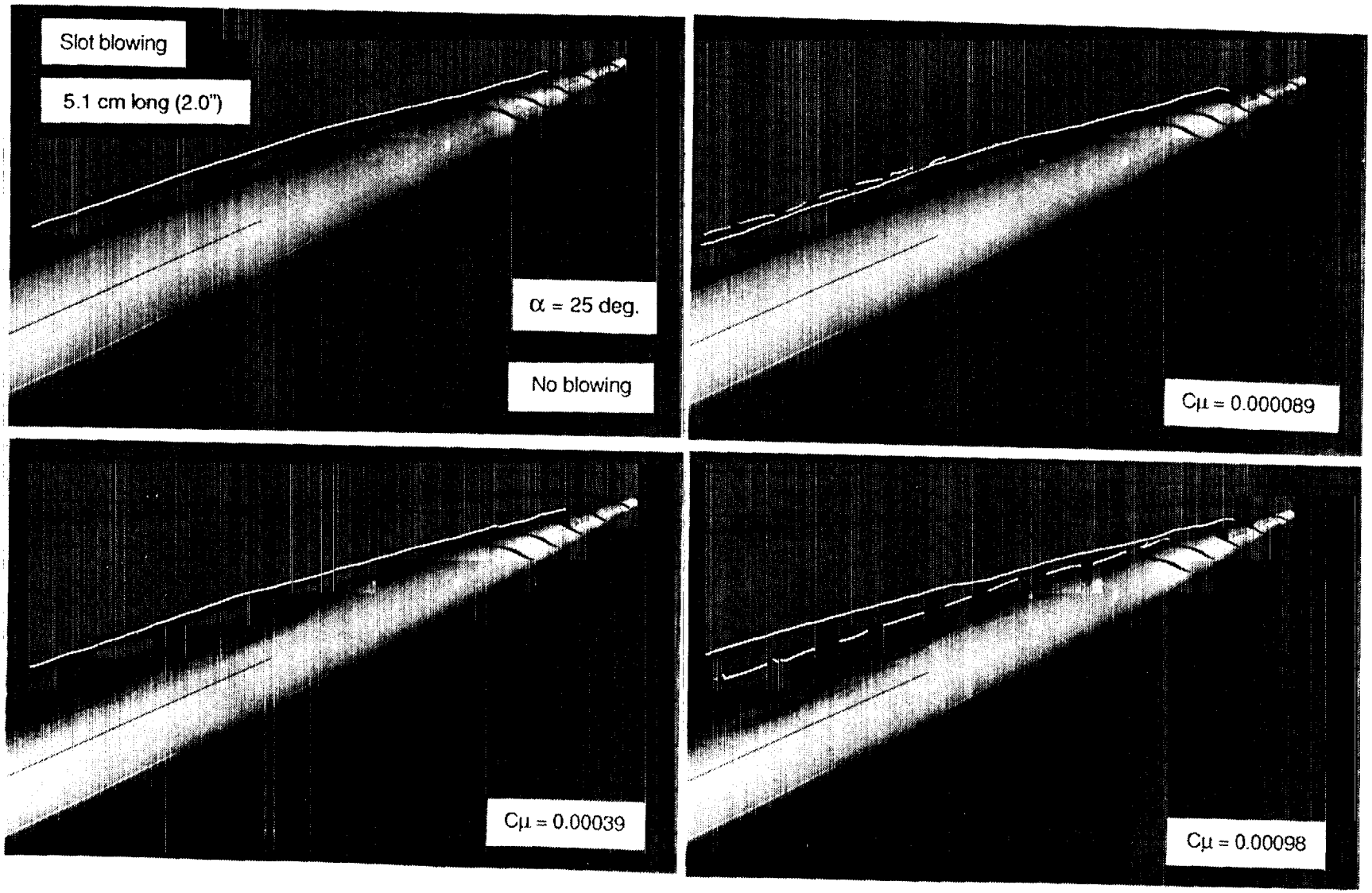

Figure 50 - Effect of Slot Blowing (Right Side, Forebody Model # 2)
5.1 cm long, $\alpha = 25°$

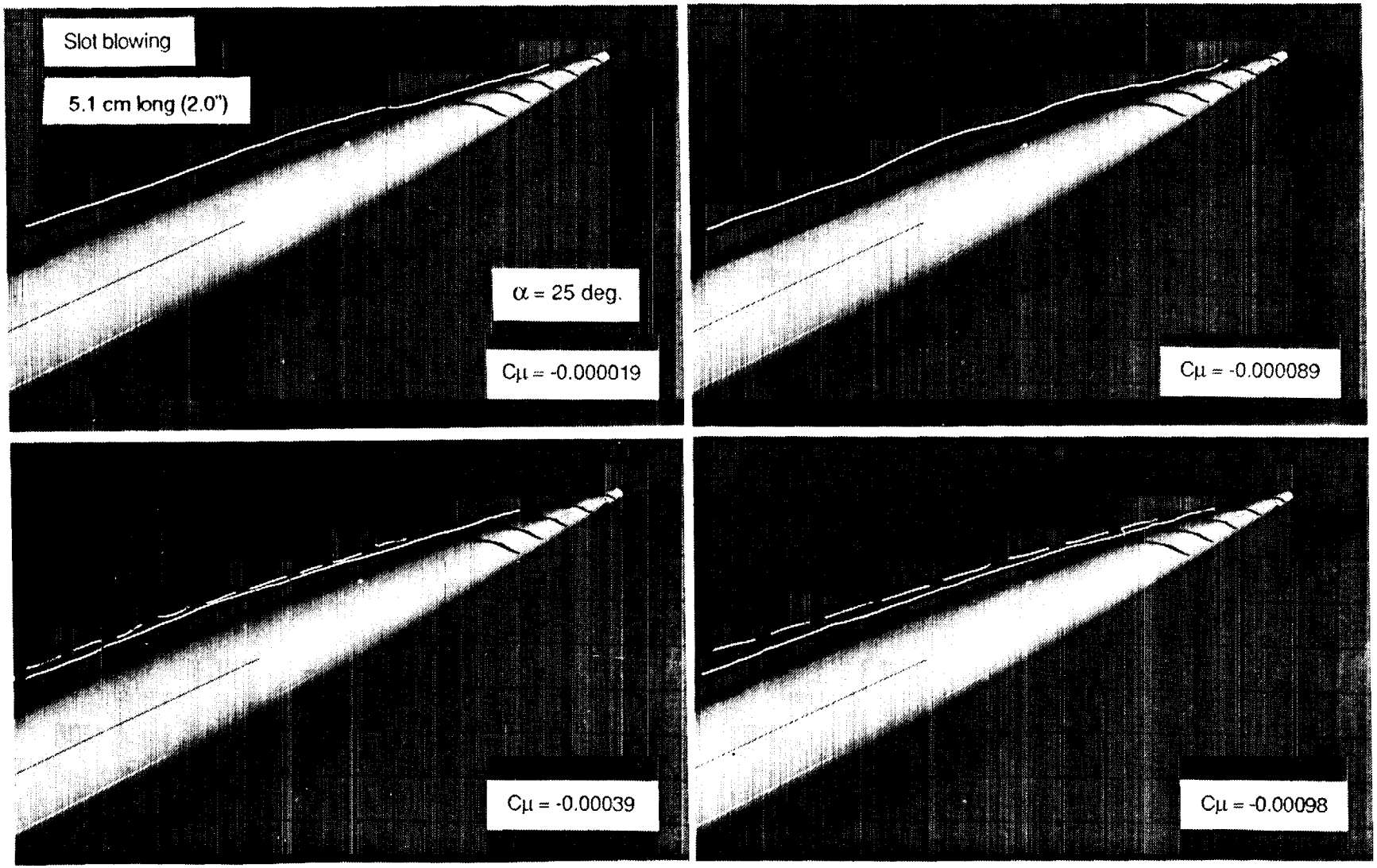

Figure 51 - Effect of Slot Blowing (Left Side, Forebody Model # 2)
5.1 cm long, $\alpha = 25^{\circ}$

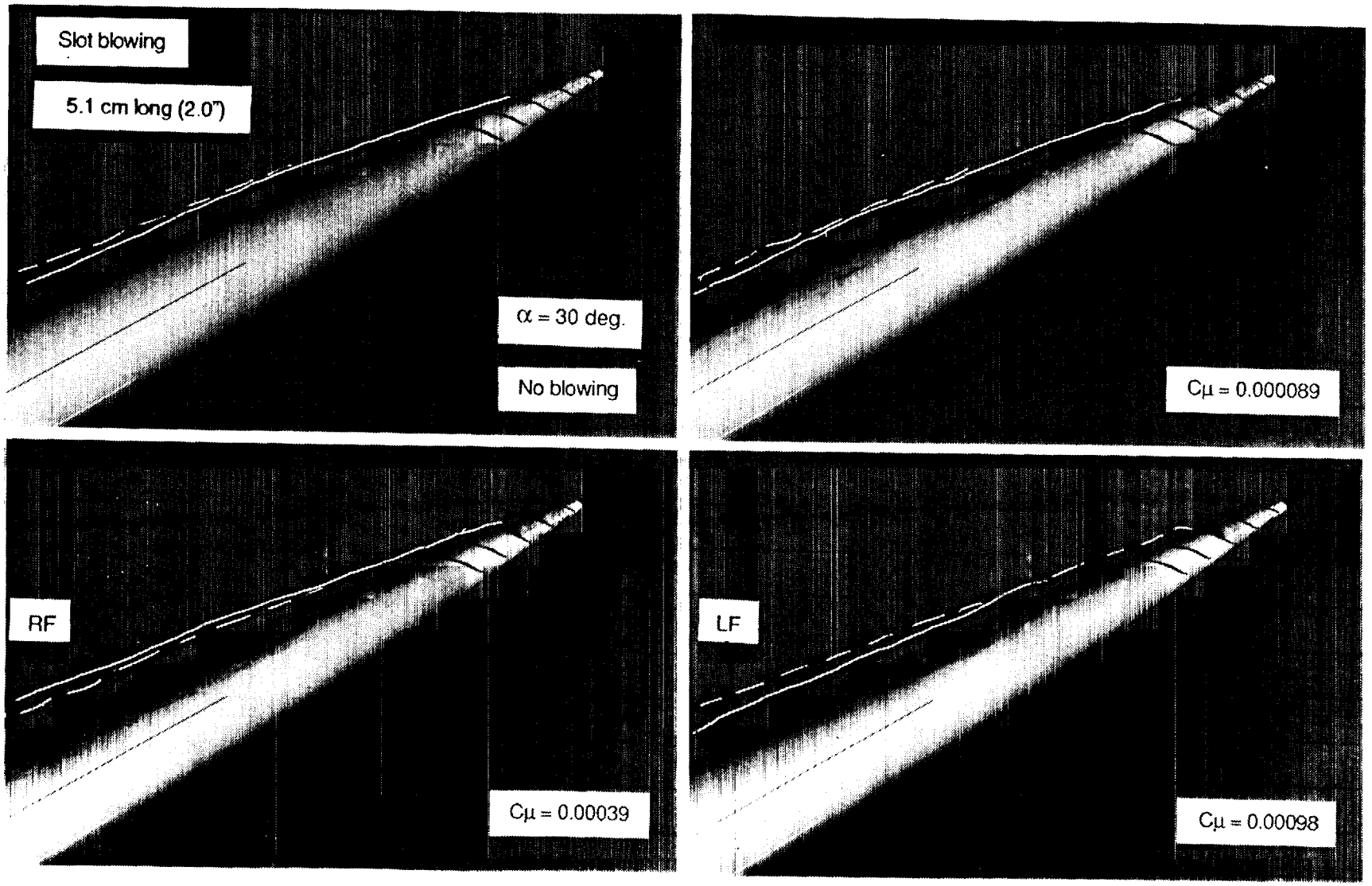

Figure 52 - Effect of Slot Blowing (Right Side, Forebody Model # 2)
5.1 cm long, $\alpha = 30°$

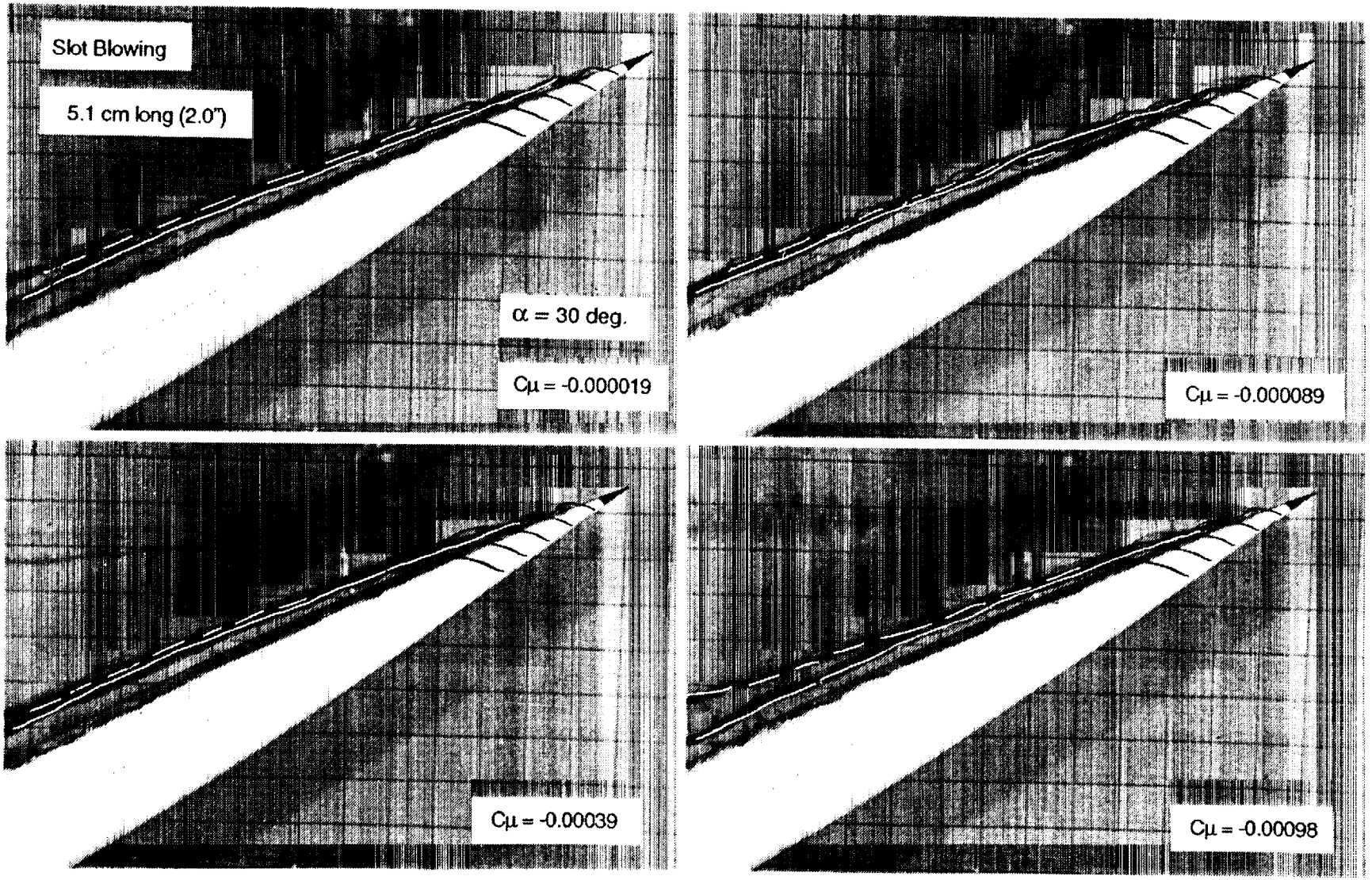

Figure 53 - Effect of Slot Blowing (Left Side, Forebody Model # 2)
5.1 cm long, $\alpha = 30^{\circ}$

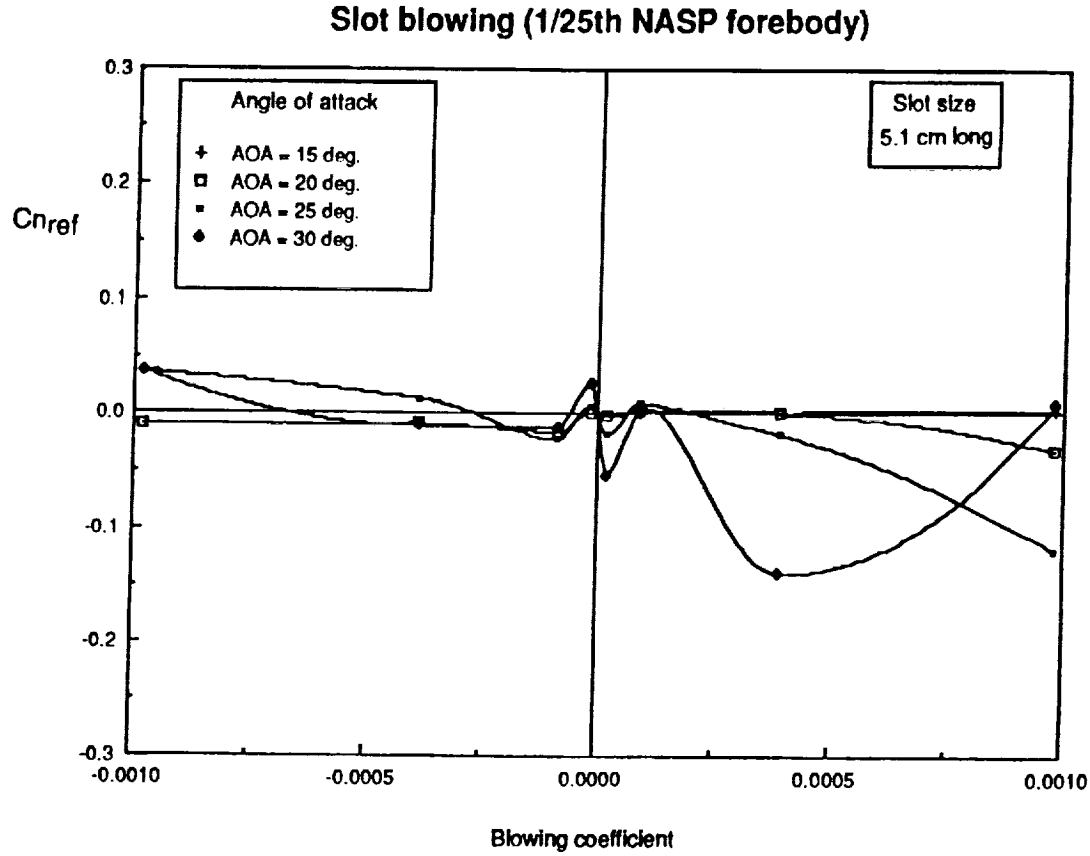

Figure 54 - Change in Reference Yawing Moment Produced by Slot Blowing 5.1 cm long, Forebody Model # 2

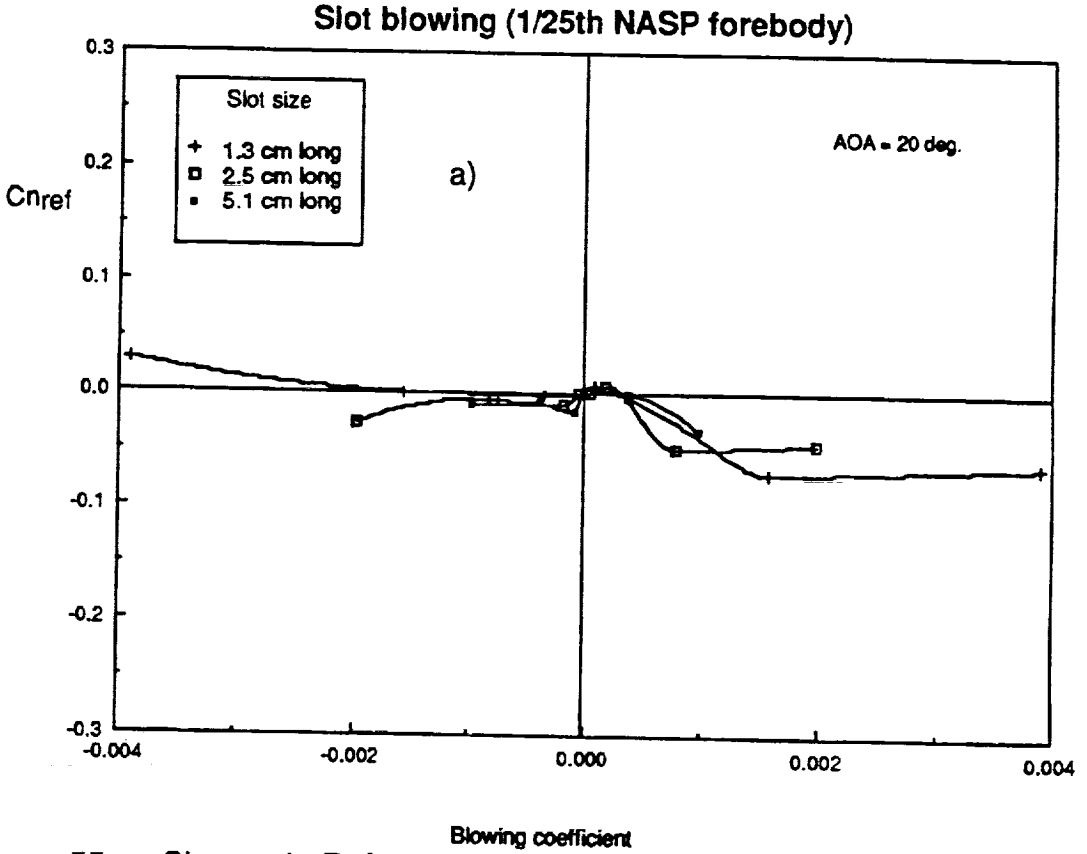

Figure 55 - Change in Reference Yawing Moment Produced by Slot Blowing Effect of Slot Length at a) $\alpha = 20°$, b) $\alpha = 25°$ and c) $\alpha = 30°$

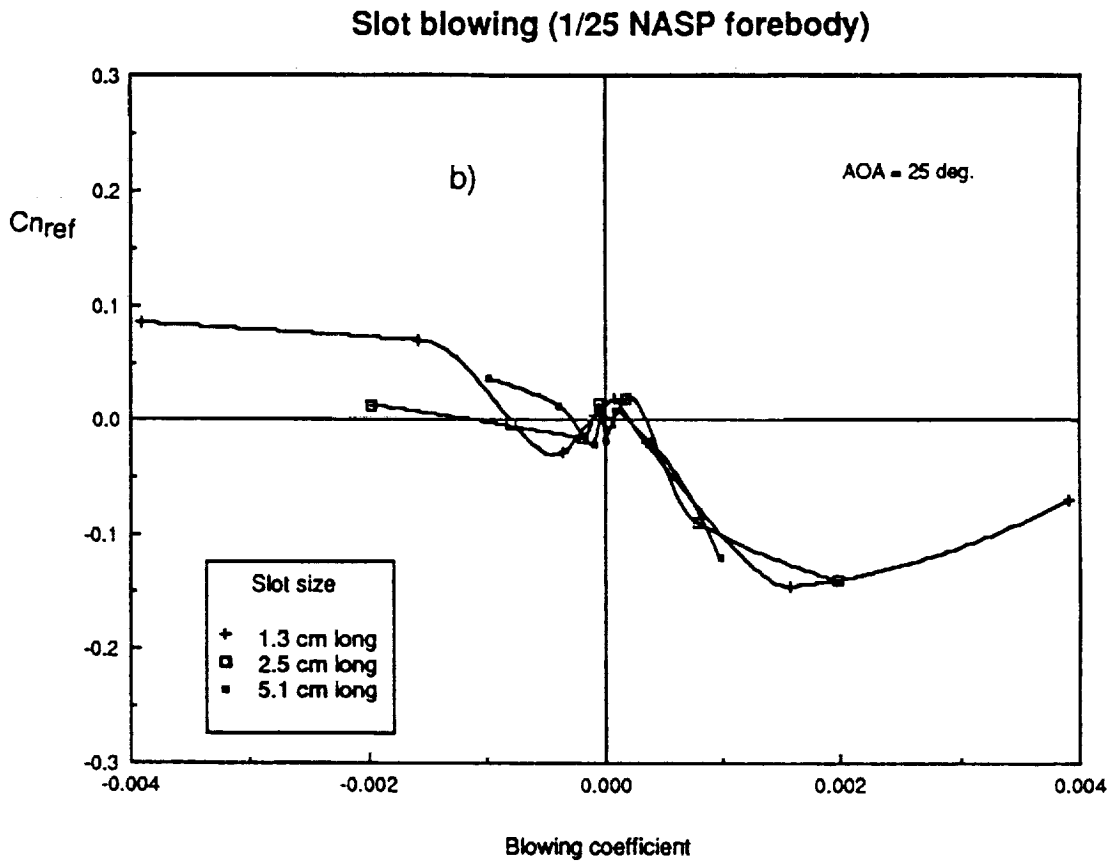

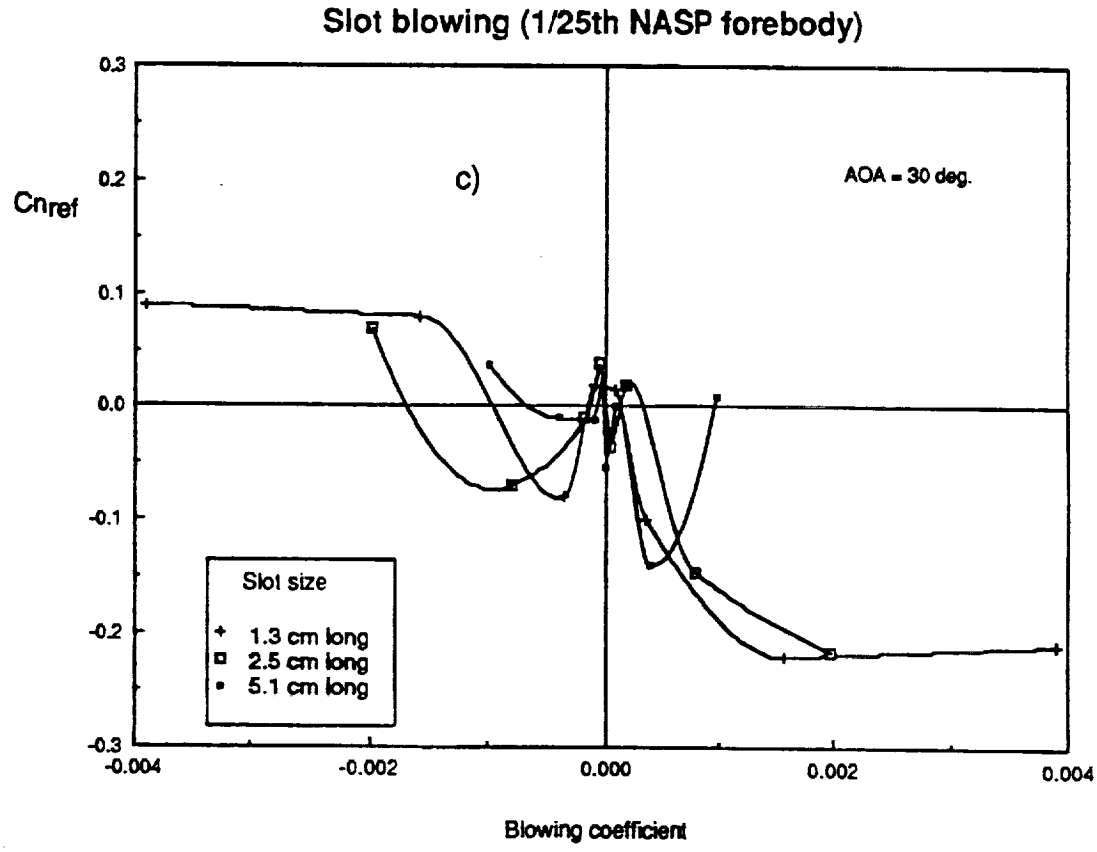

Figure 55 - Concluded

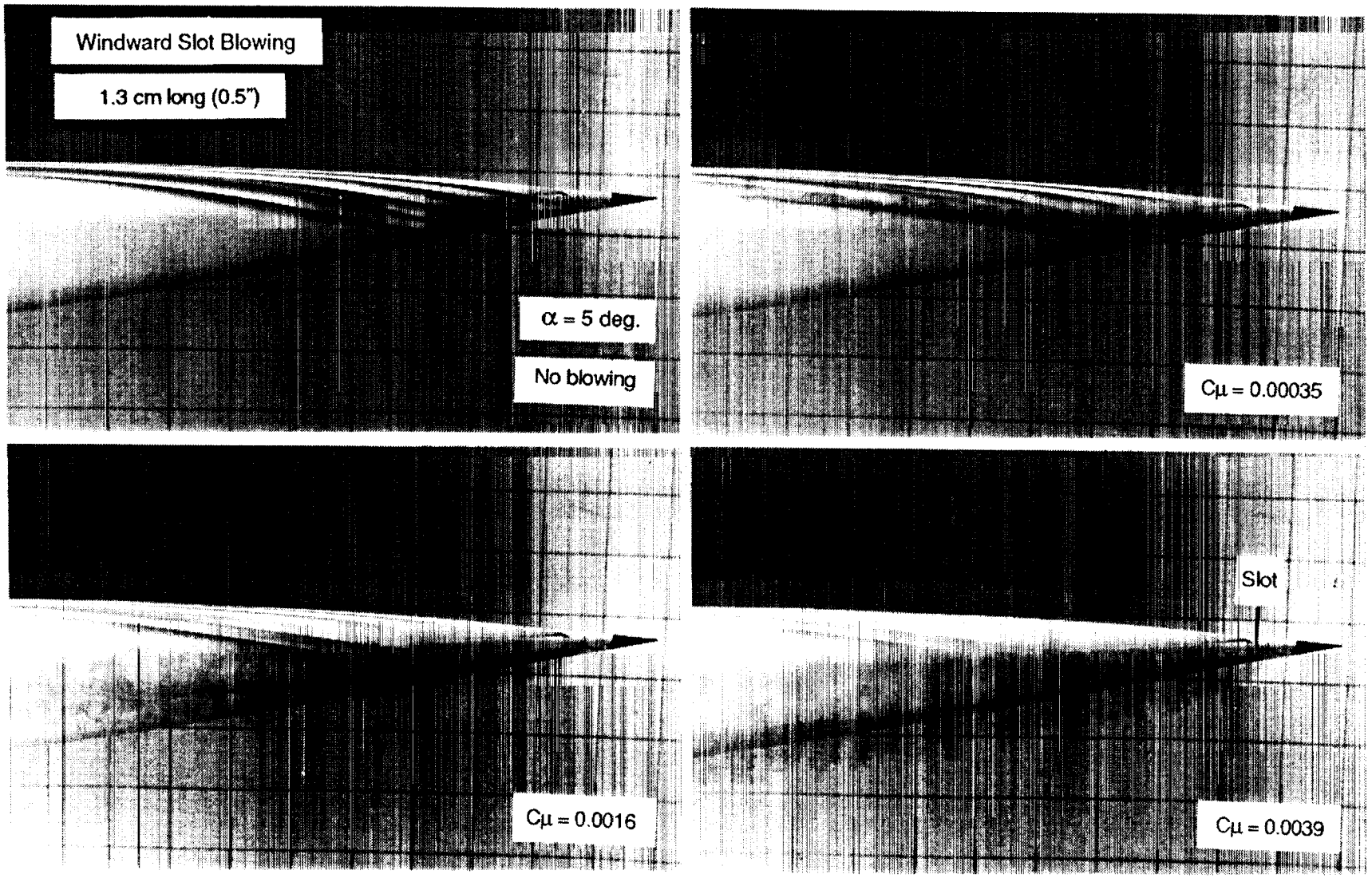

Figure 56 - Effect of Windward Slot Blowing (Right Side, Forebody Model # 2)
1.3 cm long, $\alpha = 5°$

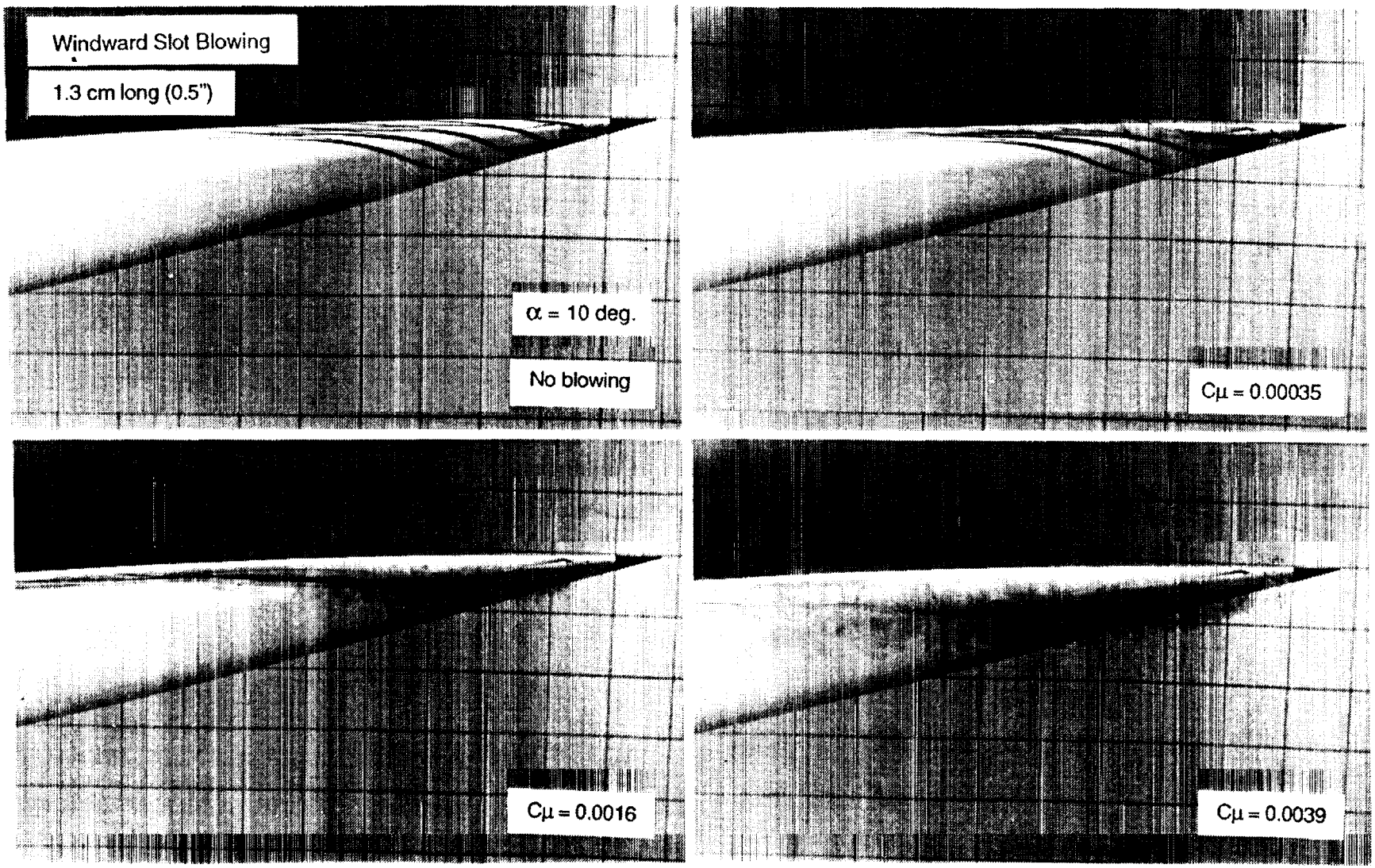

Figure 57 - Effect of Windward Slot Blowing (Right Side, Forebody Model # 2)
1.3 cm long, $\alpha = 10°$

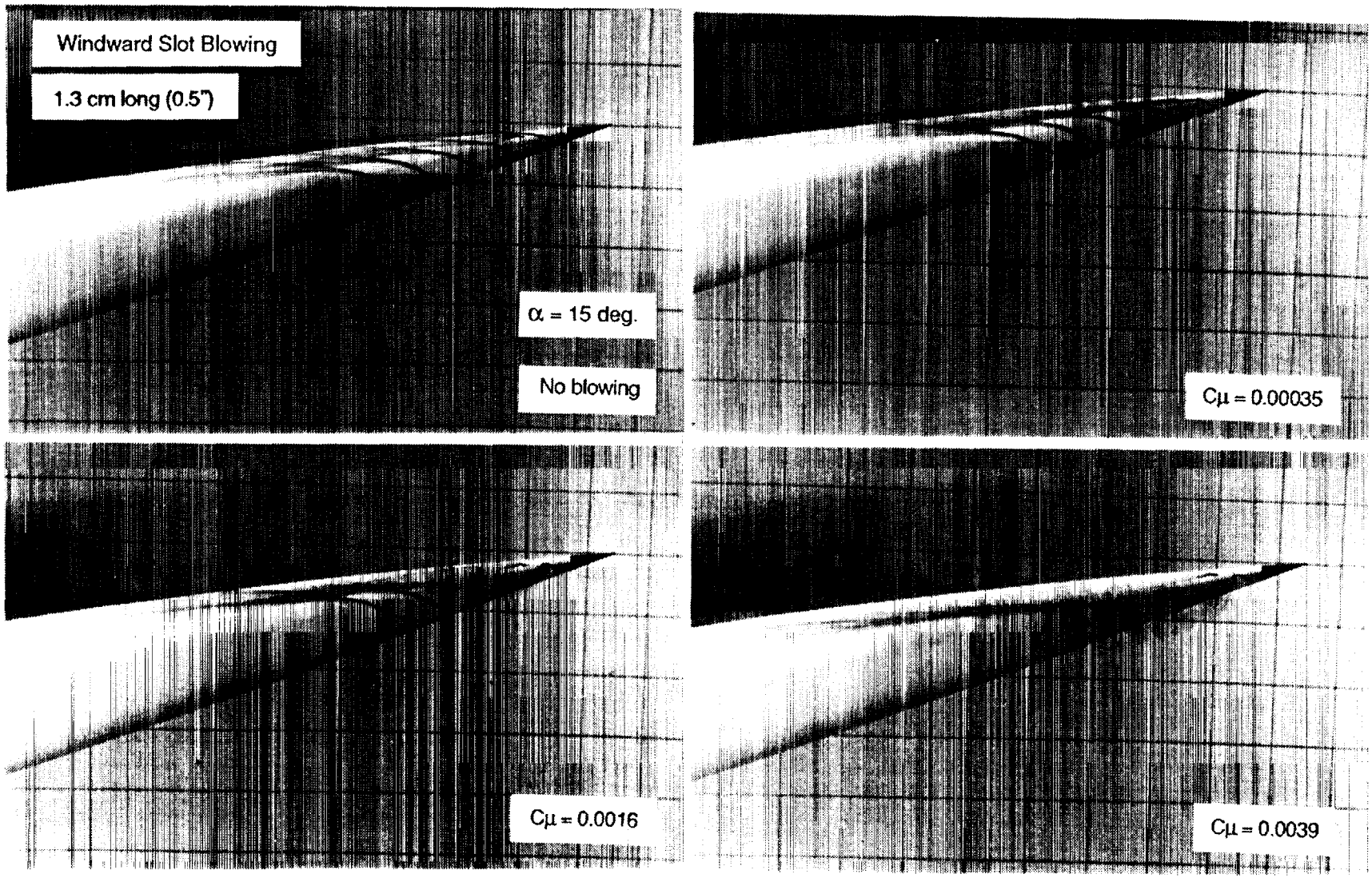

Figure 58 - Effect of Windward Slot Blowing (Right Side, Forebody Model # 2)
1.3 cm long, $\alpha = 15°$

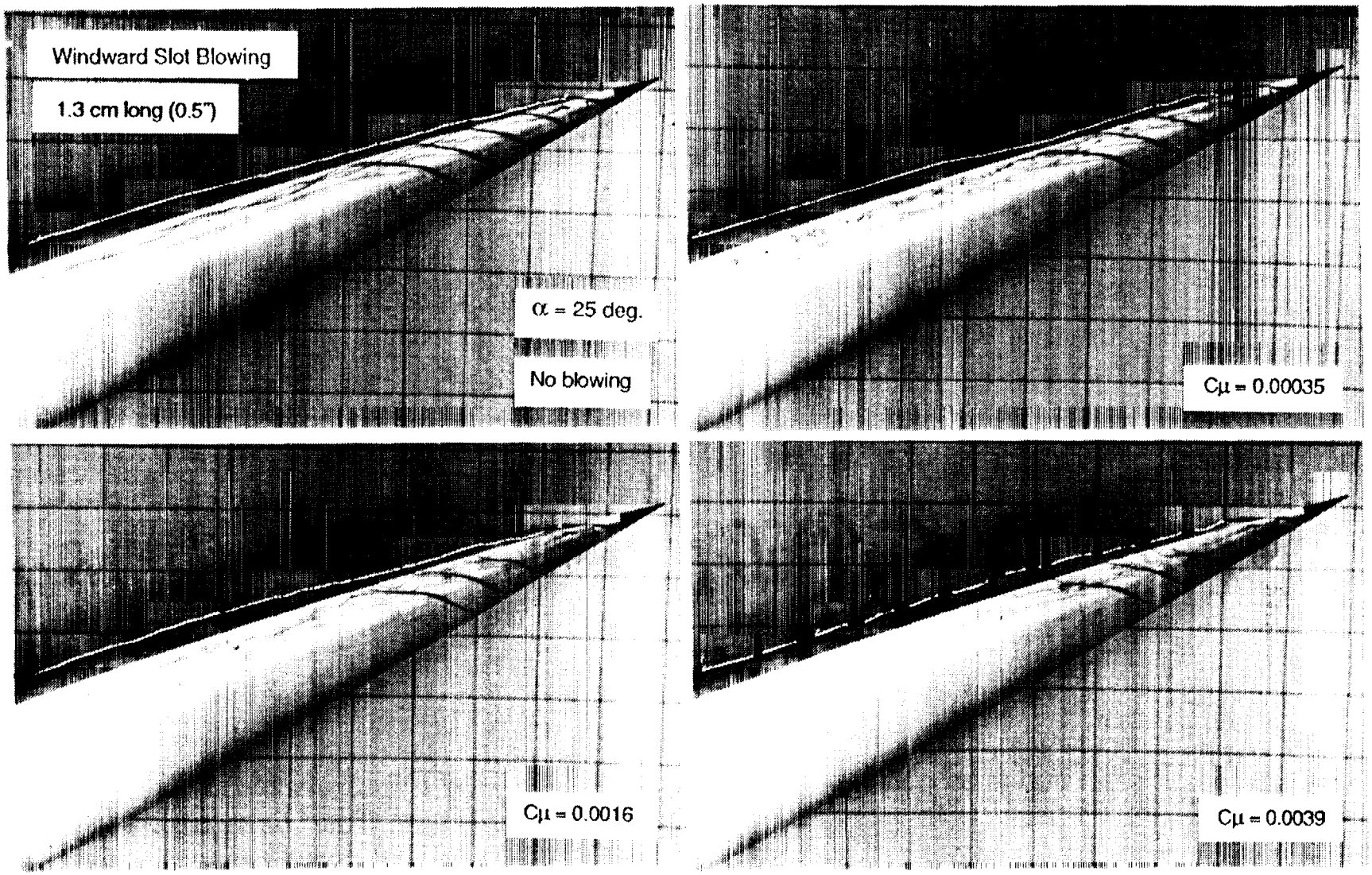

Figure 59 - Effect of Windward Slot Blowing (Right Side, Forebody Model # 2)
1.3 cm long, $\alpha = 25°$

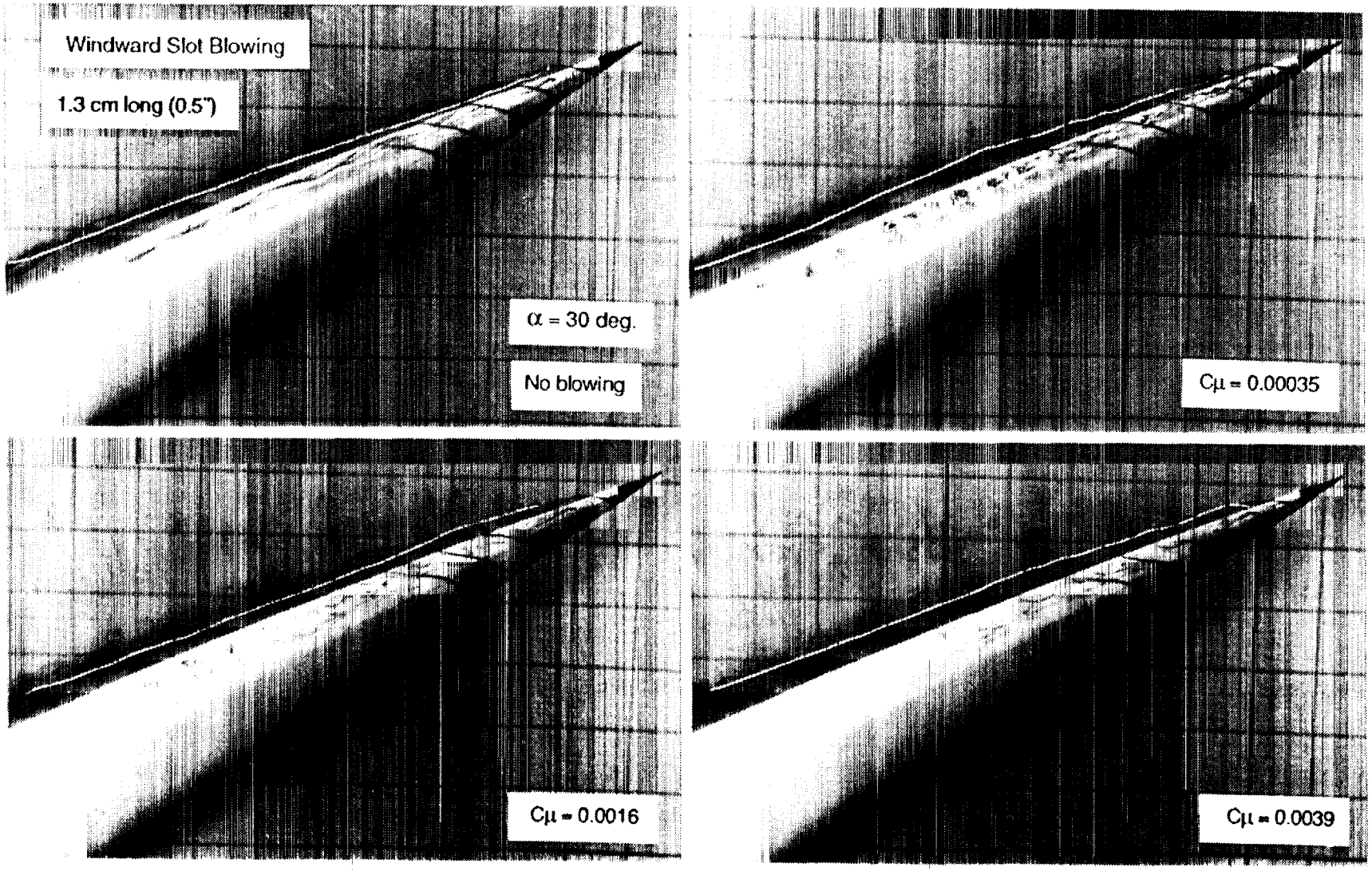

Figure 60 - Effect of Windward Slot Blowing (Right Side, Forebody Model # 2)
1.3 cm long, $\alpha = 30^{\circ}$

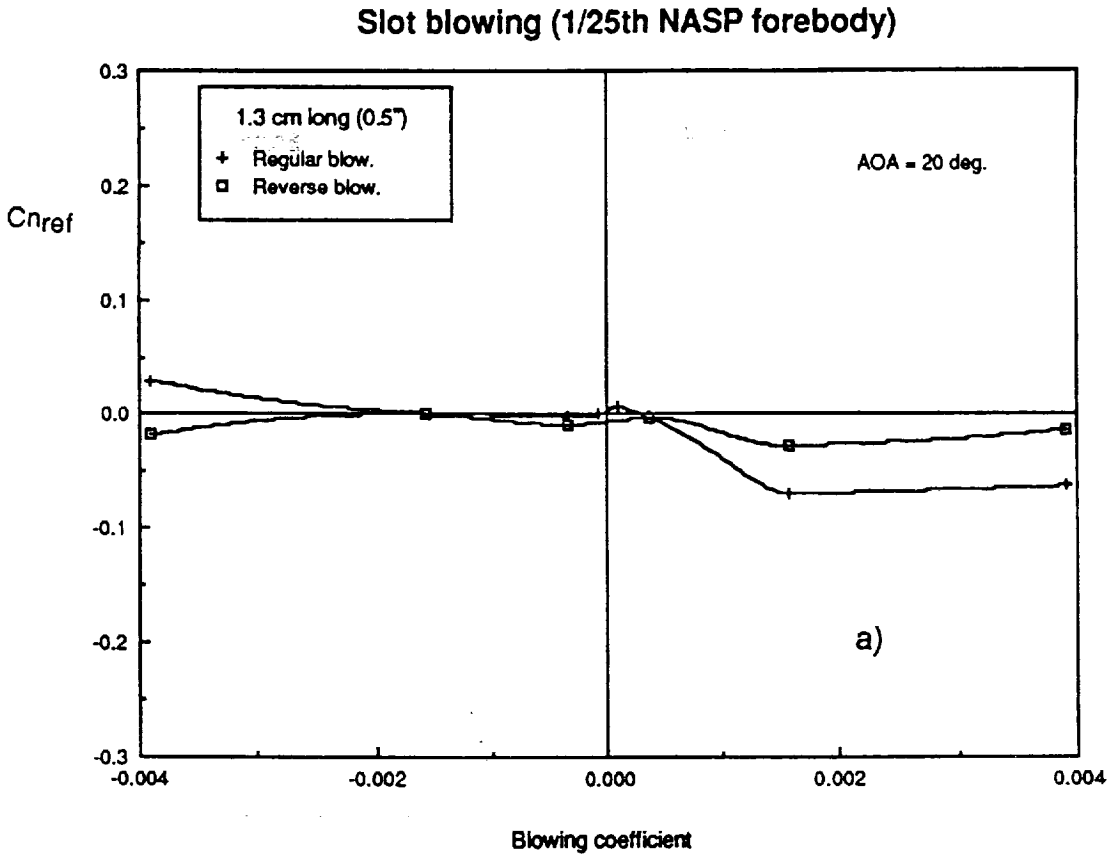

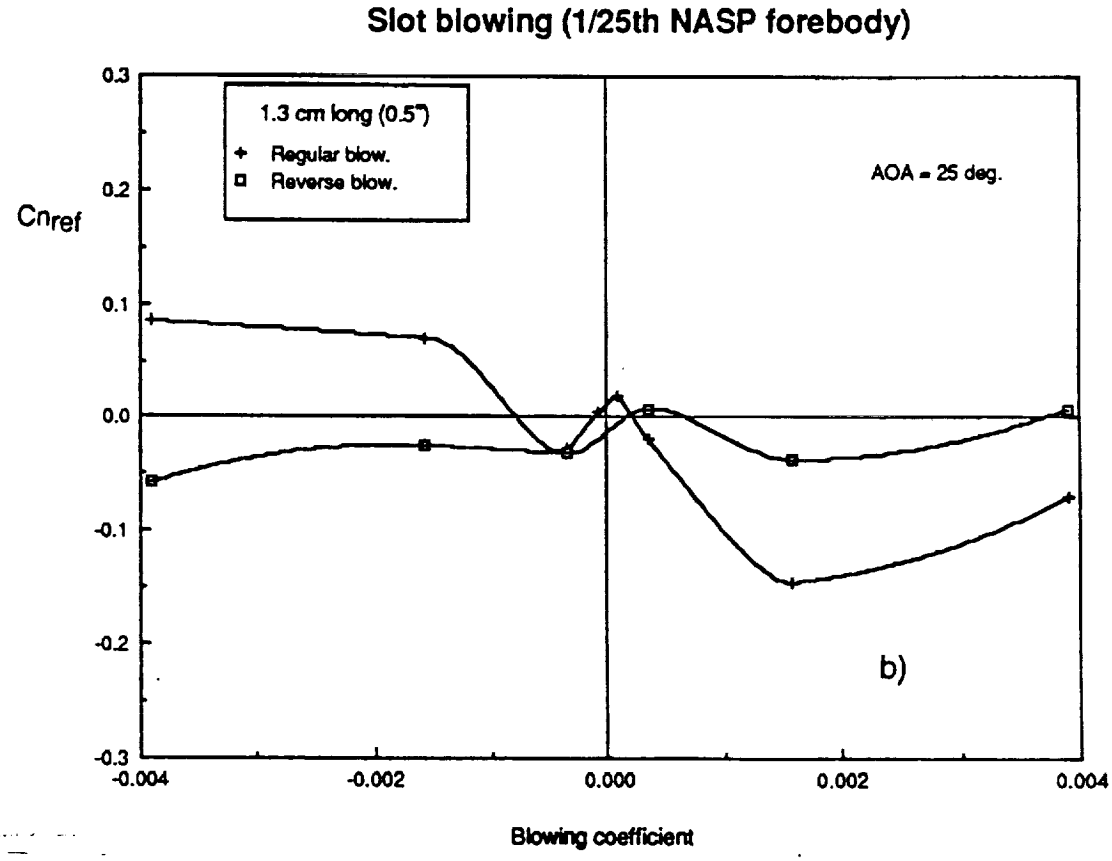

Figure 61 - Comparison Between Slot Blowing and Windward (Reverse) Slot Blowing at a) α =20°, b) α = 25° and c) α = 30°; 1.3 cm long

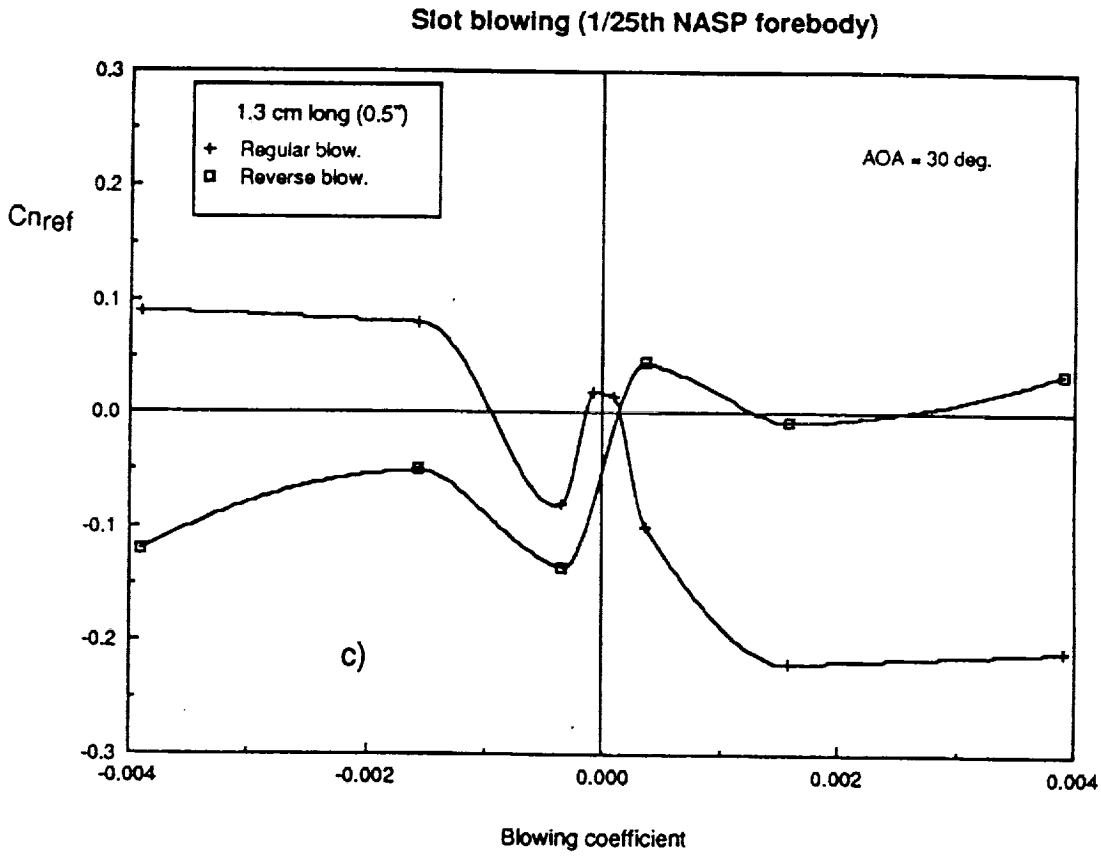

Figure 61 - Concluded

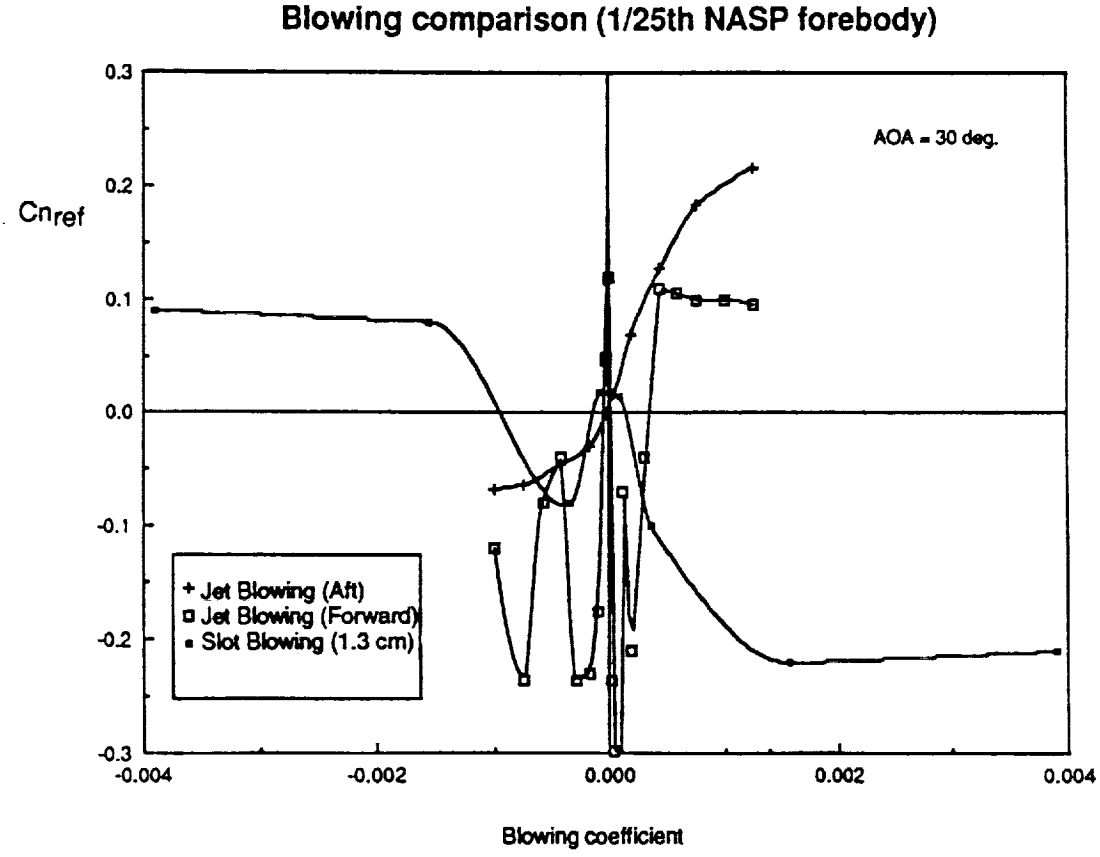

Figure 62 - Comparison Between Different Blowing Techniques; $\alpha = 30°$

REPORT DOCUMENTATION PAGE

Form Approved
OMB No. 0704-0188

1. AGENCY USE ONLY *(Leave blank)*	2. REPORT DATE	3. REPORT TYPE AND DATES COVERED
	September 1993	Contractor Report

4. TITLE AND SUBTITLE
Aerodynamic Control of NASP-Type Vehicles Through Vortex Manipulation, Volume I: Static Water Tunnel Tests

5. FUNDING NUMBERS
NAS2-13196

6. AUTHOR(S)
Carlos Suárez, T. Terry Ng, Lih-Yenn Ong, and Gerald N. Malcolm

7. PERFORMING ORGANIZATION NAME(S) AND ADDRESS(ES)
Eidetics International, Inc.
3415 Lomita Blvd.
Torrance, CA 90505

8. PERFORMING ORGANIZATION REPORT NUMBER
A-93138

9. SPONSORING/MONITORING AGENCY NAME(S) AND ADDRESS(ES)
National Aeronautics and Space Administration
Washington, DC 20546-0001

10. SPONSORING/MONITORING AGENCY REPORT NUMBER
NASA CR-177626

11. SUPPLEMENTARY NOTES
Point of Contact: Larry Meyn, Ames Research Center, MS 247-2, Moffett Field, CA 94035-1000
(415) 604-5038

12a. DISTRIBUTION/AVAILABILITY STATEMENT
Unclassified-Unlimited
Subject Category – 02

12b. DISTRIBUTION CODE

13. ABSTRACT ***(Maximum 200 words)***

Water tunnel tests were conducted on a NASP-type configuration to evaluate different pneumatic Forebody Vortex Control (FVC) methods. Flow visualization and yawing moment measurements were performed at angles of attack from 0° to 30°. The pneumatic techniques tested included jet and slot blowing. In general, blowing can be used efficiently to manipulate the forebody vortices at angles of attack greater than 20°. These vortices are naturally symmetric up to $\alpha = 25°$ and asymmetric between 25° and 30° angle of attack. Results indicate that tangential aft jet blowing is the most promising method for this configuration. Aft jet blowing produces a yawing moment towards the blowing side and the trends with blowing rate are well-behaved. The size of the nozzle is not the dominant factor in the blowing process; the change in the blowing "momentum," i.e., the product of the mass flow rate and the velocity of the jet, appears to be the important parameter in the water tunnel (incompressible and unchoked flow at the nozzle exit). Forward jet blowing is very unpredictable and sensitive to mass flow rate changes. Slot blowing (with the exception of very low blowing rates) acts as a flow "separator"; it promotes early separation on the blow side, producing a yawing moment toward the non-blowing side for the $C\mu$ range investigated.

14. SUBJECT TERMS	15. NUMBER OF PAGES
General hypersonic configuration, Forebody vortex control, Wing rock suppression, Experimental/simulation, Aerodynamic control	88
	16. PRICE CODE: A05

17. SECURITY CLASSIFICATION OF REPORT	18. SECURITY CLASSIFICATION OF THIS PAGE	19. SECURITY CLASSIFICATION OF ABSTRACT	20. LIMITATION OF ABSTRACT
Unclassified	Unclassified		